Journal of Sound and Vibration (2002) **256**(5), 873–940
doi:10.1006/jsvi.5025, available online at http://www.idealibrary.com on IDEAL®

IMPROVED MIRROR SOURCE METHOD IN ROOM ACOUSTICS

F. P. MECHEL

Landhausstrasse 12, *D*-71120 *Grafenau*, *Germany*

(*Received* 14 *August* 2001, *and in final form* 30 *November* 2001)

Most authors in room acoustics qualify the mirror source method (MS-method) as the only exact method to evaluate sound fields in auditoria. But evidently nobody applies it. The reason for this discrepancy is the abundantly high numbers of needed mirror sources which are reported in the literature, although such estimations of needed numbers of mirror sources mostly are used for the justification of more or less heuristic modifications of the MS-method. The present, intentionally tutorial article accentuates the analytical foundations of the MS-method whereby the number of needed mirror sources is reduced already. Further, the task of field evaluation in three-dimensional spaces is reduced to a sequence of tasks in two-dimensional room edges. This not only allows the use of easier geometrical computations in two dimensions, but also the sound field in corner areas can be represented by a single (directional) source sitting on the corner line, so that only this "corner source" must be mirror-reflected in the further process. This procedure gives a drastic reduction of the number of needed equivalent sources. Finally, the traditional MS-method is not applicable in rooms with convex corners (the angle between the corner flanks, measured on the room side, exceeds 180°). In such cases, the MS-method is combined below with the second principle of superposition (PSP). It reduces the scattering task at convex corners to two sub-tasks between one flank and the median plane of the room wedge, i.e., always in concave corner areas where the MS-method can be applied.

1. INTRODUCTION

The mirror source method (MS-method) generally is said to be the only precise method to evaluate sound fields in auditoria, excited by a source Q (the "original" source). It is indeed an exact method if the walls of the room are hard. If the walls are absorbent, the MS-method is an approximation with analytical derivation and analytically definable errors in the elementary process of reflection of the field of Q at a wall. The larger the sum of the heights of Q and of the immission point P above the wall, the better the precision.

The MS-method is described in text books mostly in one or two pages, and the description concentrates on the geometrical principles for the construction of mirror sources (MS). The purely geometrical considerations for the construction of MS lead to high numbers of needed MS. This is the reason why, in fact, the MS-method is not applied in practical tasks of room acoustics. It will be shown that acoustical principles reduce the number of needed MS.

A number of modifications of the MS-method are described in the literature. The main argument for such modifications is the "expected" high number of needed mirror sources. The "ray tracing method" was introduced by Krokstadt *et al.* [1], and since then further developed in many papers, especially by application of random emission of the rays [2]. Stephenson [3] substitutes the sound rays with "sound particles" shot from the sound

0022-460X/02/$35.00

source into randomly distributed directions. Vorländer [4] and Stephenson [5] compare the MS-method with the "ray tracing method" and the "sound particle method" with respect to time of computation. Vorländer gives an estimation of the needed number of MS with $N_{MS} \approx (n_w - 1)^{o_{max}}$, where n_w is the number of walls and o_{max} is the upper limit of the considered orders of wall reflections; Stephenson estimates the needed computing time in a room with $n_w = 24$ walls and $o_{max} = 7$ in units of years. One can notice that these estimations are based on purely geometrical and statistical considerations. For reduction of the computing time, the classical "ray tracing method" substitutes the sound wave by a ray, which is a straight line emanating from the source, carrying some sound energy, which is specularly reflected at the walls with a reduction of the energy according to the reflection coefficients of the walls. In further modifications, the directions of ray emission are randomly distributed (which introduces the Monte Carlo method into room acoustics). The sound field in the point of immission, P, is measured by the energy sum of the incident rays. It suggests substituting the rays by "sound particles" (also carrying some sound energy with them) that are shot from the source and reflected at the walls as in billiard playing. Because the chance for a ray or a sound particle is small to hit a point P, the receiver is extended to a "box", collecting rays or particles which pass nearby P. It is evident that many rays or particles are sent out without ever hitting P (or the box at P). To overcome this inefficiency, at least partially, in a further modification the rays are spreading as a cone. Some heuristic assumptions must be made in this "cone approach" concerning the interaction of a cone with a scattering object. It should be remarked that the problems of hitting P by a ray or a particle are pseudo-problems, due to the artefacts of rays and sound particles; a similar problem does not exist in analytical acoustics. The reported high numbers of needed mirror sources come from statistical investigations about the number of rays or particles which must be emitted randomly in order that summation at P of rays or particles gives a prescribed precision, and by a not justified identification of that number with the number of needed mirror sources.

As a consequence of the fundamental ideas of the modifications of the MS-method, all modifications use as field quantity either energetic quantities or the absolute magnitude of the sound pressure (squared) as sound field descriptors; thus, magnitudes of the sound pressure from different paths of propagation are summed up in the immission point. It is clear that interference patterns of the sound pressure around a point of immission cannot be evaluated with such methods.

It should also be noticed that all modifications use reflection coefficients $|R|^2$ or absorption coefficients $\alpha = 1 - |R|^2$ for the characterization of absorbent walls. Mostly, the absorption coefficient for diffuse sound incidence or for "diffuse reflection" is used. Diffuse reflection, however, is another artefact in itself. An angular dependence of the sound absorption is re-introduced by Lambert's law (an approximation taken from the optical scattering at rough surfaces). It cannot be a task of the present paper to give a detailed survey of the numerous papers about the MS-method, and the author should not be misunderstood as though he were stating that the mentioned modifications of the MS-method are the only existing forms of the MS-method in the literature.

In contrast to the mentioned modifications, the aim of the present paper is a description and use of the MS-method as a method of computation of the *complex*, time harmonic sound pressure (with time factor $e^{j\omega t}$ which will be dropped) of the sound pressure field $p(P)$ in a room. Other aims are as follows: presentation of the acoustical foundations of the MS-method; derivation of acoustical and analytical criteria for the interruption of MS-production; reduction of the MS-method in three-dimensional (3-D) rooms to a sequence of applications of the MS-method in two-dimensional (2-D) sub-spaces; combination of the MS-method with a principle of superposition (PSP), in order to make

the MS-method applicable in rooms with convex corners (e.g., for orchestra pits); representation of the sound field in room edges by equivalent "corner sources".

These steps reduce the number of needed equivalent sources and make the so-modified MS-method applicable in practical tasks of room acoustics. If new approximations are introduced, care is taken that their errors remain in the range of errors of the original MS-method with absorbing walls.

The described combination of a classical topic (the MS-method) with rather simple improvements nearly unavoidably makes the style of writing "tutorial". Fundamental facts will be described verbally, supported with sketches where appropriate; important relations will be presented as formulas. It is not intended to present computer programs or detailed algorithms. However, relevant formulas will be given with some completeness, so that a skilled programmer can write a program for the MS-method (the used geometrical relations are described in Appendix A). In order to make the progress visible, the method will be applied to a model of a concert hall, which is simple enough to trace the steps of computation, but not too simple.

The sketches which are used to visualize a statement will mostly be 2-D not only because 2-D presentations are easier to draw, but also because finally the application of the MS-method in 3-D rooms will be "broken down" to a sequence of 2-D tasks.

2. THE OBJECT

The geometrical object is a room formed by plane walls W_w. It is clearly defined what is inside and outside of the room. The (original) source Q and the field point P always are inside. A right-handed Cartesian system of co-ordinates x, y, z is laid over the room.

We shall distinguish between 3-D rooms with a point source as the original source, and 2-D rooms in which all walls are normal to a common plane (i.e., corners are parallel to each other). 2-D rooms further will be called "strictly 2-D" if the original source, and hence all MS, are line sources.

It is proposed sometimes to model small-size scatterers (such as pillars or handrails) with plane facets and to apply the MS-method to those facets. The subdivision of the room envelope into too small wall sections in combination with the MS-method not only produces analytical and numerical nonsense (the scattered waves at such small facets are very different from MS-waves), but also the computational work increases immensely by the subsequent generation of MS at such small faces. It would be easier and faster to solve the task of scattering at suitable scatterers (e.g., cylinders or spheres). As a general rule for the dimensions of walls to be considered, one can neglect walls with dimensions smaller than about λ_0.

3. WALLS

The walls W_w are plane. They are described by lists of edges, $W_w = \{E_{w1}, E_{w2}, E_{w3}, \dots\}$, which are ordered so that the sense of rotation in that order and the direction pointing to the inside of the room make a right-handed system. Because the first three edges will be used for the determination of the unit normal vector of the wall, these edges should not be collinear, and they should agree with the general sense of rotation of wall edges. Edges may be cyclically interchanged in a wall list. The order $w = 1, 2, 3, \dots$ of the walls is arbitrary.

Wall couples form a room wedge; they either have a (straight) real corner if the walls are intercepting, or they have a virtual corner. The walls of a couple include a wedge angle

Θ (measured inside the room). Corners are "concave" when $0 < \Theta \leqslant \pi$, and "convex" for $\pi < \Theta \leqslant 2\pi$. Walls are parallel to each other, with the virtual corner at infinity, if $\Theta = 0$; and they are collinear if $\Theta = \pi$. These situations must be treated as special cases.

The acoustic qualification of a wall will use its surface admittance G_w. The MS-method applies for the acoustic qualification of a wall its reflection factor $R_w(\theta)$ for a plane wave with incidence at the polar angle θ formed by the normal to the wall and the connection line of the MS with P. $R_w(\theta)$ depends on that angle, and thereby on the position of P, as

$$R_w(\theta) = \frac{\cos\theta - Z_0 G_w}{\cos\theta + Z_0 G_w}, \tag{1}$$

where Z_0 is the characteristic wave impedance. If the wall is bulk reacting one further has $G_w = G_w(\theta)$.

4. SOURCES

The original source Q and mirror sources (MS) may jointly be called sources; a clearer distinction will be made when necessary. Sometimes we shall speak of a "mother source" which creates at a wall W (sometimes called "mother wall") an MS as "daughter source". The symbol S will be used for mirror sources (mainly in the sketches); the symbol q will be used for a source, either the original source Q or a mirror source S.

The fundamental task of the MS-method is the reflection of a source at an infinite wall (see section 5). Analytical solutions seem to exist only for monopole point and line sources (parallel to the wall). Generally, the MS-method is applied also for a directional source with

$$p_Q(r,\vartheta) = D(\vartheta)H_0^{(2)}(k_0 r) \quad \text{in strictly 2-D rooms with a line source,} \tag{2a}$$

$$p_Q(r,\vartheta,\varphi) = D(\vartheta,\varphi)h_0^{(2)}(k_0 r) \quad \text{in 2-D or 3-D rooms with a point source,} \tag{2b}$$

where $D(\vartheta)$ or $D(\vartheta,\varphi)$ are source directivities, $\mathrm{H}_0^{(2)}(x)$ are cylindrical, and $h_0^{(2)}(x)$ spherical Hankel functions of the second kind. It should be mentioned that these forms of the source field do not satisfy the wave equation (a directional factor cannot be associated with a Hankel function of zero order). A similar violation of the wave equation is made by the MS-approximation of the reflected wave at an absorbent wall :

$$p_s(r',\theta) = R(\theta)H_0^{(2)}(k_0 r'), \qquad p_s(r',\theta) = R(\theta)h_0^{(2)}(k_0 r'), \tag{3a, b}$$

where the co-ordinates r', θ are centred at the position of the MS. Such violations of the wave equation are tolerated in the MS-method. Comparisons of results of the MS-approximation with more precise evaluations of the reflected sound field show that, in most cases, the mentioned errors can be accepted, indeed.

5. FOUNDATION OF THE MIRROR SOURCE APPROXIMATION (in 2-D)

As mentioned already, the legitimization of the MS-method comes from an analytical solution of the fundamental task of reflection of the field of a line source (in 2-D; a point source in 3-D) at a possibly absorbent, but in any case infinite, plane wall (see Figure 1; see e.g. reference [6] for line source reflection, and reference [7] for point source reflection).

An exact form of the reflected field p_r is (see reference [6] for the path $C(\varphi)$ of integration)

$$p_r(r',\theta_s) = \frac{1}{\pi}\int_{C(\varphi)} R(\varphi + \theta_s)\mathrm{e}^{-\mathrm{j}k_0 r'\cos\varphi}\,\mathrm{d}\varphi. \tag{4}$$

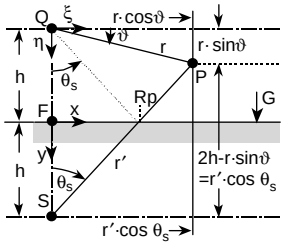

Figure 1. A line source in Q with a height h above the absorbing plane, which is characterized by a normalized surface admittance G. S is the mirror-reflected point to Q and P is the field point.

One gets by saddle point integration

$$p_r = \sqrt{\frac{1}{\pi k_0 r'}}\, \mathrm{e}^{-\mathrm{j}k_0 r'}\left[\Phi(0) + \frac{1}{4k_0 r'}\Phi''(0) + \cdots + \frac{1\cdot 3\cdot 5\cdot \ldots (2n-1)}{(2n)!\,(2k_0 r')^n}\Phi^{(2n)}(0)\right], \tag{5}$$

with

$$\Phi(s) = R(\varphi(s) + \theta_s)\frac{2j}{\sqrt{2j + {}^2}} = \frac{\cos(\varphi(s) + \theta_s) - Z_0 G}{\cos(\varphi(s) + \theta_s) + Z_0 G}\frac{2j}{\sqrt{2j + s^2}}, \tag{6}$$

$$\varphi(s) = \pm \arccos(1 - \mathrm{j}\cdot s^2), \quad s \gtrless 0, \quad \varphi(0) = 0, \quad \frac{\mathrm{d}\varphi(s)}{\mathrm{d}s} = \frac{2j}{\sqrt{2j + s^2}}. \tag{7}$$

Inserting this into equation (5) and collecting terms with derivatives $R^{(n)}(\theta_s)$ of equal order n finally gives

$$\begin{aligned} p_r(r', \theta_s) = {} & \sqrt{\frac{2j}{\pi\, k_0 r'}}\, \mathrm{e}^{-\mathrm{j}k_0 r'} \\ & \times\left[\left(1 + \frac{j}{8k_0 r'} - \frac{9}{128(k_0 r')^2} - \frac{75j}{1024\,(k_0 r')^3} + \frac{3675}{32768\,(k_0 r')^4} + \frac{59535}{262144\,(k_0 r')^5}\right)R(\theta_s)\right. \\ & + \left(\frac{j}{2} - \frac{5}{16\,k_0 r'} - \frac{259j}{768(k_0 r')^2} + \frac{3229}{6144(k_0 r')^3} + \frac{352407}{327680(k_0 r')^4}\right)\frac{R^{(2)}(\theta_s)}{k_0 r'} \\ & + \left(-\frac{1}{8} - \frac{35j}{192k_0 r'} + \frac{329}{1024(k_0 r')^2} + \frac{17281j}{24576(k_0 r')^3}\right)\frac{R^{(4)}(\theta_s)}{(k_0 r')^2} \\ & + \left(-\frac{j}{48} + \frac{7}{128k_0 r'} + \frac{1463j}{10240\,(k_0 r')^2}\right)\frac{R^{(6)}(\theta_s)}{(k_0 r')^3} \\ & \left. + \left(\frac{1}{384} + \frac{11j}{1024k_0 r'}\right)\frac{R^{(8)}(\theta_s)}{(k_0 r')^4} + \frac{jR^{(10)}(\theta_s)}{3840(k_0 r')^5}\right]. \end{aligned} \tag{8}$$

The factor in front of $R(\theta_s)$ is just the asymptotic expansion of $H_0^{(2)}(k_0 r')$. Thus, in a first approximation (with respect to an angular variation of $R(\theta_s)$)

$$p_r(r', \theta_s) \xrightarrow[k_0 r' \gg 1]{} R(\theta_s)\, H_0^{(2)}(k_0 r'). \tag{9}$$

This is the *mirror source approximation* (MS-approximation). One should keep in mind: the MS-solution is only approximate if $R(\theta_s) \neq \text{const}(\theta_s)$, i.e., for $G \neq 0$ or $|G| \neq \infty$; then it violates the wave equation; it determines precisely the meaning of $R(\theta_s)$; with that definition (and only with that) it satisfies the wall boundary condition, it supposes $k_0 r' \gg 1$, i.e., large distances dist(S, P); or more precisely: a great sum of the heights of Q and P over the wall; it supposes that P is not under an angle θ_s with a strong angular variation of $R(\theta_s)$; for grazing incidence, i.e., Q and P on the wall, the influence of higher terms $R^{(n)}(\theta_s)$ in equaton (8) is important; the derivation further supposes that the wall does not guide a surface wave (but this is only rarely the case in a restricted frequency range below a high-quality resonance; but even then equation (8) is an approximation to the field in points not too close to the wall; see reference [7] for a detailed discussion of the influence and the conditions of surface waves).

There exists an analogous derivation of the MS-approximation for a point source in 3-D with similar conditions and restrictions (see reference [7]).

The mentioned facts have important consequences: on the one hand, it makes no sense to try to compute with a higher precision than the precision of the fundamental process of the MS-method; on the other hand, the approximate character of this process does not give a privilege to fantastic modifications of the MS-method.

6. GENERAL CRITERIA FOR MIRROR SOURCES

Mirror sources are created at a wall by a source inside the wall by the following steps: mirror-reflect the source position to behind the wall; multiply its source factor with $R(\theta_s)$; if the source has a directivity factor $D(\vartheta, \varphi)$, reflect that directivity, i.e. rotate it.

Any factor of the (possibly spherical) Hankel function of the field of a single source is called the "source factor".

The form of the MS and the used co-ordinates should, if possible, be so that these steps can be performed easily in the computations.

The right of an MS to exist is the satisfaction, together with its mother source, of the boundary condition at the wall at which it was created by its mother source. Nothing else !

The first criterion for the generation of a daughter MS at a wall is that the mother source irradiates the interior surface of that wall. As a consequence, if a source is outside a wall, it does not create a daughter source at that wall. Especially, a mirror source will never be mirror-reflected back to the position of its mother source. We call this rule the "inside criterion". The chain of MS-production is interrupted if this criterion is violated; otherwise the daughter source would be "illegal".

7. FIELD ANGLE Φ OF A MIRROR SOURCE

The field angle of an MS gives a further important criterion for the interruption of MS-production. The field angle is best explained for the case of reflection of a source Q at a plane wall which is subdivided in two parts with different reflection factors R_i in them (see Figure 2).

Although the source Q in the example of Figure 2 has only one position S for an MS, there are indeed positioned two MS with different angular ranges Φ_1, Φ_2 of their fields because there are two different source factors R_1, R_2 in both ranges. The field is unsteady at the common flank of the field angles. This is a consequence of the character of the MS-method as an approximate solution which must be tolerated (below we shall see similar

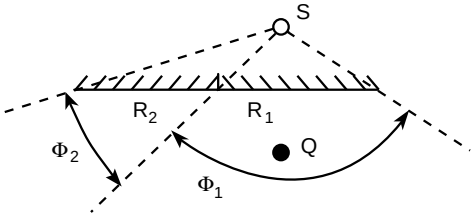

Figure 2. Definition of field angle Φ.

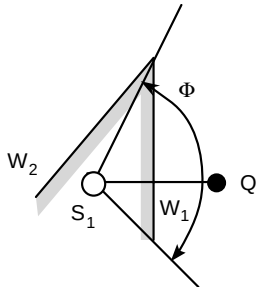

Figure 3. Combined condition that P or a wall must be inside the mother wall of a mirror source S.

consequences at other occasions). In 3-D the field angle Φ is given by a polygonal pyramid subtended by a wall W and with the source S in the apex.

The "field angle criterion" states two things. An MS creates in P a field contribution only if P is in its field angle (more precisely, on the interior side of the creating wall) and otherwise we say "the MS is ineffective in P". An MS generates a daughter MS at a wall W only, if the wall is inside the range of its field angle (again on the interior side of the creating wall); otherwise no boundary condition must be satisfied at W for MS, and therefore the daughter MS would be "illegal".

The additions in parentheses will be important for convex corners (see below). We can describe the effect of the field angle with the word "visibility". A source q sees an object only if that object is inside its field angle. If q does not see P , then q is ineffective; if q does not see a wall W, then q does not produce a daughter source with W.

The chain of MS-production is continued for an ineffective MS (because a daughter MS may become effective), but the chain is interrupted at an illegal MS.

Some problems are caused by walls W which are only partially inside Φ. In a strict procedure, one would have to subdivide the wall at the intersection with the flanks of Φ, but such a "dynamical" definition of walls would produce much computational work. It is sufficient, within the frame of precision of room acoustical computations, to check whether the wall section inside Φ exceeds some size limit (e.g., λ_0); if not, that wall is neglected for that MS. It is a good compromise between precision and amount of computation to check whether the centre C of W is inside Φ. This check is done by a repeated test whether C is inside the walls of the polygonal pyramid subtended by W and with the MS at its apex. The repetition can be interrupted if C is outside one of the pyramid walls.

In general, MS with increasing order are displaced farther and farther away from the interior of the considered room. Thus their field angles become smaller and smaller; so fewer walls have to be considered for the production of further MS. This elementary fact cuts down the feared tree-like branching of MS production.

The mentioned additional condition that either P or another wall must be in the field angle *on the interior side* of the generating wall is important, as can be seen from Figure 3.

In Figure 3 the source Q creates at W_1 an MS S_1 , which in the shown case is outside both walls W_1, W_2. The inside criterion would interrupt a further production of MS anyhow. If, however, Q is displaced farther away from the wall W_1, then S_1 may fall on the interior side of W_2. Nevertheless S_1 will not produce an MS at W_2, because W_2 would be in Φ but not on the interior side of the generating wall W_1.

The additional condition (W_2 inside W_1) is relevant only for convex corners.

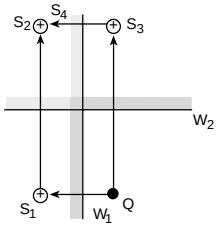

Figure 4. Concave rectangular corner.

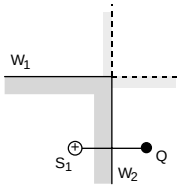

Figure 5. Convex rectangular corner.

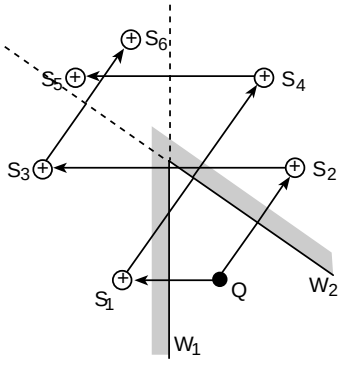

Figure 6. Concave acute-angled corner.

8. A FEW EXAMPLES OF MS-PRODUCTION

We consider in the examples only couples of intercepting walls forming a space wedge. If the wedge angle Θ of a couple of walls is a rational multiple of π, the MS beginning with some higher order will fall upon positions of MS of lower orders. The concave rectangular wedge is liked as an example (Figure 4).

The outer sides of the (possibly extended) walls are greyed. The chain of the MS-production ends in Figure 4 with S_2, S_4 , because both MS are outside both walls. The source factors of both MS S_2, S_4 are equal. The question arises as to whether both coincident MS S_2, S_4 should be counted, or only one of it (see below).

Figure 5 shows a convex rectangular corner.

Only one MS can be constructed at the convex rectangular corner of Figure 5. That is evidently not enough to represent the sound field at such a corner. Consequently, the traditional MS-method fails at convex corners !

In the example of Figure 6 the MS-production ends with S_5, S_6, because both MS are outside both walls.

Depending on the wedge angle Θ and on the position of Q, different numbers of MS can be constructed (higher for small Θ, infinitely high for parallel walls with a part of the room between the walls, i.e., for $\Theta = 0$).

9. COMPUTATIONAL PARTS OF THE MS-METHOD

The traditional MS-method consists of three computational parts: find the positions of the MS (considering the inside and field angle criteria); determine the source factors of the MS, i.e., of the reflection factors $R(\theta_s)$ (depending on the acoustical quality of the mirror wall and of the relative positions of MS and P); evaluate the contributions of the MS to the field in P.

Most programming is needed for the finding of the MS positions, although the single steps are elementary geometrical tasks. Less intensive in programming is the evaluation of the reflection factors of absorbent walls. This task will be delegated to subroutines for the wall surface admittance G. Most simple is the evaluation of the field contributions in P; only a number of Hankel functions of zero order must be evaluated; this sub-task is fast-computing for spherical Hankel functions (which are given by $\cos(x)$, $\sin(x)$), and is fast-computing also for cylindrical Hankel functions when using the known polynomial approximations for Bessel and Neumann functions of zero order.

The traditional MS-method proceeds with the order o of mirror reflections in the production of MS of the order o, $S(o)$. At the order $o = 1$ the MS $S(1)$ are determined in turn for all walls (consider the inside criterion for convex corners!); at the order $o = 2$ all $S(1)$ are potential mother sources for the generation of the MS of second order $S(2)$ at all walls (except the wall at which $S(1)$ was produced), unless the inside and field angle criteria exclude $S(2)$; continue until a final interrupt criterion is met.

10. INTERRUPT CRITERIA IN THE MS-METHOD

The MS-method is often blamed for its apparent exorbitantly high numbers of involved mirror sources. In such statements, inherent interrupt criteria of the MS-method are ignored.

Conditions for the interrupt of the chain of MS-production are as follows.

(1) The source q is outside the mirror wall W: There exists no boundary condition for q at W; the MS-chain can be interrupted.
(2) A wall W is outside the field angle Φ of q: q does not produce a daughter MS at W. For walls with a common corner this is equivalent to (1).
(3) An MS would fall into the interior room space: then there would be, except for Q, a new pole position of the field; this offends the condition of regularity of the field; the MS is illegal. This case is met with only for convex corners.
(4) If the new MS would fall on Q: from then on the MS positions would be repeated; this violates the source condition which demands that the volume flow through a small enclosure around Q must be the same as of the original source. The MS is illegal.
(5) The product ΠR, which is the source factor of q, would become $\Pi|R| <$ limit, which is a pre-set limit. This would make the field contribution negligible, also for all daughter sources of q.
(6) If the sound field is the target quantity (not the reverberation time; see below for that), the distance $dist(q, P)$ of a source q from P may be limited to be $< d_{max}$. For point

sources the amplitude ratio of q in P, relative to the amplitude of Q in P, is $dist(Q, P)/dist(q, P)$. This ratio generally becomes even smaller for daughter sources of q.

(7) A limitation $\Pi|R|dist(Q, P)/\text{dist}(q, P) <$ limit d_{max} would be more significant.

(8) With some arbitrariness one sets an upper limit of the orders $o = 1, 2, \ldots, o_{max}$ of the MS.

The product $\Pi_{o>0} R_o(\theta_s)$ of the reflection factors $R_o(\theta_s)$ of the orders o form the source factor of an MS of reflection order o. It will be symbolized below with ΠR, or $\Pi|R|$ if the product of magnitudes of reflection factors will be used.

In interrupt checks using $\Pi|R|$ it may be sufficient to use for the reflection factors R (or their magnitudes $|R|$) approximate values, for example the reflection factor for normal sound incidence or the reflection coefficient $|R|^2$ from the absorption coefficient for diffuse sound incidence. Then the construction of the MS becomes independent of the position of P. The reflection factors are the only quantities which introduce the frequency into the construction of the MS . If one takes for the interruption check a lower limit or an average value of $|R|$ over the considered frequency interval, the construction of the MS is independent of the frequency also. One should apply tests with the true $|\Pi R|$ in the step of evaluation of the field contributions of the sources, when the ΠR are available. But then these tests must be applied on a smaller number of MS than in the phase of MS-construction.

11. INSIDE CHECK

Checks for interrupt and efficiency form the main part of the computational work in the original MS-method. They are fundamental tasks of computational geometry. But because they are repeated very often, they should compute fast. One can break down all tests to "inside checks". An inside check examines whether a point q is on the interior side of a plane, in the plane, or on the exterior side of the plane (the sides are defined by the rotational sense of the edges E_k of a wall $W = \{E_1, E_2, E_3, \ldots\}$, and they are clear for the flanks of the pyramid of the field angle Φ). One could do the inside check with the help of direction cosines of the connecting lines between q and the E_k. The evaluation of angles, however, is slow. An equivalent check (in 2-D) uses the vector product of the vectors $(q \to E_1), (q \to E_2)$:

$$(q \to E_1) \times (q \to E_2) \left\{ \begin{array}{ll} > 0, & \text{left-rotating} \\ = 0, & \text{collinear} \\ < 0, & \text{right-rotating} \end{array} \right\} \quad \text{triple}(q, E_1, E_2). \tag{10}$$

This check needs two multiplications and one subtraction. A corresponding check in 3-D uses the vector triple product (scalar product of a vector and a vector product) if the wall is given by three of its edges. If the parameters of the reduced normal form of the wall equation

$$ax + by + cz + d = 0 \tag{11a}$$

are known, the inside check needs three multiplications and three additions (see Appendix A) with $q = \{x, y, z\}$:

$$ax + by + cz + d \left\{ \begin{array}{ll} > 0, & q \text{ inside the } W \text{ plane} \\ = 0, & q \text{ on the } W \text{ plane} \\ < 0, & q \text{ outside the } W \text{ plane} \end{array} \right\}, \tag{11b}$$

if W, q form a right-handed system; otherwise the signs change.

Another, often used, test examines if a point P is inside the polygonal pyramid which has the point q as apex and is subtended by a wall W. This test is done by a repetition of inside checks for P and the triangles forming the sides of the pyramid. The loop over the triangles can be aborted with a negative answer for the test, if one of the inside checks fails (distinguish whether W and q are a right-handed or left-handed system).

The shading of a point P or a wall W by a convex corner, and the visibility of P or W from a point q through an aperture (formed by convex corners with a free interspace between them) are also tested with inside checks (see later).

12. WHAT IS NEEDED FOR THE TRADITIONAL MS-METHOD

One needs as input: the list of walls $\{W_1, W_2, W_3, \dots\}$ which themselves are lists of edges $\{E_1, E_2, E_3, \dots\}$, $E_i = \{x_i, y_i, z_i\}$; the source point $Q = \{x_Q, y_Q, z_Q\}$; the field point $P = \{x, y, z\}$; the list of wall admittances $G = \{G_1, G_2, G_3, \dots\}$; the limits o_{max}, limit, d_{max} for the order o, the source factors $\Pi|R|$, the distances $dist(q, P)$, respectively.

It is supposed that $dist(Q, P)$, the wall centres C_w, and the parameters a, b, c, d of the reduced normal forms of the wall equations $ax + by + cz + d = 0$ are evaluated (see appendix A) before the construction of the MS.

One needs, for the evaluation of the reflection factors and of the contributions in P: (1) the position q of a source (either Q or an MS); (2) the counting index w of the wall W at which q was generated; (3) the distance $dist(q, P)$; (4) the amplitude factor $\Pi R(\theta_s)$; (5) a flag which signals with $flag = 0$ that q is an effective source, and with $flag = 1$ that q is ineffective.

These data are collected in "source lists" $\{q, w, dist(q, P), \Pi R(\theta_s), \text{flag}\}$, and the source lists for a given reflection order $o = 0, 1, 2, \dots, o_{max}$ are collected in tables:

$$tab(o) = \{\dots, \{q, w, dist(q, P), \Pi R(\theta_s), flag\}, \dots\}.$$

The counting index of a source list within $tab(o)$ is s. The source table for the order $o = 0$, i.e., for the original source $q = Q$, has the form $tab(0) = \{\{Q, 0, dist(Q, P), 1, 0\}\}$ (for rooms with concave corners; see below for rooms with convex corners).

One can delegate the task of mirror reflection of a mother source q_m, represented by its source list $\{q_m, w_m, dist(q_m, P), \Pi_m R(\theta_s), \text{flag}_m\}$, at a wall W_w, given by its index w, including all tests of interrupt and effectivity, into a subroutine, which should be carefully checked and economized with respect to computing time. That subroutine returns the source list $\{q, w, dist(q, P), \Pi R(\theta_s), flag\}$ of the daughter source, if no interrupt criterion is met; the value 0 , if an interrupt criterion is met.

Such a subroutine for 3-D rooms with concave corners is a program of about 25 program lines in Mathematica® language (the geometrical sub-tasks inside the subroutine are delegated to subroutines, in turn).

The original MS-method works in three nested loops: (1) the outer loop over the order $o = 1, 2, \dots, o_{max}$ and it produces the source table $tab(o)$; (2) the middle loop over the counting index $s = 1, 2, \dots$ of the sources in $tab(o-1)$; (3) the innermost loop over the counting index $w = 1, 2, \dots$ of walls: it calls the above-mentioned subroutine; if that subroutine does not return 0, the new source list is appended to $tab(o)$.

This original MS-method is attractive by its computational simplicity. A frame program for the evaluation of $tab(o)$ in Mathematica® typically is a program of about 12 lines, if the frame program calls a subroutine for the MS-evaluation with all checks inside that subroutine. It may be of some advantage to perform the checks of legitimacy of a new MS (mother source inside the mirror wall; mirror wall in the field cone of the mother source) in

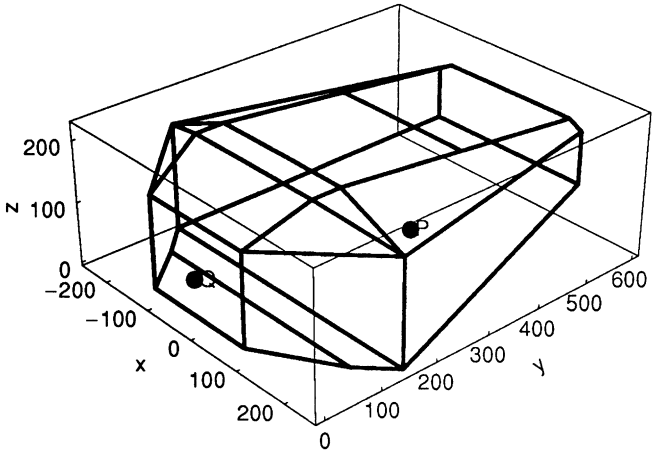

Figure 7. Wire-plot of the model room.

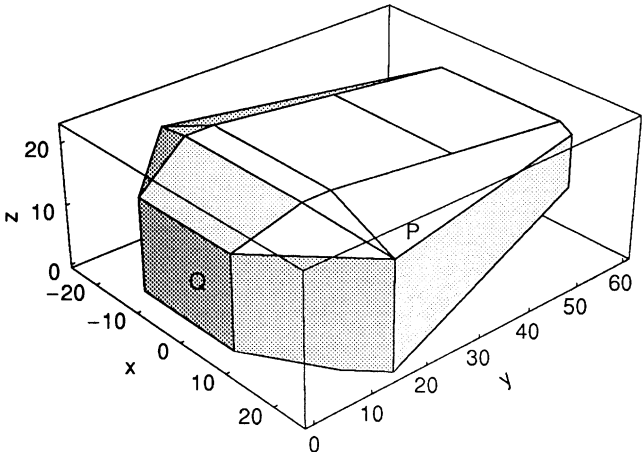

Figure 8. Outside view of the model room.

the frame program (this is true especially when the MS-method is applied to rooms with convex corners; see section 14).

The returned tables $tab(o)$ contain also ineffective sources ($flag = 1$). One can select the effective sources with $flag = 0$ and collect them in tables called $tab_{eff}(o)$. So one has available all data which are needed to evaluate and sum up the field contributions in P of the effective sources.

13. A CONCAVE MODEL ROOM, AS AN EXAMPLE

We consider a 3-D model room which could go as a simple concert hall (see Figures 7 and 8). It has $w = 1, 2, \ldots, 19$ walls, two of them (5, 19) are coplanar, and two couples, (2, 6), (4, 8), have parallel walls on opposite sides of the room. The floors of the stage and of the seat area are inclined relative to each other. Balconies cannot be modelled with concave rooms. The

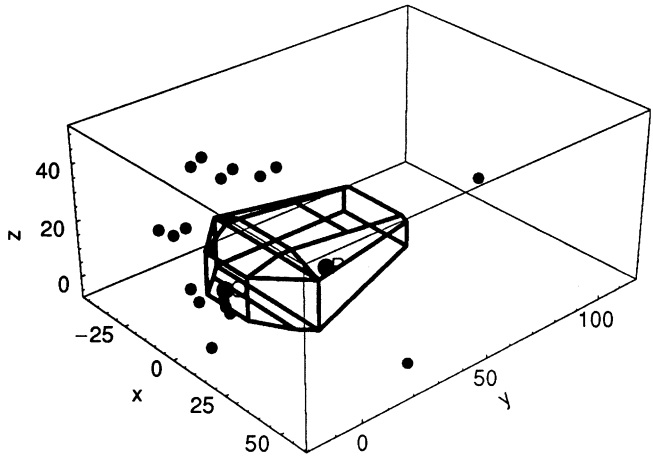

Figure 9. Mirror sources of order $o = 1$, with only back-reflection criterion. Number of MS: 19.

sections through the room, from which the geometrical input data were taken, are given in Appendix B, together with the list of co-ordinate values of the edges, of Q, and P. From these data the following 3-D plots are computed (such plots are parts of the checks of input data). Figure 7 shows the room as a 3-D wire-plot, together with the source Q and the field point P. Figure 8 shows an outside view of the room. The co-ordinate units are arbitrary. In Figure 8 and in later diagrams for the mirror sources, they are scaled down with a factor 1/10.

The normalized wall admittances $Z_0 G_w$ for the shown example are entered as constant complex values (see Appendix B). They produce absorption coefficients α_{dif} for diffuse sound incidence as given below (see Appendix B for the wall counting index):

$\alpha_{dif} = \{0{\cdot}10, 0{\cdot}10, 0{\cdot}40, 0{\cdot}71, 0{\cdot}20, 0{\cdot}60, 0{\cdot}20, 0{\cdot}40, 0{\cdot}20, 0{\cdot}40, 0{\cdot}40, 0{\cdot}20, 0{\cdot}20, 0{\cdot}20, 0{\cdot}20, 0{\cdot}20, 0{\cdot}20, 0{\cdot}20, 0{\cdot}50\}$.

The graphs in Figures 9–11 show mirror sources (as points) for some orders o if only back-reflection (into the position of the mother source) is avoided. Such diagrams would be the basis for published numbers of "needed" mirror sources.

The next diagrams show the effective mirror sources with all interrupt criteria applied; the numbers of MS are indicated in the plot label. As criterion for exclusion of a wall as mirror wall, it was checked whether the wall centre is inside the field angle cone of the mother source. It should be noticed that already for the order $o = 1$ the number of MS is reduced from 19 to 10 (mainly by the efficiency check).

The published estimates $N(N-1)^{(o-1)}$ for the needed MS of order o in a room with N walls would give for the order $o = 6$ (with $N = 19$ for our room), a number 35 901 792 !!

By the way, the computing time for $tab_{eff}(o)$ up to $o = 6$ was 116 s (on a 400 MHz laptop computer with non-compiled Mathematica® programs).

The strong reduction of the numbers of MS in Figures 12–14, as compared with those in Figures 9–11, has two reasons: first, the application of the inside criterion for sources relative to the mirror walls and of the inside criterion for walls inside the field cone of the (mother) source; second , the application of the criterion of efficiency of a source. The numbers of MS in orders o for different applied criteria are collected in Table 1.

Table 2 collects, in each order o, minimum and maximum reductions in the level of the sound pressure contribution in P due to $\Pi|R|$, $dist(Q, P)/dist(q, P)$, and their product.

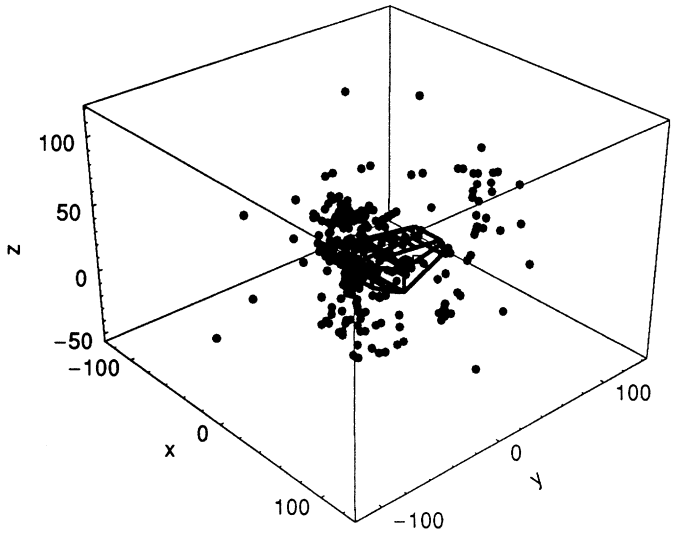

Figure 10. Mirror sources of order $o = 2$, with only back-reflection criterion.Number of MS: 342.

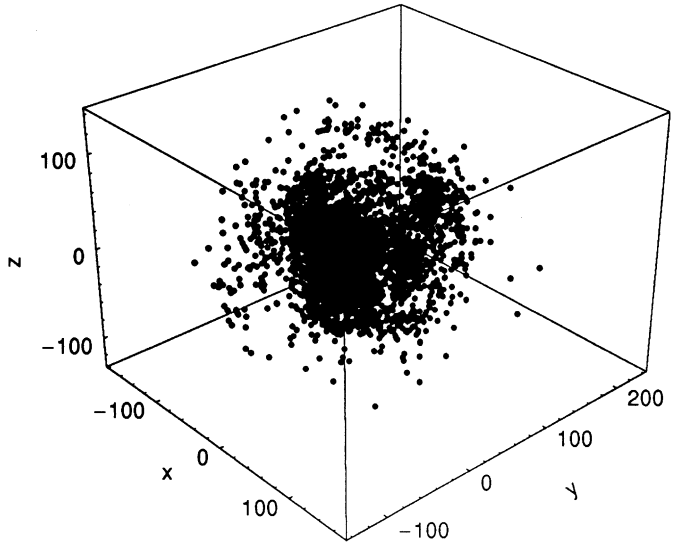

Figure 11. Mirror sources of order $o = 3$, with only back-reflection criterion. Number of MS: 6156.

The limits were set to $\Pi|R| > 0{\cdot}01 \sim -40$ dB; $dist(q, P) > 10dist(Q, P)$ (corresponding to -20 dB of the distance ratio); so none of the two limitations restricted the number of effective mirror sources. The table also shows that a limitation of the orders to $o \leqslant o_{max} = 6$ is reasonable, because the highest contribution of a mirror source for $o = 6$ is $-14{\cdot}53$ dB below the contribution of the original source Q. In addition, the number of effective MS would be further reduced if the product $\Pi|R|dist(Q, P)/dist(q, P)$ (say with a setting to -40 dB) were used for termination.

As an example of application, we plot the profiles of the sound pressure level in places $X = (x, y, z_P)$ around $P = (x_P, y_P, z_P)$ as 3-D plots of $20\lg|p(X)/p(P)|$ over k_0x, k_0y for two

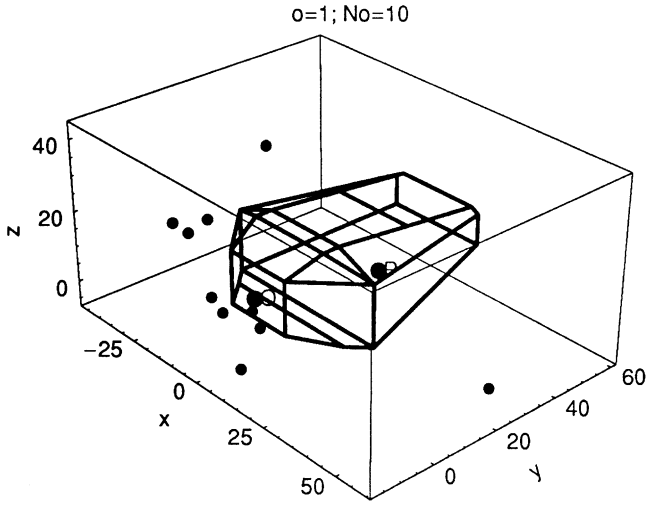

Figure 12. Effective mirror sources of order $o = 1$, with all interrupt criteria. Number of MS: 10.

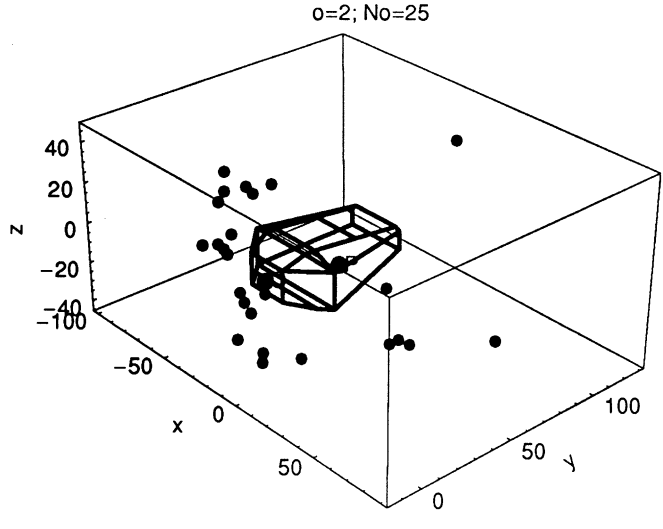

Figure 13. Effective mirror sources of order $o = 2$,with all interrupt criteria. Number of MS: 25.

frequencies. It is supposed that the distances $dist(X, P)$ are small enough to neglect the influence of variation of X on $R(\theta_s)$. Figure 17 is for a low frequency and Figure 18 for a five times higher frequency; the frequency is determined by the scale factor of the co-ordinates $scal = 2\pi/\lambda_0$ (the computing time for a diagram was 16 s; the order limit was $o_{max} = 6$; therefore the number of mirror sources are those of Table 1 and of Figures 12–16).

Figure 17 indicates a standing wave pattern with deep minima mainly in the x direction. Figure 18 represents a superposition of standing wave patterns in several directions, with not so deep minima.

Such patterns could not be computed with modified MS-methods using $|p_s(P)|$ or rays or sound particles as field descriptors.

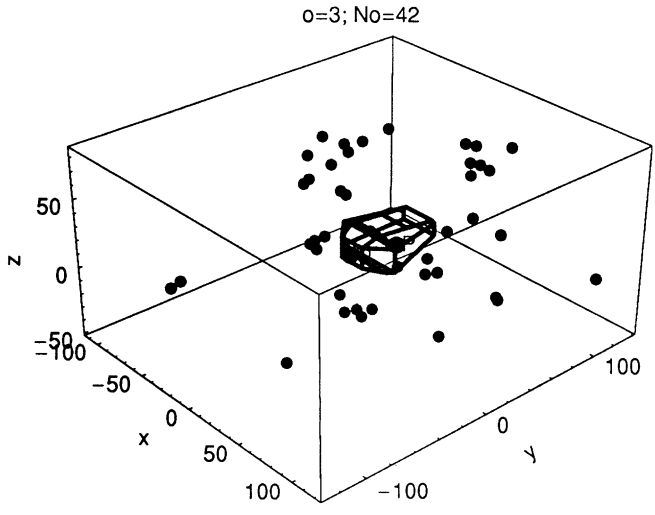

Figure 14. Effective mirror sources of order $o = 3$,with all interrupt criteria.Number of MS: 42.

TABLE 1

Numbers of MS *in several orders o for different interrupt criteria applied*

o	Back-reflection	Inside q and wall	Efficiency
1	19	19	10
2	342	97	25
3	6 256	261	42
4	110 808	478	69
5	1 994 544	755	99
6	35 901 792	1 059	141

TABLE 2

Minimum and maximum reductions in the level of field contributions in the order o by the source factor ΠR*, the distance ratio* $dist(Q,P)/dist(q,P)$*, and their product*

o	$\lvert\Pi R\rvert$		$dist(Q,P)/dist(q,P)$		$\Pi\lvert R\rvert dist(Q,P)/dist(q,P)$	
	min	max	min	max	min	max
1	7·34	0·566	4·69	0·122	7·46	0·948
2	21·05	1·32	10·23	0·331	25·57	4·36
3	22·61	1·69	14·2	4·36	32·29	6·93
4	22·96	3·06	15·91	4·86	36·02	8·89
5	36·21	3·58	18·86	7·34	49·29	12·86
6	37·72	4·19	19·01	8·98	52·91	14·53

14. THE MS-METHOD IN ROOMS WITH CONVEX CORNERS

As was shown above, the original MS-method fails for the description of the sound field around convex corners (we shall solve this problem below). But one can apply the

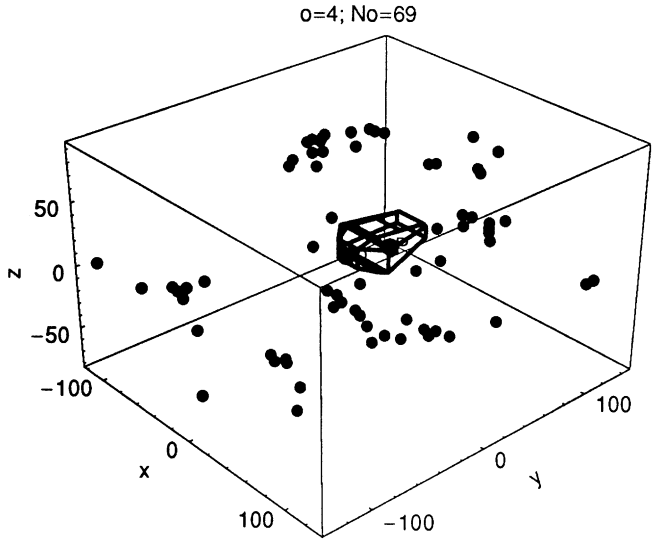

Figure 15. Effective mirror sources of order $o = 4$, with all interrupt criteria. Number of MS: 69.

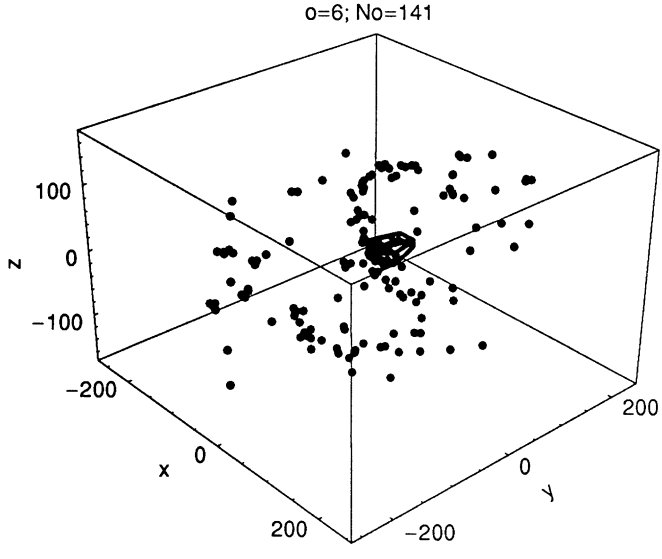

Figure 16. Effective mirror sources of order $o = 6$, with all interrupt criteria. Number of MS: 141.

traditional form of the MS-method in such rooms, if one supposes that the scattered sound field in the shadow zone behind a convex corner can be neglected in comparison with the contributions of mirror sources which radiate into the shadow zone without scattering at the convex corner.

Evidently, there are two aspects of this supposition. For explanation, suppose the model room of the previous section (which has only concave corners) is augmented by an orchestra pit below the stage with a balustrade between the orchestra pit and the auditorium (as usual). In the first case, let the source be on the stage (as in the previous section); then the

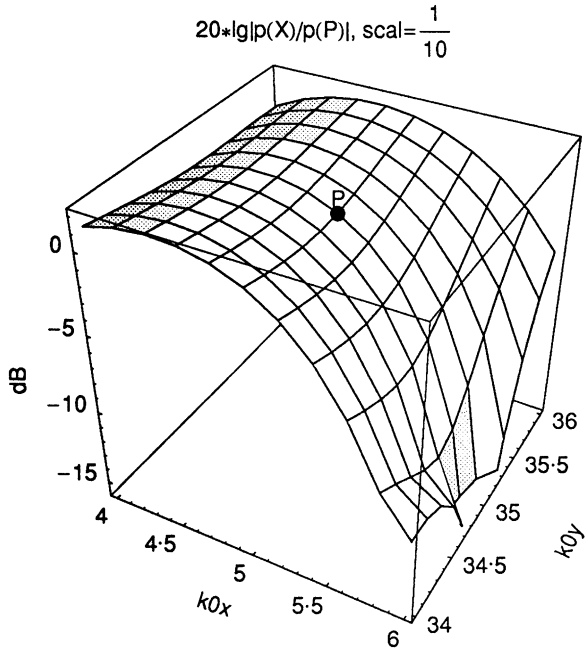

Figure 17. Profile of the sound pressure level around P, for a low frequency.

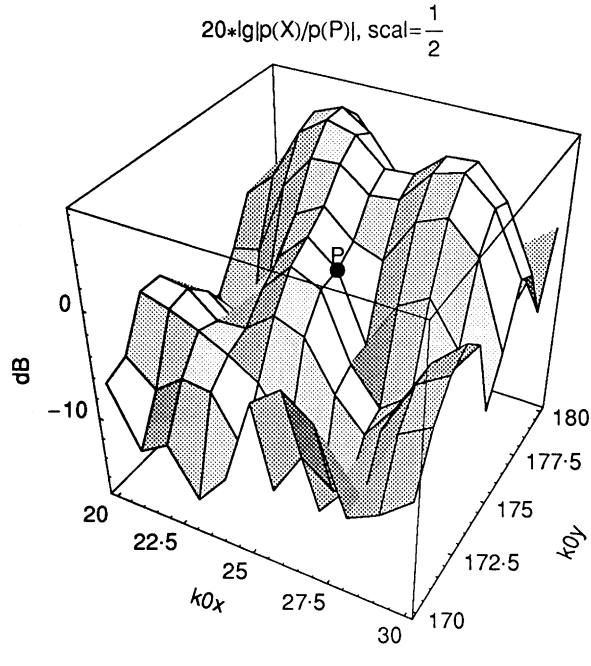

Figure 18. Profile of the sound pressure level around P, for a higher frequency.

orchestra pit is a coupled space which, most probably, does not influence very much the sound field in the receiver point P. In the second case, let the source be in the orchestra pit (a not unusual situation in opera houses ...). The interaction of the source with the room for

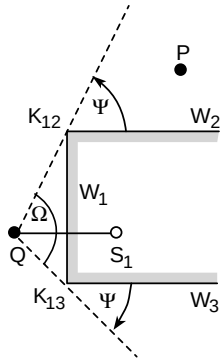

Figure 19. Illustration of shading by convex corners.

a significant part of transmission goes via a scattering either at the corner of the balustrade or at the corners between the stage and the orchestra pit. It should be clearly stated that this situation cannot be treated with sufficient precision with the method of this section, which is based on neglecting the scattering at convex corners. However, the traditional MS-method with convex corners will be described below just for this situation, as an example, because it clearly demonstrates the peculiarities of convex corners.

The mentioned supposition introduces the concept of "shading" into the MS-method. We consider the aspects of shading, and anticipate that a distinction must be made between the cases that the source q was created at the convex corner or not. As an example for sources q not created at the convex corner, we take the original source Q in the sketches below.

It is an important statement that a convex corner can be treated in the computations like a concave corner, if the source q "sees" both flanks of the corner (from inside), because then no shadow is created. This condition is easily checked by "q inside both flanks". Figure 19 illustrates the case of shading.

W_1 is a wall ending on both sides in convex corners; thus, Q has two shadow angles ψ with W. If P is in one of the shadow angles, Q is ineffective. The two shadow angles ψ cover a sub-range of the shade angle Ω which Q spans with W. P will be shaded relative to Q if it is inside Ω. Q creates at the shown walls only one legal daughter source S_1. Because it is outside all walls, it will not create further daughter sources.

If the source in Figure 19 is not Q but an MS q_m created at a wall W_m (not shown in Figure 19), the source angle Ω shown in Figure 19 should not be confused with the field angle Φ_m of q_m (which is subtended by the mother wall W_m and having q_m in the apex).

Figure 20 shows a possible situation at a strongly convex corner, in which the legal daughter source S_1 of Q lies inside the room.

The relations concerning Q in Figure 20 are similar to those in Figure 19 (Q is ineffective if the field point is in P'). If we consider the mirror source q, it does not produce a daughter source at W_2 although it is inside that wall. Now Φ_q is the field angle of q as defined and used in previous sections. The prescription that q shall not produce a daughter source at W_2 is covered, when we expand the condition for walls W at which a source q can produce a daughter source (W is inside Φ_q) by the additional requirement, that W is inside the mother wall (here W_1) of q. With that expanded rule, q can legally produce a daughter source at W_3.

The convex corner of Figure 20 is treated like a concave corner, if the source is in the range indicated with "no shadow". This "no shadow" range gets larger for "mildly convex" corners. Thus, the sound field evaluated in a room having only mildly convex corners will

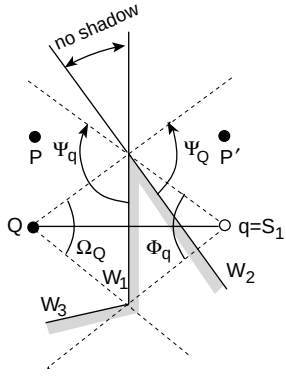

Figure 20. Shading of a mirror source q by convex corners.

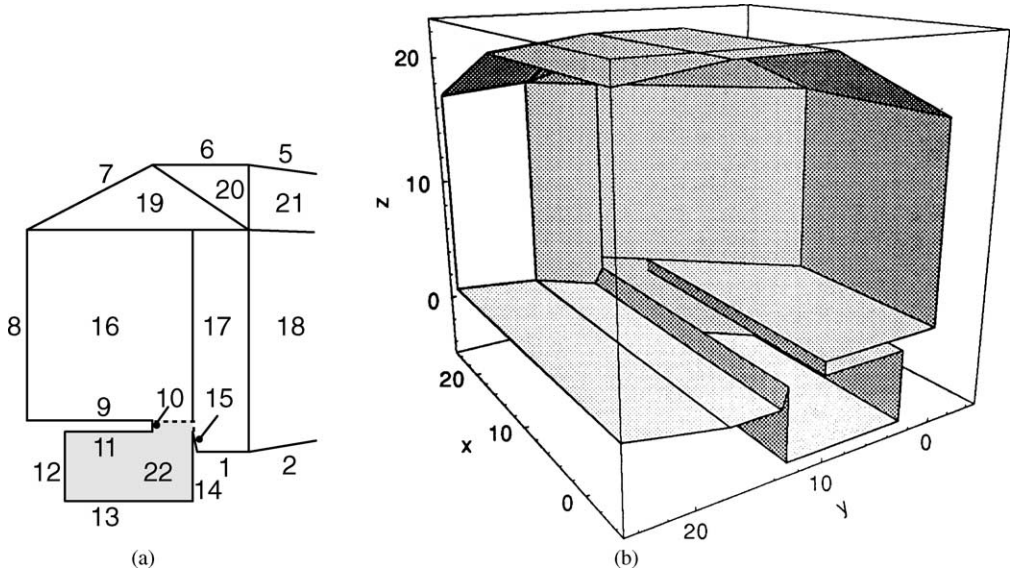

Figure 21 (a) Concept of "excluded walls" in rooms with convex corners. (b) 3-D view from inside to the stage and the orchestra pit of (a).

not be much different from the field in a similar room with only concave corners (as would be expected).

A further category of interrupts of MS-production is illustrated with a vertical section through a stage with an orchestra pit below it (see Figures 21(a, b), which are taken from the model room of the next section).

The walls (14,15) in Figure 21(a) form the balustrade with a convex corner. The wall couples (9,10), (10,11), (14,15) form convex corners. The walls (1,6), (6,9), (6,13), (8,14), (10,14), (11,13), (12,14) are parallel to each other in the usual sense, that they include a part of the room between them (mathematically they are anti-parallel, i.e., their normal vectors have opposite directions).

One must distinguish between (mathematically) parallel walls, which have parallel normal vectors, and anti-parallel walls, with parallel normal vectors, but of opposite directions. Coplanar parallel walls may appear also in concave rooms, where they are

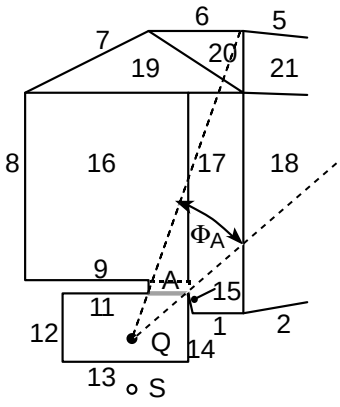

Figure 22. Shading by apertures.

treated correctly by the criterion that a mirror wall must be inside the field angle cone of the mother source. In rooms with convex corners, parallel walls may have an offset relative to each other (such as (1,9), (1,13), (6,11), (8,10), (8,12), (9,13), (10,12), (10,15) in Figure 21(a)). Because scattering into the shadow zone of a convex corner is excluded by supposition, the sound field in front of one wall of such couples does not influence the boundary condition at the other wall. We shall speak of "excluded" walls, or of "exclusive" couples, to indicate that an MS created at one wall of the couple cannot produce a daughter MS at the other wall. Some of the excluded walls in the above example would be "caught" by the criterion that a mother source must be inside a mirror wall and that the mirror wall must be inside the field angle cone of the mother source on the interior side of the mother wall. But the couple (8,10), for example, might escape such tests.

The computationally most complicated modification of the MS-method in rooms with convex corners comes from the problem of "visibility" (of the field point P or of possible mirror walls) in such rooms, especially if they have more than just one convex corner. The problem is illustrated in Figure 22, which is a repetition of Figure 21(a), but now with the source Q and one of its mirror sources S indicated.

The source Q (and similarly S) "sees" the point P or a mirror wall only if they are inside the angle Φ_A, which is formed by a polygonal pyramid with Q in the apex and subtended by the "aperture area" A, which, in the shown situation, spans between the convex corners of the top of the balustrade and the lower corner of the stage ramp (grey line in the sketch). In most cases, it will be necessary to determine the edges of the aperture A "manually". One can attribute to A an interior side and an exterior side by the sequence of its edges (for example, the normal unit vector of A shows in the upward direction of Figure 22). The original source Q on one side of A gives a field contribution in P on the other side of A (i.e., is effective) only if P is inside Φ_A. Similarly, Q will create a mirror source with a wall on the other side of A only if the wall is inside Φ_A. The same statements hold for mirror sources S created at walls (e.g., 11, 12, 13, 14) on one side of A. These rules hold also inversely (i.e., in Figure 22 if Q is above A and P below, or for mirror sources created at walls above A and interactions with walls below A). The position of A depends on the position of the source q (e.g., for the MS produced by Q at wall 14, one corner of A is the upper corner of the stage head). It may be doubted if such "dynamical" determination of A and re-grouping of walls in subgroups "above" and "below" A does pay, on the background of the rather coarse approximation which we describe here.

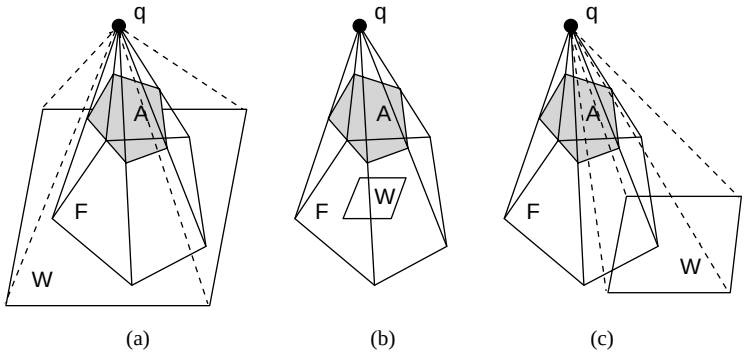

Figure 23. Cases of visibility of a wall W through an aperture A.

The "inside check" for P inside the *cone*(q, A) is simple; see section 11. In concave rooms, we have similarly tested if a mirror wall is inside the field angle Φ of a source by checking whether the wall centre is inside Φ. This kind of check for the visibility of a wall W using its centre C for the check would be too rough; important sound paths from one sub-space (e.g., the orchestra pit) to the other sub-space (e.g., the stage or the auditorium) could be missed with that kind of test.

The source q and the aperture A produce a "bright patch" F in the plane of an opposite wall W (F is the polygon formed in the plane of W by the intersection points X_i of the side corners of the cone(q, A) with the plane of W; they can be evaluated). Three cases of visibility should be distinguished; they are shown in Figures 23(a–c).

One could describe the condition of visibility by the requirement that at least one edge of F is within W or at least one edge of W is within F. The implementation of this test would need the evaluation of the intersection points X_i and the test if a "point is within a polygon" (which should not be confused with a "point is inside the polygon plane"). One can avoid these (computer-intensive) sub-tasks by using the *cone*(q, W). Then the visibility check reduces to the tests "at least one edge of A inside the *cone*(q, W)" or "at least one edge of W inside the cone(q, A)".

The MS-method in rooms with convex corners (in the supposed approximation which neglects corner scattering) has the same aim as in concave rooms, namely to find source lists $\{q, w, dist(q,P), \Pi R, flag\}$ for legal sources q. As in section 12 the frame program operates in three nested loops over the order o, the counting index s of the sources in the order o–1, the counting index w of the walls. Because of the many decisions which must be made by the frame program, anyhow, it is advisable to write a sub-routine for the mirror source evaluation, which is applicable for flanks of concave and convex corners, i.e., which internally only makes interrupt checks related to $\Pi|R|$ and to *dist*(q,P) and efficiency tests for the new MS, whereas the frame program performs all interrupt tests. One can summarize the modifications of the MS-method in rooms with convex corners as follows.

(1) Find the lists of wall couples forming convex corners and of exclusive couples.
(2) Determine the aperture A (if any).
(3) An efficiency check must be performed already for the order $o = 0$, i.e., for $q = Q$. (Q is ineffective, if P is on the other side of A, but not in Φ_A of Q; or, for a single convex corner when A is not defined, if P is in the shade angle Ω_Q (a pyramid with Q in the apex and subtended by a wall W which is a flank of the convex corner).) Therefore, determine *tab*(0) in the frame program.

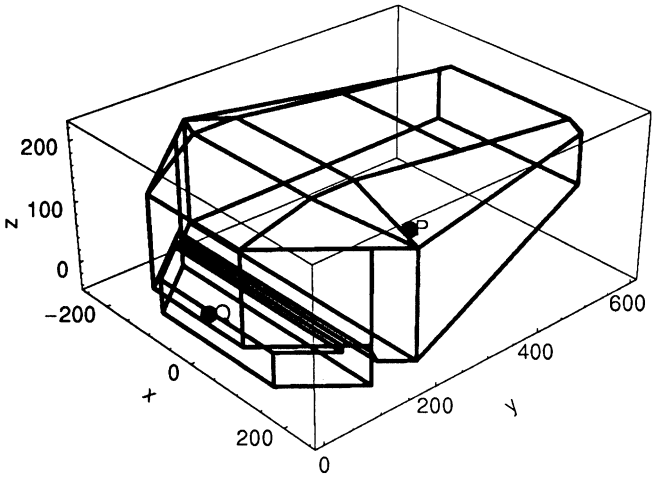

Figure 24. 3-D wire plot of the room, showing the positions of the source Q and of the field point P.

(4) The source lists of the order $o = 1$ (i.e., with Q as mother source) must also be determined separately in the frame program (because Q has no mother wall).
(5) For orders $o > 1$, the frame program in its innermost loop over the wall indices w has to check the interrupt conditions: $w = w_m$, the index of the mother wall; the mother source q_m outside the wall with $W(w)$; $\{w, w_m\}$ or $\{w_m, w\}$ belong to the list of excluded couples; for walls w, w_m on the same side of A, if the centre of the wall w is outside the $cone(q_m, W(w_m))$; for walls w, w_m on different sides of A, if $W(w)$ is not visible for q_m through A.
(6) If none of the tests in (5) is positive, the frame program calls a subroutine for the evaluation of the source list of a new mirror source.

The subroutine causes an interrupt (skip of w), if $\Pi|R| <$ limit or $dist(q, P) > d_{max}$. It further makes the efficiency tests. These efficiency checks should be clear from the explanations given above.

As compared with the scheme of computation in rooms with only concave corners, the MS-method in rooms with convex corners has much more checks to be performed; consequently, the number of effective mirror sources will be smaller than in a concave room with the same number of walls.

15. A MODEL ROOM WITH CONVEX CORNERS

The model room of this section widely corresponds to the model room in section 13 , but an orchestra pit is added below the stage (the cut drawings and the data of the room are contained in Appendix B). Figures 21(a, b) show parts of the room. *A* 3-D wire-plot of the walls (unscaled) is contained in Figure 24, and 3-D view from outside is shown in Figure 25 (scaled with the factor 1/10 as in the subsequent diagrams with mirror sources). The original source Q is placed in the orchestra pit; the receiving point P has its former position. The number of walls of the room is $n_w = 29$. There are three important convex corners: the upper corner of the balustrade at the orchestra pit, and the upper and lower corners of the head of the stage floor.

Table 3 gives the numbers of legal and effective mirror sources in the orders $o = 1, 2, \ldots, o_{max} = 6$.

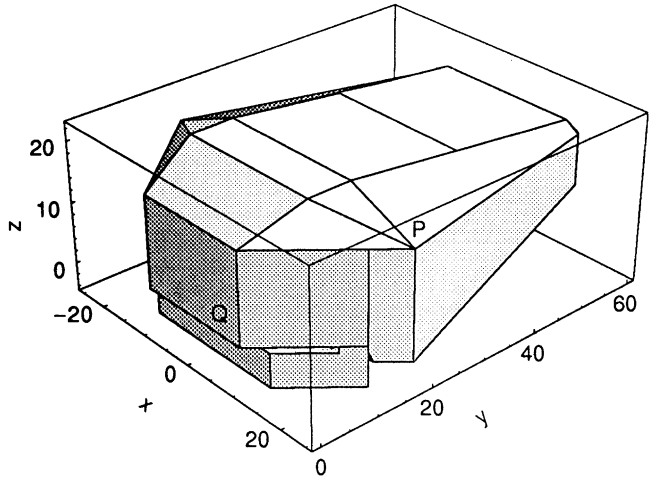

Figure 25. 3-D view of the room of Figure 24 from outside, with scaled co-ordinates.

TABLE 3

Number of legal and effective MS in the orders $o = 1, 2, \ldots, 6$

Type	$o = 1$	$o = 2$	$o = 3$	$o = 4$	$o = 5$	$o = 6$
Legal	24	109	286	637	1 306	2 467
Effective	0	19	44	96	186	272

All MS of the order $o = 1$ are ineffective, like the original source Q. The total number of effective sources is 617 up to $o = 6$; the predicted number in [4] would be (with $n_w = 29$)

$$1 + \sum_{o=1}^{6} n_w(n_w - 1)^{(o-1)} = 517\,585\,882.$$

Figures 26–29 show legal and effective MS in 3-D plots for some orders o (legal first, then effective, except for $o = 1$ where no effective MS exists).

Table 4 gives the lowest values for the source factor $\Pi|R|$ (in dB) and the lowest and highest values of the product $\Pi|R|dist(Q,P)/dist(q/P)$ (in dB) within the orders.

The table shows that, when using the product $\Pi|R|\,dist(Q,P)/dist(q/P)$ as interrupt criterion, some MS in the orders $o = 5, 6$ could be dropped, but the last row shows that the order $o_{max} = 6$ may not be high enough.

Again, we plot the sound pressure level profile around P (see the explanation to Figures 17 and 18 for the assumptions made) and refer the level to the sound pressure which the free source Q would produce in P. Figure 30 is for a higher frequency: $20|g|p(X)/pQ(P)|$, with a scale factor scal $= \frac{1}{2}$.

The contributions of the higher order MS (the orders $o = 0, 1$ are missing) lift the sound pressure level in the room significantly over the level in free space.

16. ADVANTAGES AND DISADVANTAGES OF THE TRADITIONAL MS-METHOD

Up to now we have described the fundamentals and application of what we call the "traditional MS-method". With this section the modification of that method will be

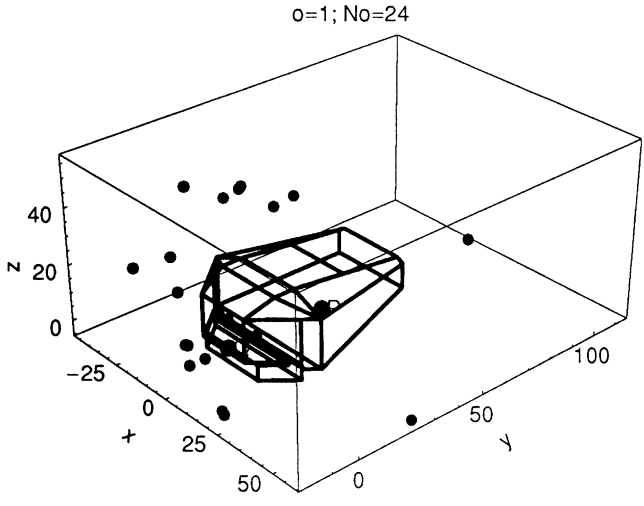

Figure 26. Legal MS for $o = 1$.

prepared. But the previous sections should not be misunderstood to be just an introduction (which as such surely would be too long …). It is a subject in itself to free the MS-method of its negative image as being inapplicable in realistic tasks, and some of the problems appearing below can only be understood with a detailed knowledge of the traditional MS-method.

This aspect can be up-valued by recalling the well-known problems in the standardized measurement of the sound absorption coefficient α_{dif} for "diffuse" sound incidence in a reverberant room; the results of measurements with the same test absorbers in different rooms by experience differ by large factors. Reverberant rooms are simple, at least if there are no "diffusers" in the room; the room is concave with typically 6–10 constructional walls, plus one "wall" for the test object. Diffusers in the shape of plane panels distributed over the volume could also be introduced in the MS-method; diffusers in the shape of wall bosses are treated with the MS-method for rooms with convex walls. The MS-method in its described implementation returns the (complex !) sound pressure distribution at the absorber surface, and with an easy modification also the normal particle velocity. Thus, the absorbed sound power can be evaluated. Two comments may be appropriate in this context. First, one cannot sum up the contributions of the individual sources to the absorbed power; this would be possible only if the sound waves from different sources would be incoherent to each other. But all sources are "driven" by the same signal generator. Therefore, one must determine the absorbed sound power as mentioned above. Second, the traditional MS-method cannot explain the so-called "border effect" of finite-size absorber patches. The border lines of the test absorber (even when the absorber is flush with the floor) are wall corners at the limit to convex corners. Edge scattering within the MS-method needs the modification of that method which will be described below. But the MS-method could be used to investigate the roles of the room shape and of the source, receiver, absorber positions on the absorption coefficient.

The advantages of the traditional MS-method are its analytical and, to some degree, its algorithmic simplicity. There are some disadvantages on the other hand.

The first of them may be considered as a matter of taste. The MS-method resembles a trial-and-error method by its many checks and rejections of potential mirror sources. It

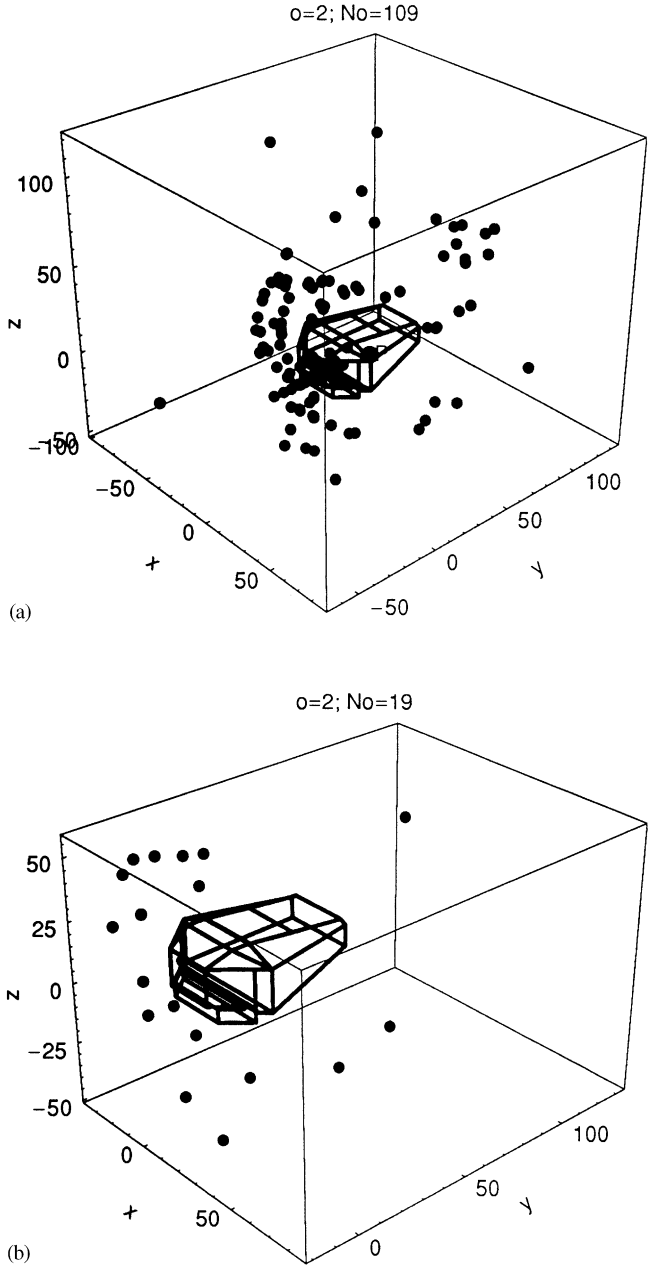

Figure 27. (a) Legal MS for $o = 2$. (b) Effective MS for $o = 2$.

would be an advantage to introduce "larger units" of sources which can be analytically determined.

The second disadvantage lies in the fact that the MS-method can differentiate between more or less important mirror sources only at the end of the procedure when the effective MS are constructed. The traditional MS-method proceeds with the order o of reflection, and for every order checks each wall for a possible effective daughter source. If one computes up to an upper limit o_{max}, at some corners (with not very small wedge angle Θ)

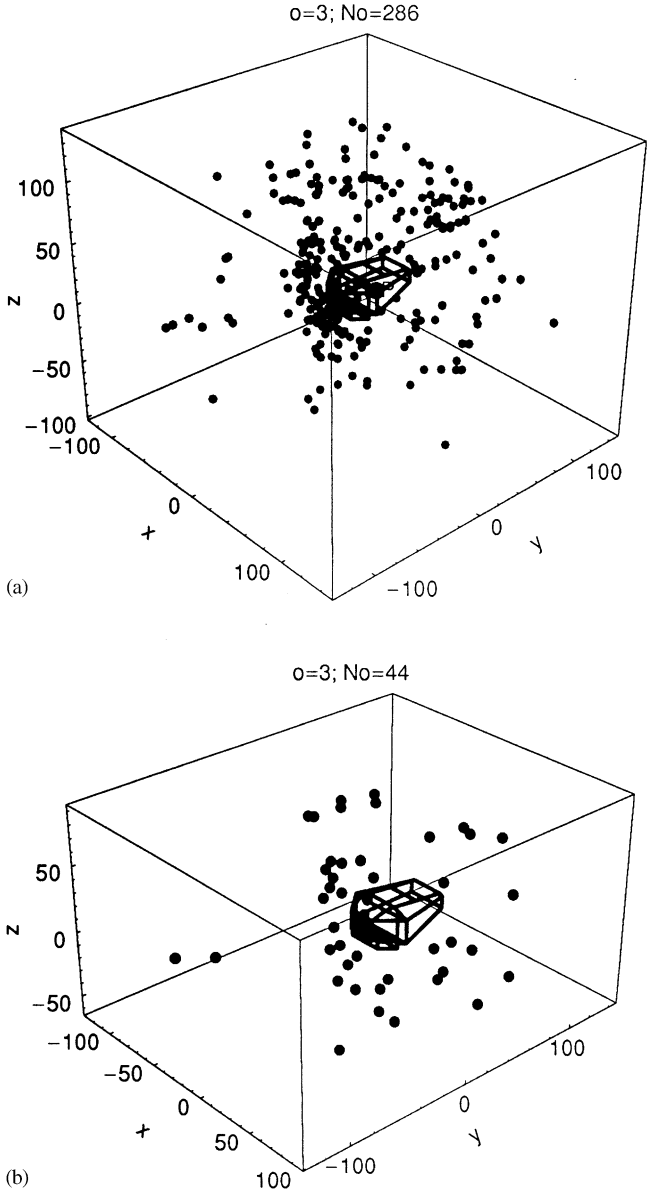

Figure 28. (a) Legal MS for $o = 3$. (b) Effective MS for $o = 3$.

unnecessarily many candidates for a legal MS are tested, while for other wall couples (especially anti-parallel walls) possibly important mirror sources are missed by the stop at o_{max}. The basic idea of a modification lies in the question as to whether it is possible to group the mirror sources differently, so that the members of a group can be determined more easily, and that the groups contain the more important mirror sources. This problem will be the subject of section 18.

The third fundamental disadvantage was mentioned already; it is the inability of the traditional MS-method to scope with scattering at convex corners. This problem will be solved within the frame of a modified MS-method in a later section. Before that we describe a kind of reciprocity which is useful in many instances.

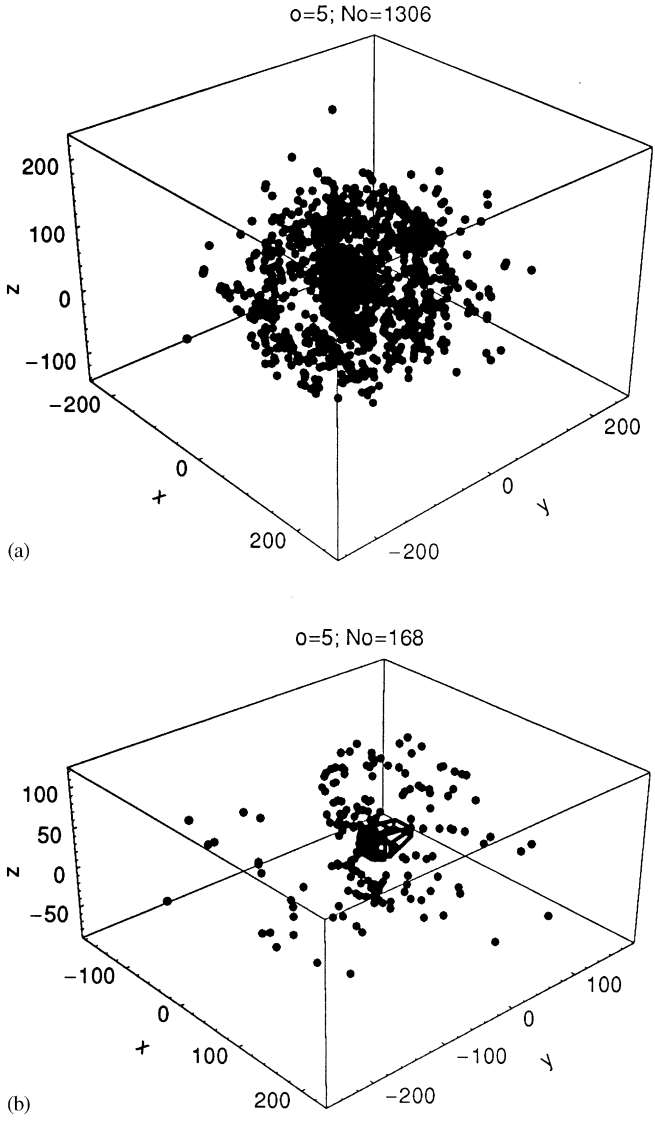

Figure 29. (a) Legal MS for $o = 5$. (b) Effective MS for $o = 5$.

TABLE 4

Level changes of contributions in the order o

Level change by	$o = 2$	$o = 3$	$o = 4$	$o = 5$	$o = 6$
$\Pi\|R\|$, min	−4·38	−19·02	−23·81	−31·05	−34·59
$\Pi\|R\|dist(Q,P)/dist(q/P)$, min	−12·37	−25·17	−30·88	−37·89	−47·13
$\Pi\|R\|dist(Q,P)/dist(q/P)$, max	− 3·37	− 4·22	− 3·38	− 4·25	− 6·98

17. A KIND OF RECIPROCITY IN THE MS-METHOD

Evidently, a source q, generated by a mother source q_m at a mirror wall W, will produce in a receiver point P the same contribution $p(P)$, which the mother source q_m would produce in

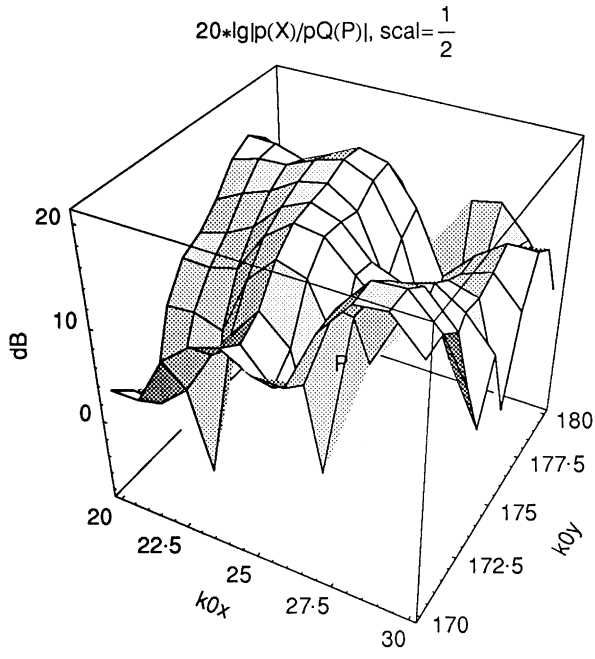

Figure 30. Sound pressure level profile around the point P of immission.

the point P', which is the mirror-reflected point to P with respect to W, after multiplication with $R(\theta_s)$.

So one could set up a "mirror-receiver-method" instead of a "mirror-source-method" by remoulding all interrupt and efficiency rules. Numerically, there would be no advantage as compared with the MS-method for isotropic sources Q. If, however, the original source Q has a directivity $D(\vartheta, \varphi)$, the mirror-receiver-method avoids the mirror reflection of the directivity.

In connection with isotropic sources Q, the mentioned rule of reciprocity may facilitate some argumentation and solution of geometrical sub-tasks. One case of that kind is the model for "switch-off" of a steady sound field in the context with the reverberation time in a later section.

18. COLLECTION OF THE MS FOR WALL COUPLES

This section prepares all following modifications of the MS-method. It is based on the easily proven fact that the original source Q and all mirror sources which are created by it and its daughter sources at a couple of walls are arranged on a circle ("MS-circle") which contains Q and has its centre in the foot point Z of Q (normal projection) on the intersection line of the walls. So we are dealing with flanks of a corner; the corner is "real" if the flanks are intercepting, or the corner is "virtual" if other walls are arranged between the flanks. The corners (either real or virtual) may be concave or convex, but for the moment we consider only concave corners. A special case are anti-parallel flanks; their (necessarily virtual) corner line is at infinity; the MS-circle becomes a straight line through Q normal to the flanks.

Because the plane containing the MS-circle is normal to the corner line, we are dealing with a 2-D problem (a further advantage of grouping the mirror sources in groups of MS at

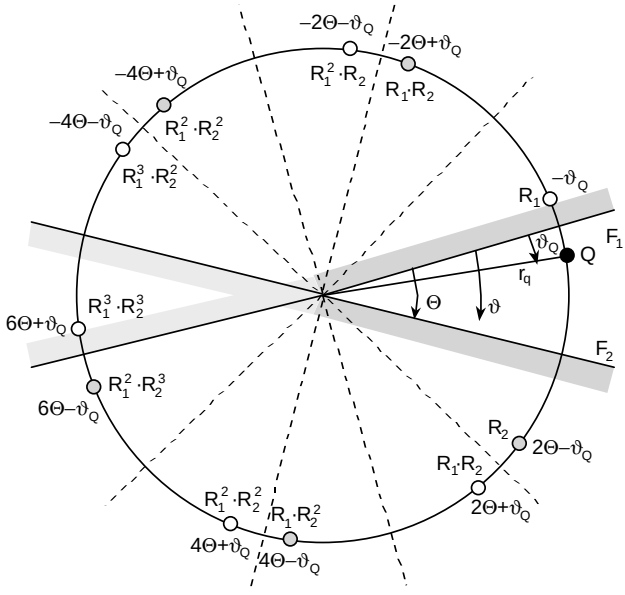

Figure 31. Mirror sources produced by a couple of flanks of a concave corner.

wall couples). This is suggesting to discuss the problem in a cylindrical co-ordinate system r, ϑ centred in Z and with the reference for ϑ preferably (but not necessarily) in one of the flanks. The radius of the MS-circle will be symbolized by r_q and the angle for Q with ϑ_Q, whereas the angle for an MS will be called ϑ_q. The co-ordinates of the field point P are r, ϑ, ζ, where ζ is the co-ordinate along the corner line, with $\zeta = 0$ for Z, Q, q. The transformation between the Cartesian co-ordinates x, y, z of the room and the cylindrical co-ordinates r, ϑ, ζ of a flank couple is described in Appendix A.

Figure 31 shows a couple of flanks F_1, F_2, the original source Q and its mirror sources on the MS-circle.

Figure 31 shows all legal MS (the number is rather high because the wedge angle Θ is small, by intention). The source at $6\Theta - \vartheta_Q$ formally could be mirror-reflected once again, but then the daughter source would coincide with the MS at $6\Theta + \vartheta_Q$ with the same source factor, so by the coincidence criterion this daughter source would be illegal. The indicated source factors as products of R_1, R_2 should not be interpreted too literally; the factors in the powers of these reflection factors may contain different angles θ_s.

The MS on both circular arcs $\vartheta < 0$ and $\vartheta > 0$ have source angles ϑ_q within the limits

$$\Theta - \pi \overset{!}{<} \vartheta_q = -2s\Theta \pm \vartheta_Q \overset{!}{<} -\pi; \quad s = 0, \pm 1, \pm 2, \ldots \cdot \tag{12}$$

The mirror sources lastly were generated at F_1 for $s < 0$; they would produce a daughter source on the lower circular arc with F_2 if that is not excluded by the inside criterion, and *vice versa* for $s > 0$.

Range (12) leads to limits for the counter s:

On the upper arc $\vartheta < 0$:

$$0 \geqslant s' > \frac{1}{2}\left(\frac{\pi \pm \vartheta_Q}{\Theta} - 1\right), \tag{13a}$$

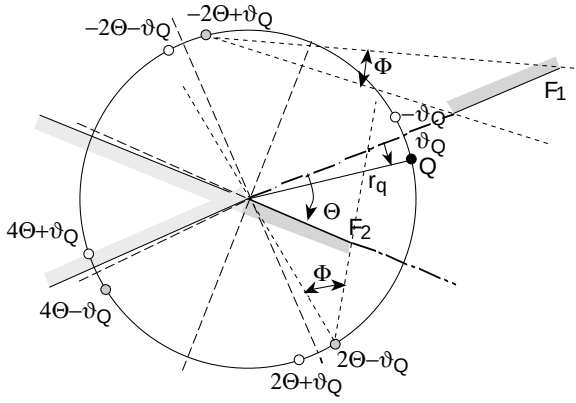

Figure 32. Some special cases of visibility of walls of a wall couple.

on the lower arc $\vartheta > 0$:

$$0 < s < \frac{\pi \mp \vartheta_Q}{2\Theta}. \tag{13b}$$

The sum of the counters is restricted to

$$s + |s'| < \frac{\pi}{\Theta} - \frac{1}{2}. \tag{14}$$

Thus, the number of MS decreases with increasing Θ. If $\Theta = \pi$, only the MS with $n = 0$ is legal. Evidently, anti-parallel wall couples with $\Theta = 0$ are a special case, which will be discussed separately below.

One needs, for the implementation of the MS-method, the distance between q and P, and the angle θ_s formed by the connection line (q, P) with the normal of the flank. The distance between q and P is

$$dist(q,P) = \sqrt{\zeta^2 + r^2 + r_q^2 - 2r\, r_q \cos(\vartheta - \vartheta_q)}. \tag{15}$$

The cosine $\cos(\theta_s)$ is easily evaluated in the Cartesian co-ordinates, but this would need a co-ordinate transformation for all q. It is better to use the cylindrical co-ordinates of P and to evaluate $\cos(\theta_s)$ in that system. This task will be described in Appendix A.

The advantage of the described grouping is evident: one need not find the MS by trial and error, but they are evaluated in a straightforward method, if the flanks have a real corner (where exclusion by interrupt and efficiency checks play no role). Further, one is sure to have covered all MS for a wall couple. The question is, whether one possibly introduces too many MS if the flanks have a virtual corner. See Figure 32 for that question.

Figure 32 illustrates the case when both flanks F_1, F_2 are on different sides of the MS-circle. The MS lastly generated at the outer flank F_1 never "see" the other flank F_2, and the MS lastly generated at F_2 may have F_1 in their field angles Φ, or not.

Conclusion: For flanks with virtual corner the tests "F_i in *cone*(q, F_j)" must be made as interrupt checks; however, there are easy to describe situations in which the number of these tests can be reduced. Similarly, the efficiency checks, which ask whether the projection P' of P into the plane of the MS-circle is in the angle Φ, not only are simplified because these checks now are 2-D checks, but conditions which make such checks unnecessary can be

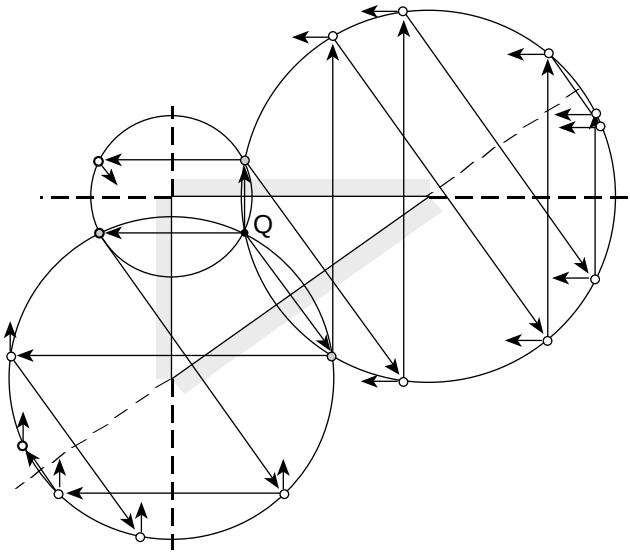

Figure 33. Mirror sources of a triangular room, collected on MS-circles.

formulated. The tests "F_i in $cone(q, F_j)$" remain 3-D if the flanking walls have a virtual corner and no intersection with the MS-circle.

The set of mirror sources so constructed (we call it "corner set") is "complete"; the sum of their contributions to $p(P)$ is a precise field description (with the principal limitation of precision of the MS-method), if only the flanking walls of the couple would exist. We call their sound field the "corner field". If P lies in between the flanks, it is plausible that this field represents the most important contributions of wall reflections in P. Further contributions come from other wall couples and their corner sets if P is in the field angle Ψ of those couples (see below), and by reflections of the corner set of a wall couple at other walls within Ψ. The combination of corner sets to the ensemble of mirror sources of a room ("room set"), or the completion of corner fields to the room field, will be discussed in the next section.

19. COMBINATION OF CORNER FIELDS TO THE ROOM FIELD

The room may have N walls W. First find solutions for corners with couples W_i, W_j, $i, j = 1, 2, \ldots, N$; $i \neq j$; that is $N(N-1)/2$ combinations (the combination W_i, W_j is equivalent to the combination W_j, W_i).

For the preparation of the next idea, we take the most simple examples of 2-D triangular and rectangular rooms. If the room had a 3-D tetrahedral shape, for example, the main difference would be the inclination of the MS-circles relative to each other (it is simpler to compute the situation in a 3-D room than to present it in a graph). Below, MS from the traditional MS-method are drawn with interrupts according to the inside criterion. This will be sufficient for the ensuing argumentation.

The MS created at a wall couple are collected on circles. In Figure 33 for the triangular room three of the MS appear twice (they are marked with a grey fill); they are the MS of first order. In Figure 34 for the rectangular room the vertical and horizontal lines through Q represent the limit cases of MS-circles for the two anti-parallel wall couples. In this figure, the four MS of first order appear three times. Long arrows in the figures indicate where the

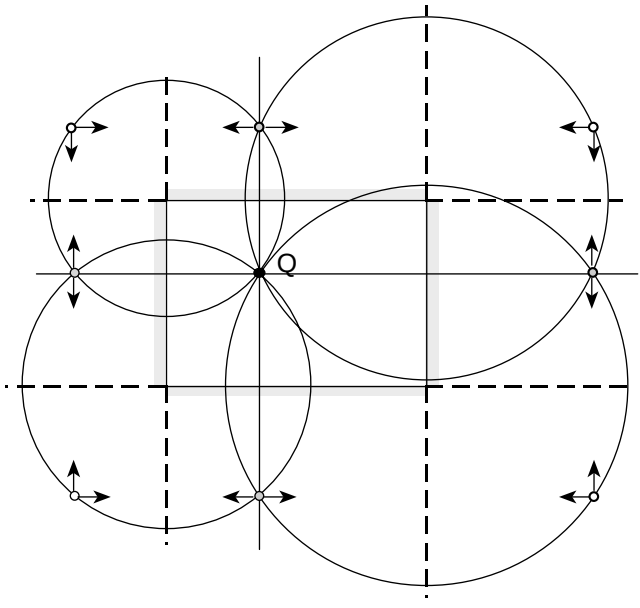

Figure 34. Mirror sources of a rectangular room, collected on MS-circles.

MS come from. Short arrows indicate at which wall the shown MS should be mirror-reflected in the next step of MS-production. These arrows point to opposite walls.

In Figure 33, the original source Q appears three times in the corner sets, and the MS of first order appear two times.

In Figure 34, the original source Q appears four times in the corner sets, and the MS of first order appear three times.

The fact that the MS of a wall couple are placed on a circle around the wall corner with Q on it, and that the continuation of MS-production would imply opposite walls, suggest collecting the MS of a wall couple into one equivalent source for the corner field. The following rules are evident from the above discussion: exclude the original source from the field of that source; exclude the MS of first order from that source; define the field angle Ψ of the source.

We shall see in the next section that the new source is placed in the foot point Z of Q on the corner line. The field angle Ψ therefore is the angle defined by the two flanks and the corner line as apex line.

20. COLLECTION OF THE MS OF A WALL COUPLE IN A CORNER SOURCE

Up to now the graphs in the previous section indicate nothing more than an involved, but legitimate procedure of MS-production. The main difference to the previous sections is the kind of grouping of the MS.

Now we take advantage of the fact that the MS of a wall couple are arranged on a circle around the intersection line (normal to that line) which also contains Q. The intersection line between the walls must not really exist (see the rectangular room). But first we exclude the special case of parallel walls (it is specially treated below). The radius of the MS-circle is designated as r_q.

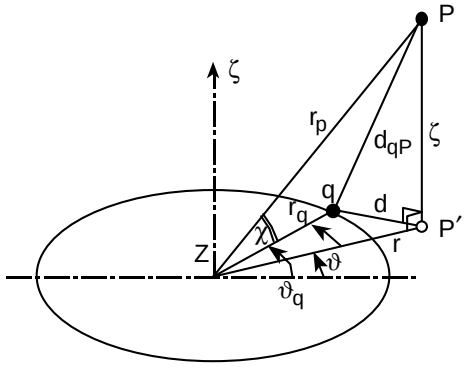

Figure 35. Geometrical quantities in the evaluation of the field of sources in a corner set.

The field of an MS in P is described by

$$p_q(P) = \Pi R h_0^{(2)}(k_0 d_{qP}) = \frac{\Pi R}{k_0 d_{qP}} [\sin(k_0 d_{qP}) + \mathrm{j}\cos(k_0 d_{qP})]$$

$$= j\Pi R \frac{\mathrm{e}^{-\mathrm{j}k_0 d_{qP}}}{k_0 d_{qP}}, \tag{16}$$

with $d_{q\mathrm{P}} = dist(q,P)$. The addition theorem for spherical Bessel functions (see reference [8, p. 440, equations. (10.1.45), (10.1.46)]) when applied to the above expression leads to

$$h_0^{(2)}(k_0 d_{qP}) = \sum_{n \geqslant 0} (2n+1) P_n\left(\frac{r}{r_p}\cos(\vartheta_q - \vartheta)\right) \begin{Bmatrix} j_n(k_0 r_p)\, h_n^{(2)}(k_0 r_q);\ r_p < r_q \\ j_n(k_0 r_q) h_n^{(2)}(k_0 r_p);\ r_p > r_q \end{Bmatrix}, \tag{17}$$

where $j_n(x)$ are spherical Bessel functions of order n, $h_n^{(2)}(x)$ are spherical Hankel functions of the second kind, $P_n(x)$ are Legendre polynomials, and the geometrical quantities are taken from Figure 35.

The circle in Figure 35 is the MS-circle; q is a source on it with the cylindrical co-ordinates r_q, ϑ_q, $\zeta = 0$; P is the field point with the cylindrical co-ordinates r, ϑ, ζ; P' is the projection of P on the plane of the MS-circle. The following relations exist between the geometrical quantities:

$$d_{qP}^2 = r_q^2 + r_p^2 - 2r_q r_p \cos\chi,$$

$$r_p^2 = r^2 + \zeta^2, \tag{18}$$

$$d_{qP}^2 = d^2 + \zeta^2,$$

$$d^2 = r_q^2 + r^2 - 2r_q r \cos(\vartheta_q - \vartheta), \tag{19}$$

from which

$$\cos\chi = \frac{r}{r_p}\cos(\vartheta_q - \vartheta) \tag{20}$$

follows. The first line in equation (18) was used for the addition theorem.

Summation over the sources on the MS-circle gives, for the field contribution in P of those sources,

$$p(P) = \mathrm{j} \sum_s \Pi_s R(\theta_s) \sum_{n \geqslant 0} (2n+1) P_n\left(\frac{r}{r_p} \cos(\vartheta_{qs} - \vartheta)\right) \begin{Bmatrix} j_n(k_0 r_p)\, h_n^{(2)}(k_0 r_q); & r_p < r_q \\ j_n(k_0 r_q)\, h_n^{(2)}(k_0 r_p); & r_p > r_q \end{Bmatrix}. \quad (21)$$

The summation index s can be taken from equation (12), if all sources should be added. As explained above, it is recommended to avoid the summation over Q and the MS of first order (their field contributions will be added to the field in their traditional forms); and illegal or inefficient sources will also be left out of the summation over s. Equation (21) represents an important group of mirror sources in an explicit formula. The terms represent radially standing waves in r_p if $r_p < r_q$, and outward propagating waves if $r_p > r_q$. The sound field is steady at $r_p = r_q$. The sum satisfies the boundary conditions at the flanks, Sommerfeld's farfield condition, the source condition and the edge condition (which requires that the volume flow through a small cylinder around a corner or a sphere around an edge does not exceed the volume flow through a similar cylinder or sphere, respectively, around the original source Q; the edge condition mostly is used for the selection of permitted radial functions, like Sommerfeld's farfield condition). But equation (21) in general does not satisfy the wave equation, because the factors $\Pi_s(\theta_s)$ in general are neither constant nor do they have the form which is required by the wave equation for angular factors to Bessel functions of the order n. But satisfaction of the wave equation could not be expected with the MS-method as base for equation (21).

This representation however has a numerical problem: the convergence and the precision are critical for $r_p = r_q$, i.e., if the field point lies on the sphere which has the MS-circle as equator circle. Physically, the numerical problem comes from the fact that the sphere surface contains the poles of the sources q. The evaluation of equation (21) at $r_p = r_q$ needs a careful check of the summation limit for n (a detailed discussion of the convergence check can be found in reference [9]). This problem in general does not appear after a mirror-reflection of equation (21) at an opposite wall (see below). One could avoid it by using at or near $r_p = r_q$ the traditional MS-method, but this would need the programming of both methods. An easier method in the case $r_p = r_q$ is the evaluation of equation (21) on both sides of that limit, at some distance, and then to take the mean value.

The fact that a set of spherical Bessel and Hankel functions with integer orders must be evaluated makes no problem; the set can be obtained from two start values of the order by the known recursions of such functions, and also the Legendre polynomials are easily computed. The radial arguments are constant for all sources on the MS-circle and for a fixed immission point P.

Important conclusions can be drawn from equation (21). The components of the sum over n are spherical wave terms, which are centred in the centre Z of the MS-circle on the corner line. Therefore, we say that equation (21) represents the field of a "corner source". It can be introduced into a continued MS-generation like any directional source. The advantages of the corner source are evident. Its position need not be found in a complicated search algorithm; it is explicitly defined by the room geometry and the position of Q. Also its field angle Ψ is immediately given, it is the angle between the flanking walls. The difference to the field angle Φ of a traditional MS is remarkable (Φ is the angle of the cone subtended by the mother wall and the MS in the apex). Efficiency checks (P in Ψ ?) and interrupt checks (an opposite wall in Ψ ?) are much easier to perform.

It is not proven, but plausible, that one can stop the field evaluation after the corner sources of all wall couples have been evaluated and mirror-reflected once at their opposite (visible) walls. All really important field contributions will be obtained with that procedure.

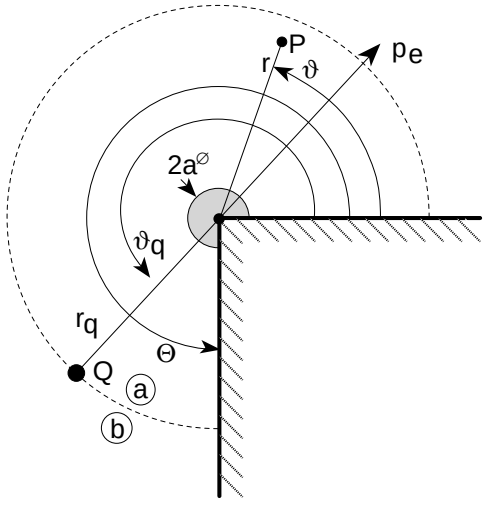

Figure 36. Modal composition of the field around a corner.

The mirror reflection of the corner source is done by a simple modification of equation (21) if one applies the reciprocity of section 17. One need not evaluate the positions of the mirror-reflected sources, but one mirror-reflects P, multiplies the $\Pi R(\theta_s)$ in the sum over s with the new reflection factor, and evaluates equation (21) with the geometrical parameters of the new position of P (which can also be determined directly from the room input data and the position of P). This procedure avoids the reflection of the directivity of the corner source.

21. A NON-HYBRID FORM OF THE CORNER SOURCE

The corner source according to equation (21) may be called a "hybrid" source, because, on the one hand, it is composed of analytical wave terms (in the n-sum), but the trial-and-error procedure of the MS-method is still contained (in a reduced form) in the determination of the summation indices s.

Independent solutions for the sound field of a (point or line) source in the wedge space limited by two flanking walls can be derived which also correspond to a corner source, but now they also obey the wave equation if the walls are hard (or ideally soft), and satisfy the wave equation with a better approximation than the mirror source solution if the flanks are absorbent.

Such solutions are described in reference [9] for corners with hard flanking walls, and in references [10, 11] for corners with absorbent walls. Results of theory shall be repeated below (for completeness, and in 2-D, for simplicity) for corners with hard flanking walls. The theory in reference [9] at the same time includes a cylindrical scatterer sitting on the corner. This case, which may be met with in room acoustics, was mentioned above. It may be of some interest to see how it can be handled.

The basic idea of such solutions is to expand the sound field as sums of "corner modes", which are fundamental solutions of the wave equation and the boundary conditions, and which are orthogonal over the azimuth ϑ within the wedge angle Θ. If one expands the sound field of the original source Q in such modes, their sum automatically satisfies the boundary conditions.

The object, for which the result will be given below, is shown in Figure 36. A corner (not necessarily convex as shown) with hard walls, forming a wedge angle Θ, and a cylindrical

scatterer with radius a is irradiated by a line source Q, parallel to the corner, placed in (r_q, ϑ_q). The total sound field $p(r, \vartheta)$ is composed of azimuthal modes of the corner problem, i.e., elementary solutions which satisfy the boundary conditions at the flanks.

Two radial zones must be distinguished: zone (a) with $a \leqslant r < r_q$, and zone (b) with $r > r_q$.

The fields of both zones can be formulated as zone (a)

$$p_a(r,\vartheta) = \sum_{n \geqslant 0} A_n H^{(2)}_{\eta_n}(kr_q)[H^{(1)}_{\eta_n}(kr) + R_n H^{(2)}_{\eta_n}(kr)] \cos(\eta_n \vartheta), \tag{22}$$

zone (b)

$$p_b(r,\vartheta) = \sum_{n \geqslant 0} A_n [H^{(1)}_{\eta_n}(kr_q) + R_n H^{(2)}_{\eta_n}(kr_q)] H^{(2)}_{\eta_n}(kr) \cos(\eta_n \vartheta). \tag{23}$$

k is the radial component of the wave number, with $k^2 = k_0^2 - k_z^2$, and $k = k_0$ if the axial wave number k_z is zero (no field variation along z). η_n are solutions of the characteristic equation from the boundary conditions (zero normal particle velocity) at the flanks

$$(\eta_n \Theta) \tan(\eta_n \Theta) = 0. \tag{24}$$

Thus $\eta_n = n\pi/\Theta$, $n = 0, 1, 2, \ldots$. (Here again $\Theta = 0$ is a special case). R_n are the modal reflection factors at the surface of the cylinder which is supposed to have a surface admittance G

$$R_n = -\frac{Z_0 G H^{(1)}_{\eta_n}(ka) + j(k/k_0) H'^{(1)}_{\eta_n}(ka)}{Z_0 G H^{(2)}_{\eta_n}(ka) + j(k/k_0) H'^{(2)}_{\eta_n}(ka)} = -\frac{(\eta_n/k_0 a - jZ_0 G) H^{(1)}_{\eta_n}(ka) - (k/k_0) H^{(1)}_{\eta_n+1}(ka)}{(\eta_n/k_0 a - jZ_0 G) H^{(2)}_{\eta_n}(ka) - (k/k_0 H^{(2)}_{\eta_n+1}(ka)}. \tag{25}$$

The mode amplitudes A_n are determined from the source condition which requires that the volume flow of the field through a small cylinder around Q is the same as of the original source Q and which can be formulated as

$$v_{rb}(r_q + 0) - v_{ra}(r_q - 0) \stackrel{!}{=} q\delta(\vartheta - \vartheta_q), \tag{26}$$

where q is the volume flow of Q per unit length. With that quantity q for the characterization of the strength of Q, the free field of Q is

$$p_Q(\rho) = \tfrac{1}{4} Z_0 k_0 \rho q H^{(2)}_0(k\rho), \tag{27}$$

where ρ is the radius measured from Q. With the synthesis of the Dirac delta function $\delta(\vartheta - \vartheta_q)$ with angular modes, one gets

$$A_n = \frac{\pi}{4} k_0 r_q \frac{Z_0 q}{\Theta N_n} \cos(\eta_n \vartheta_q) = \frac{\pi}{\Theta N_n} \frac{p_Q(0)}{H^{(2)}_0(kr_q)} \cos(\eta_n \vartheta_q). \tag{28}$$

There in N_n are mode norms with the values $N_n = 1$ for $n = 0$, and $N_n = 2$ for $n > 0$. $p_Q(0)$ is the value of the source free field at the position of the corner.

The sound field, which is determined with these results, can be split into two parts: one part created by the corner (remaining if no scattering cylinder is present), and one part created by the scattering cylinder, using the factors

$$C_n = \frac{Z_0 G J_{\eta_n}(ka) + j(k/k_0) J'_{\eta_n}(ka)}{Z_0 G H^{(2)}_{\eta_n}(ka) + j(k/k_0) H'^{(2)}_{\eta_n}(ka)},$$

$$C_n \xrightarrow[Z_0 G \to 0]{} \frac{J'_{\eta_n}(ka)}{H'^{(2)}_{\eta_n}(ka)}, \quad C_n \xrightarrow[Z_0 G \to \infty]{} \frac{J_{\eta_n}(ka)}{H^{(2)}_{\eta_n}(ka)}, \quad C_n \xrightarrow[ka \to 0]{} 0, \tag{29}$$

with the results

zone (a)

$$p_a(r,\vartheta) = p_{a,Corner} + p_{a,Cyl}$$
$$= \frac{2\pi}{\Theta}\,\frac{p_Q(0)}{H_0^{(2)}(kr_q)}\sum_{n\geqslant 0}\frac{\cos(\eta_n\vartheta_q)}{N_n}H_{\eta_n}^{(2)}(kr_q)J_{\eta_n}(kr)\cos(\eta_n\vartheta)$$
$$-\frac{2\pi}{\Theta}\,\frac{p_Q(0)}{H_0^{(2)}(kr_q)}\sum_{n\geqslant 0}C_n\frac{\cos(\eta_n\vartheta_q)}{N_n}H_{\eta_n}^{(2)}(kr_q)H_{\eta_n}^{(2)}(kr)\cos(\eta_n\vartheta), \tag{30}$$

zone (b)

$$p_b(r,\vartheta) = p_{b,\,Corner} + p_{b,\,Cyl}$$
$$= \frac{2\pi}{\Theta}\,\frac{p_Q(0)}{H_0^{(2)}(kr_q)}\sum_{n\geqslant 0}\frac{\cos(\eta_n\vartheta_q)}{N_n}J_{\eta_n}(kr_q)H_{\eta_n}^{(2)}(kr)\cos(\eta_n\vartheta),$$
$$-\frac{2\pi}{\Theta}\,\frac{p_Q(0)}{H_0^{(2)}(kr_q)}\sum_{n\geqslant 0}C_n\frac{\cos(\eta_n\vartheta_q)}{N_n}H_{\eta_n}^{(2)}(kr_q)H_{\eta_n}^{(2)}(kr)\cos(\eta_n\vartheta). \tag{31}$$

The splitting of the field into the two zones (a), (b) basically corresponds to the application of the addition theorem for cylindrical functions, used already in section 20; the numerical difficulties mentioned there for $r = r_q$ exist here also. They are avoided if the incident field does not come from a line source, but is a plane wave in the direction ϑ_q. Then zones (a), (b) no longer must be distinguished, and the total field in the wedge is

$$p(r,\vartheta) = p_{Corner} + p_{Cyl}$$
$$= \frac{2\pi}{\Theta}\,p_Q(0)\sum_{n\geqslant 0}\frac{e^{j\eta_n\pi/2}}{N_n}J_{\eta_n}(kr)\cos(\eta_n\vartheta_q)\cos(\eta_n\vartheta)$$
$$-\frac{2\pi}{\Theta}\,p_Q(0)\sum_{n\geqslant 0}C_n\frac{e^{j\eta_n\pi/2}}{N_n}H_{\eta_n}^{(2)}(kr)\cos(\eta_n\vartheta_q)\cos(\eta_n\vartheta). \tag{32}$$

$p_Q(0)$ again is the value of the incident wave at the corner.

Below we shall discuss the special case of parallel walls (as announced above). This would correspond to $\Theta = 0$. This case evidently is singular, as can be seen from equation (24).

If one compares these results with equation (21) (a comparison between the present 2-D task and the above 3-D problem is possible, though not in detail, if one substitutes cylindrical Bessel functions with spherical Bessel functions, and $\cos(\eta_n\vartheta)$ with $P_n(\cos(\eta_n\vartheta))$), one sees that the geometrical sub-tasks in equation (21) (for the determination of r_p, ϑ, ϑ_q) are replaced by the sub-task of the determination of the η_n, which, however, is easy.

Paper [11] constructs corner modes in a wedge with absorbent flanks. These modes satisfy the boundary conditions, but not precisely the wave equation (which recalls the situation with mirror sources in corners with absorbent flanks). The corner modes need the solution of a rather complicated characteristic equation for the angular wave numbers, and the radial functions are hypergeometrical functions (Kummer and Tricomi functions). Most probably the application of such modes in room acoustics would be too complicated.

Paper [10] therefore applies the third principle of superposition (see below) for the construction of an approximate solution. The third principle of superposition expresses the field in a wedge with one ideally reflecting (hard or soft) and one absorbent wall with the solutions of the two problems in which the absorbent wall is first hard ("hard–hard problem" or "hard–soft problem") and then soft ("hard–soft problem" or "soft–soft problem"). The solutions of these sub-problems are either taken directly from above (hard–hard problem) or after some simple modifications.

However, the presentation of the results of that paper here would lead us too far away from the present subject, so the reader is referred to the original papers.

22. A "MIXED" METHOD FOR FIELD EVALUATION IN ROOMS

The fact that the modal synthesis of sound fields in room wedges (formed by two flanking walls) is valid both for concave and convex corners suggests a method for the evaluation of the sound field in a point P if both P and Q are positioned in the range of the same room wedge (especially if P is near the corner line). The modal synthesis delivers precisely the total sound field (i.e., with the contribution of Q included) if the wall couple were alone.

In a realistic room further field contributions in P come from mirror reflections of the corner source at the opposite walls (which again may be evaluated as the field of the corner source in the mirror-reflected point P). Under the mentioned conditions for the position of P one surely can stop the evaluation after one mirror reflection at all visible opposite walls. This mixture of modal synthesis and MS-method may be of interest under the mentioned conditions.

23. LIMIT CASE OF PARALLEL WALLS

Because only anti-parallel walls will be considered here, we shortly speak of "parallel" walls. In principle, the number of needed MS for the sound field in the space between parallel walls is infinitely high (on both sides of the walls). Up to now, we have only an interrupt criterion if the walls are absorbent due to the reduction of the source factor ΠR with increasing order.

In the limit case of parallel walls in equation (21), the limits $r, r_p, r_q \to \infty$ and $\vartheta \to 0$ are assumed; the MS-circle becomes a straight line normal to the walls.

First we derive with Figure 37 a plausible interrupt criterion for MS-production with parallel walls by consideration of allowable errors; then we sum up the MS to a single equivalent source.

The arrows in Figure 37 indicate which couples of sources satisfy the boundary condition at which wall. If one interrupts one has a couple without "partner" for the boundary condition (this is the lowest couple in the graph). An interrupt makes an error in the boundary condition at a wall. The absolute error is in the order of magnitude of the field contribution of the uncompensated source couple. It decreases with increasing order of reflection: because of the increasing distance of the source couple to the wall (geometrical reduction); because of the decrease of ΠR with absorbent walls (acoustical reduction). The relative error, which is important, further decreases with increasing order, because the reference quantity is the sum of contributions of "complete" couples.

From experiences of field evaluations in flat ducts (which is the object at hand) one can conclude that a relative boundary value error $\Delta_{rel} \approx 1/10$–$1/20$ is tolerable. Neglecting geometrical and acoustical reductions, this leads to a permitted interrupt at about $s_{hi} = 10$–20 MS. This will be sufficient if geometrical reduction with increasing order is taken into account, and if one considers that real walls never are ideally reflecting. A reflection coefficient $|R| = 0{\cdot}9$ produces for an order $o = 15$ a source factor of about $0{\cdot}9^{15} = 0{\cdot}206$.

For the summation of contributions of MS at parallel walls, one can again start with equations (17) and (21), take the first term of the asymptotic expansion of spherical Bessel and Hankel functions because of $r_p, r_q \to \infty$, which introduces products of cosine and exponential functions, reformulate these products so that only exponential functions with

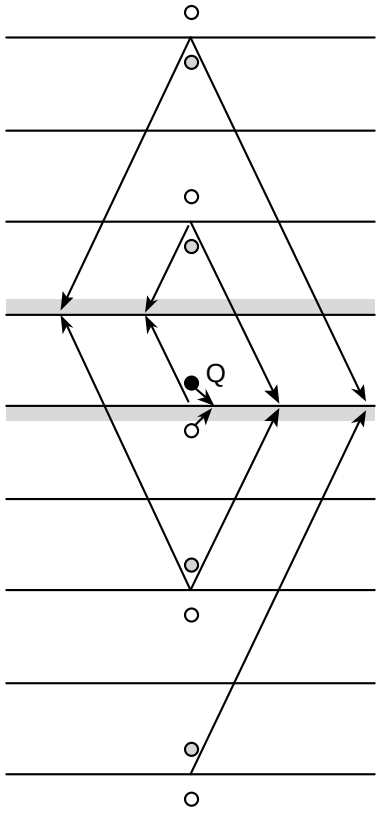

Figure 37. Interrupt criterion in the case of parallel walls.

either sums or differences of radii appear in the exponent, set exponentials with sums to zero, because of the small but existing attenuation in air, find analytical equivalents for the sum over Legendre polynomials, and obtain the result that it is reasonable to express the field of a mirror source in P as the field of the original source Q with a geometrical factor.

But, knowing this goal it is easier to derive that form of the MS-field directly. The problem is characterized geometrically by the straight line, normal to the flanks F_1, F_2, which contains the original source Q and the MS q, and the field point P. We therefore take a right-handed Cartesian co-ordinate system x', y', z' with the y'-axis on the source line, and the x'-axis in one of the flanks so that P is in the x', y' plane (it follows from the system x, y, z of the room by a rotation and shift); see Figure 38.

The source positions are given by $x' = 0$, $z' = 0$ and

$$x'_q = (2s + 1)H \pm h, \quad s = 0, \pm 1, \pm 2, \ldots, \tag{33a}$$

if the co-ordinate origin is chosen on F_1 as in Figure 38, otherwise by

$$x'_q = 2sH \pm h, \quad s = 0, \pm 1, \pm 2, \ldots. \tag{33b}$$

The field contribution $p_q(P)$ in P of a source q can be written in terms of the contribution $p_Q(P)$ of Q as

$$p_q(P) = \Pi_q R(\theta_s) \frac{k_0 d_{QP}}{k_0 d_{qP}} \mathrm{e}^{-\mathrm{j}k_0(d_{qP} - d_{QP})} p_Q(P), \tag{34}$$

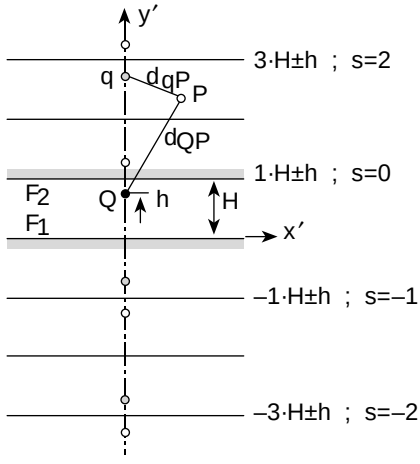

Figure 38. Summation of MS-contributions in the case of parallel walls.

with

$$d_{qP} = \sqrt{(x'_P - x'_q)^2 + (y'_P - y'_q)^2}, \qquad d_{QP} = \sqrt{(x'_P - x'_Q)^2 + (y'_P - y'_Q)^2}. \tag{35}$$

The angles θ_s for the reflection factors are easily obtained in the x' and y' co-ordinates. The equivalent source and its contribution representing all mirror sources is given by

$$p(P) = p_Q(P) \sum_s \Pi_q R(\theta_s) \frac{k_0 d_{QP}}{k_0 d_{qP}} \, \mathrm{e}^{-\mathrm{j}k_0(d_{qP} - d_{QP})}. \tag{36}$$

For the combination with corner sources of non-parallel wall couples, it is again recommended to let the original source and the MS of first order out of the summation over s. For the mirror reflection of this source at an opposite wall use the reciprocity, i.e., determine the position of the reflected field point P' in the co-ordinates x, y', z'.

If the parallel flanks F_1, F_2 are not directly opposite to each other, but with a parallel offset, interrupt checks for mirror sources are preferably performed in the co-ordinates x', y', z' (skip s for illegal sources in equation (36)), as well as efficiency checks (skip s for inefficient sources). The total source (36) is ineffective, if P is not in the space between the planes of the flanks F_1, F_2, and the mirror-reflected combined source is ineffective if P' is not in that space. So indeed one has to form two sums (36), one for the "legal" equivalent source, which is used in its mirror reflection, and one for the final evaluation of the field contribution. But the decision if equation (36) must be evaluated at all can be made before any computation.

One still has the problem with convex corners and their scattered field. This problem can be solved rather easily, within the frame of an MS-method, by combination of the MS-method with the "second principle of superposition" (PSP). We begin with the description of that principle in the next section.

24. THE SECOND PRINCIPLE OF SUPERPOSITION (PSP)

It should be stated in advance: the PSP, when applied to single concave corners, does not result in significant saving of computation, as compared to the traditional MS-method; except it is globally applied to symmetrical rooms (see below); but its application is necessary with convex corners; because it is applicable to both convex and concave corners,

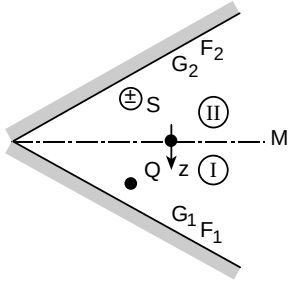

Figure 39. Application of the second PSP in room acoustics.

and some of its features are more easily explained with concave corners, these are treated here also.

One distinguishes three principles of superposition, numbered in the order of their publication. The first principle of superposition reduces the determination of the characteristic mode propagation constants in ducts with unsymmetrical absorbent linings to two corresponding tasks with symmetrical linings [12]. The second principle of superposition, first published by Ochmann and Donner [13] in a special application with silencers and then generalized in reference [14], reduces the evaluation of sound transmission through objects having a plane of symmetry to two sub-tasks in which the plane of symmetry is hard or soft respectively. The third principle of superposition gets the solution of a scattering task at an object with an absorbent surface from the solutions of two tasks in which that surface is hard and soft respectively [15].

The objects of the second principle of superposition (PSP) are an arbitrary (also multi-modal) source Q and a scattering object which has a plane of symmetry M. When the PSP is applied to room edges, the flanking walls are supposed to extend from their line of intersection to infinity. If they are absorbent, the absorption should be the same at both flanks (symmetrical flanks; see below for unsymmetrical flanks). It is not necessary that the flanking walls of a room have a real line of intersection; they may be couples of walls, with other walls forming the connection on the apex side.

We suppose equal wall admittance values G_i at both flanks F_i. We further suppose a co-ordinate system with a co-ordinate z (which favourably is an azimuthal co-ordinate) normal to the median plane M. This assumption is not necessary; it just simplifies the description.

The median plane M subdivides the wedge into two halves: (I) on the source side of M; (II) on the back side of M (as seen from Q).With the choice of z as in Figure 39, mirror-reflected points in both halves are distinguished just by $\pm z$.

The PSP composes the solution of the original scattering task by the solutions of two sub-tasks $\sigma = h, w$ of scattering in zone (I): in the first sub-task, $\sigma = h$, the plane of symmetry M is hard; in the second sub-task, $\sigma = w$, the plane of symmetry M is soft.

The field of each sub-task is composed by the source field p_Q and a scattered field $p_s^{(\sigma)}$: $p^{(\sigma)} = p_Q + p_s^{(\sigma)}$. The fields of the original task in both zones (I), (II) then are

$$p_{\mathrm{I}}(x, z) = p_Q(x, z) + \tfrac{1}{2}(p_s^{(h)}(x, z) + p_s^{(w)}(x, z)),$$

$$p_{\mathrm{II}}(x, z) = \tfrac{1}{2}(p_s^{(h)}(x, -z) - p_s^{(w)}(x, -z)) \tag{37a}$$

(x represents the co-ordinates other than z). One can decompose the field also as $p^{(\sigma)} = p_Q + p_r + p_s^{(\sigma)}$, where p_r shall be the same in both sub-tasks; then one has

$$p_{\mathrm{I}}(x, z) = p_Q(x, z) + p_r(x, z) + \tfrac{1}{2}(p_s^{(h)}(x, z) + p_s^{(w)}(x, z)),$$
$$p_{\mathrm{II}}(x, z) = \tfrac{1}{2}(p_s^{(h)}(x, -z) - p_s^{(w)}(x, -z)). \tag{37b}$$

The scattered fields here generally are different from those of equation (37a), but in our problem p_r is just a member of the scattered field terms (see below) so that these remain unchanged.

In summary: the PSP solves the scattering task on the source side (I) for the sub-tasks $\sigma = h, w$ and computes with them the field on the back side (II) (just by mirror reflection at M). One should keep in mind this "detour" of the field evaluation in (II) via zone (I).

The *derivation* of the PSP uses, additionally to the source $Q(x, z)$, sources $Q(x, -z)$ which are mirror-reflected at M; in the first sub-task the MS has the same amplitude as Q; in the second sub-task it is multiplied with −1. Equations (37a) just describe the superposition of both sub-tasks with Q and $\pm$ MS as sources. The following features should be observed:

The simplicity of the derivation shows the general validity of the PSP (under the mentioned condition of symmetry of the object).

The PSP is an exact description if the scattered fields of the sub-tasks can be determined exactly.

The PSP offers itself for a combination with the MS-method!

If, in the course of the PSP, mirror sources are created at M (to satisfy there the boundary conditions), one should remember that mirror sources at ideally reflecting planes give an exact description of the field. With absorbing flanks, the errors of the MS-method remain.

The fields of the mirror sources S_i form the "scattered fields".

If S_i was created by mirror reflection at F_1 on the source side, the sign of the MS is the same in both sub-tasks; this will be indicated in the sketches below with (+).

If S_i is created by mirror reflection at M, the sign of S_i is different in both sub-tasks; this will be marked in the sketches with ($\pm$), i.e., (+) for $\sigma = h$, (−) for $\sigma = w$. If an MS which was created at M (i.e., marked with ($\pm$)) afterwards is reflected at F_1, the double sign ($\pm$) remains.

The resulting fields of the PSP are:

$$p_{\mathrm{I}}(x, z) = \mathrm{Q} + \tfrac{1}{2}\left(\sum_i S_i^{(h)}(x, z) + \sum_i S_i^{(w)}(x, z)\right),$$
$$p_{\mathrm{II}}(x, z) = \tfrac{1}{2}\left(\sum_i S_i^{(h)}(x, -z) - \sum_i S_i^{(w)}(x, -z)\right). \tag{38a}$$

The change $h \to w$ of the median plane M does not influence the position and number of the MS; therefore the sums have the same counting and summation index i.

If the first MS is created at F_1 (on the source side), it has in both sub-tasks the same sign (it will be indicated with S_0). It can be pulled in $p_{\mathrm{I}}(x, z)$ outside the parentheses and needs no superscript (h) or (w). The remaining MS under the sums (with superscripts) have undergone at least one mirror reflection at M. So one can write

$$p_{\mathrm{I}}(x, z) = Q + S_0(x, z) + \tfrac{1}{2}\left(\sum_i S_i^{(h)}(x, z) + \sum_i S_i^{(w)}(x, z)\right),$$
$$p_{\mathrm{II}}(x, z) = \tfrac{1}{2}\left(\sum_i S_i^{(h)}(x, -z) - \sum_i S_i^{(w)}(x, -z)\right). \tag{38b}$$

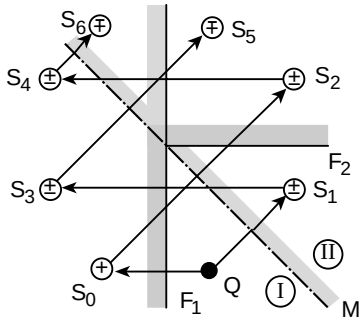

Figure 40. MS-production at the flank F_1 and the median plane M for a concave rectangular corner.

We have encountered a special treatment of the MS of first order S_0 at F_1 already in other contexts.

One must distinguish with the production of MS in the PSP:

(1) "Mirror reflected …" (a) at the wall F_1; then the sign is the same as for the mother source, but if F_1 is absorbent, a reflection factor R arises; (b) at M; then the sign in the sub-task h is that of the mother source, in the sub-task w the sign is changed; i.e., the new factor in the source factor ΠR is $R = \pm 1$.

(2) Two sub-tasks—(a) $\sigma = h$: no sign change at mirror reflections; (b) $\sigma = w$: sign change for mirror reflections at M (but not at F_1).

(3) Two "paths" of MS-production—(a) first path: begins with mirror-reflection at F_1; MS on this path will be designated with even indices $i = 0, 2, 4, \ldots$; (b) second path: begins with mirror reflection at M; MS on this path will have odd indices $i = 1, 3, 5, \ldots$.

Whereas the sub-tasks h, w do not change the position of an MS of some order, the positions of the MS of both paths are generally different from each other.

As a detailed example, we take the concave rectangular edge; see Figure 40.

In Figure 40 MS-production is continued (irrespective of the inside criterion) until the MS begin to fall on positions of formerly created MS. The paths from then on would begin to be continued backwards (with multiple covering of the positions).

The following schemes represent the chains with multiple reflections at F_1 and M for both paths. Mirror reflection at F_1 is marked by a simple arrow $\rightarrow$ and reflection at M by a double arrow $\Rightarrow$. The cases $\sigma = h$ are arranged in the upper line, and $\sigma = w$ in the lower line. MS in vertical columns of the scheme have equal positions. The flanking wall F_1 first is supposed to be hard.

In the schemes below, the sums appearing in the PSP (for one path; recall that MS in a column of the scheme have equal positions) under the symbols of the MS are written:

$$\sum S = \sum_{i \geqslant 0} S_i^{(h)} + S_i^{(w)} \quad \text{in zone (I)},$$

$$\Delta S = \sum_{i \geqslant 0} S_i^{(h)} - S_i^{(w)} \quad \text{in zone (II)}.$$

First path:

$$Q \xrightarrow[w]{h} S_0 \begin{matrix} \nearrow + S_2 \to + S_4 \Rightarrow + S_6 \to + S_8 \Rightarrow + S_{10} \to + S_{12}, \\ \searrow - S_2 \to - S_4 \Rightarrow + S_6 \to + S_8 \Rightarrow - S_{10} \to - S_{12}, \end{matrix}$$

$$\sum S = \sum_{i \geqslant 0} S_i^{(h)} + S_i^{(w)} = 2S_0 \quad 0 \quad 0 \quad 2S_6 \quad 2S_8 \quad 0 \quad 0,$$

$$\Delta S = \sum_{i \geqslant 0} S_i^{(h)} - S_i^{(w)} = 0 \quad 2S_2 \quad 2S_4 \quad 0 \quad 0 \quad 2S_{10} \quad 2S_{12}, \tag{39a}$$

Second path:

$$Q \begin{matrix} \nearrow + S_1 \to + S_3 \Rightarrow + S_5 \to + S_7 \Rightarrow + S_9 \to + S_{11}, \\ \searrow - S_1 \to - S_3 \Rightarrow + S_5 \to + S_7 \Rightarrow - S_9 \to - S_{11}, \end{matrix}$$

$$\sum S = \sum_{i \geqslant 0} S_i^{(h)} + S_i^{(w)} = 0 \quad 0 \quad 2S_5 \quad 2S_7 \quad 0 \quad 0,$$

$$\Delta S = \sum_{i \geqslant 0} S_i^{(h)} - S_i^{(w)} = 2S_1 \quad 2S_3 \quad 0 \quad 0 \quad 2S_9 \quad 2S_{11}. \tag{39b}$$

If one sums up the MS of both paths, the PSP gives

$$p_{\mathrm{I}}(x, z) = Q(x, z) + S_0(x, z) + \sum_{n=1,\,3,\,5\,\ldots} \sum_{k=1}^{4} S_{4n+k}(x, z),$$

$$p_{\mathrm{II}}(x, z) = \sum_{n=0,\,2,\,4\,\ldots} \sum_{k=1}^{4} S_{4n+k}(x, -z). \tag{40}$$

Now we complete the scheme for the case of (symmetrical) absorption at the walls. The reflection factors R_i in an order of MS are not changed by $h \to w$, except the sign.

First path:

$$Q \xrightarrow[w]{h} R_0 S_0 \begin{matrix} \nearrow + R_0 S_2 \to + R_0 R_4 S_4 \Rightarrow + R_0 R_4 S_6 \to + R_0 R_4 R_8 S_8 \Rightarrow \cdots, \\ \searrow - R_0 S_2 \to - R_0 R_4 S_4 \Rightarrow + R_0 R_4 S_6 \to + R_0 R_4 R_8 S_8 \Rightarrow \cdots. \end{matrix}$$

$$\sum S = \sum_{i \geqslant 0} S_i^{(h)} + S_i^{(w)} = 2R_0 S_0 \quad 0 \quad 0 \quad 2R_0 R_4 S_6 \quad 2R_0 R_4 R_8 S_8,$$

$$\Delta S = \sum_{i \geqslant 0} S_i^{(h)} - S_i^{(w)} = 0 \quad 2R_0 S_2 \quad 2R_0 R_4 S_4 \quad 0 \quad 0, \tag{41}$$

Second path:

$$Q \begin{matrix} \nearrow + S_1 \to + R_3 S_3 \Rightarrow + R_3 S_5 \to + R_3 R_7 S_7 \Rightarrow + R_3 R_7 S_9 \to \cdots, \\ \searrow - S_1 \to - R_3 S_3 \Rightarrow + R_3 S_5 \to + R_3 R_7 S_7 \Rightarrow - R_3 R_7 S_9 \to \cdots. \end{matrix}$$

$$\sum S = \sum_{i \geqslant 0} S_i^{(h)} + S_i^{(w)} = 0 \quad 0 \quad 2R_3 S_5 \quad 2R_3 R_7 S_7 \quad 0,$$

$$\Delta S = \sum_{i \geqslant 0} S_i^{(h)} - S_i^{(w)} = 2S_1 \quad 2R_3 S_3 \quad 0 \quad 0 \quad 2R_3 R_7 S_9. \tag{42}$$

25. SOME EXAMPLES FOR THE MS AND PSP-METHOD

The most important advantage of the combination MS and PSP is the fact that with it convex corners become tractable; the traditional MS-method there fails completely.

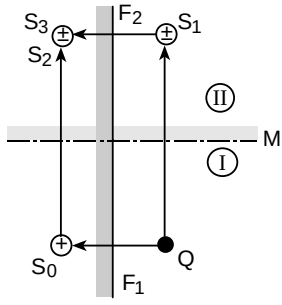

Figure 41. Application of the PSP in the case of a plane wall.

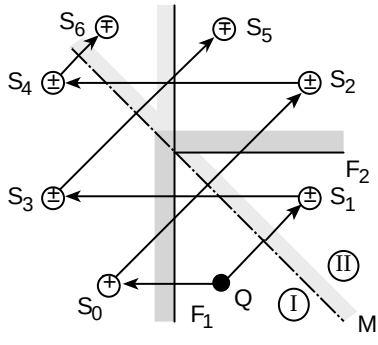

Figure 42. Application of the PSP in the case of a concave rectangular corner.

Because the wedge angle of a couple of walls always is $\Theta \leqslant 2\pi$, the angle between F and M always is $\leqslant \pi$; zone (I) in which the scattered field has to be determined is concave; the MS-method there can be applied.

In concave corners the application of the PSP possibly produces a higher precision because the MS have new positions. But this should be checked.

The following sketches mainly suppose hard flanks (for simplicity reasons); absorbing flanks are specially mentioned.

A very simple, but instructive, example is the case of a source Q above a plane wall; see Figure 41.

The MS are shown in Figure 41 until interruption by the inside criterion. There is coincidence of S_2, S_3 (with the same source factor R for absorbent F_1, F_2).

It is an important question if such coinciding MS have to be counted a multiple number of times or if the MS-production is interrupted when coincidence begins. S_1, S_2, S_3 compensate each other in the sum ΣS of $p_{(I)}$. The field in (I) is built up by Q, S_0, as expected. In the difference ΔS of $p_{(II)}$ the contributions of S_1, S_2, S_3 would sum up, if the MS would be used as drawn. As a consequence, the field would be unsteady at M.

Consequently, coincidence of MS with the same source factor ΠR should be avoided! Taking this interrupt criterion into account, the field is correctly given by the MS and PSP-method. This method thus has a further interrupt criterion, as compared with the traditional MS-method.

The example of Figure 41 also illustrates well the procedure in the MS and PSP-method for the evaluation in zone (II): One first evaluates with the significant MS the scattered field in zone (I), and then mirror-reflects that field at M into zone (II).

Another instructive example is the concave, rectangular edge; see Figure 42.

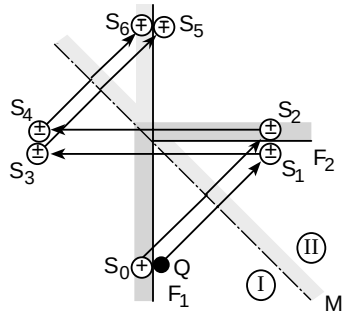

Figure 43. A concave rectangular corner with the source Q approaching a flank.

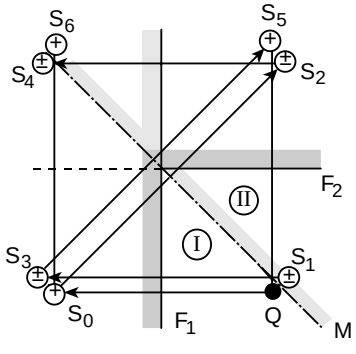

Figure 44. A concave rectangular corner with the source Q approaching the median plane M.

The MS are drawn in Figure 42 as far as it is permitted by the inside and coincidence criteria. (a further reflection of S_5 at F_1, which would be permitted by the inside criterion, would produce coincidence with S_6).

According to equation (40), the field $p_I(x, z)$ is created by the superposition of the fields of Q, S_0, S_5, S_6, and the field $p_{II}(x, -z)$ by the mirror sources S_1, S_2, S_3, S_4. The boundary conditions at the flanks F_1, F_2 evidently are satisfied. Because both groups of MS can be transformed into each other by a rotation with $\pi/4$ and a mirror reflection, the field is also steady at M; thus it is a solution of the task.

A special case which can be easily understood is obtained if the source Q approaches the flank F_1. With a hard flank F_1 again the case of a source above a hard wall F_2 is achieved; see Figure 43.

The effective source in Figure 43 is a double source $Q + S_0$. As expected, the field is symmetrical relative to F_1 and F_2. It is also steady at M. The field is completely and precisely represented.

In a further limit case, Q approaches the median plane M; the field again is rightly represented as can be seen from Figure 44.

The MS in Figure 44 again are drawn according to the inside and coincidence criteria. The source Q and the MS marked with (+) determine the field in (I); the MS marked with ($\pm$) compose (first in (I)) to the field in (II). The boundary conditions at F_1, F_2 and condition of steadiness at M are satisfied.

The presented examples again illustrate the importance of the determination of p_{II} via the detour over zone (I). The examples contain MS with ($\pm$) in (II). Without the detour, this

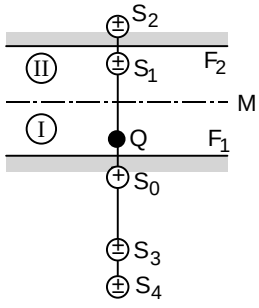

Figure 45. PSP in the case of parallel walls.

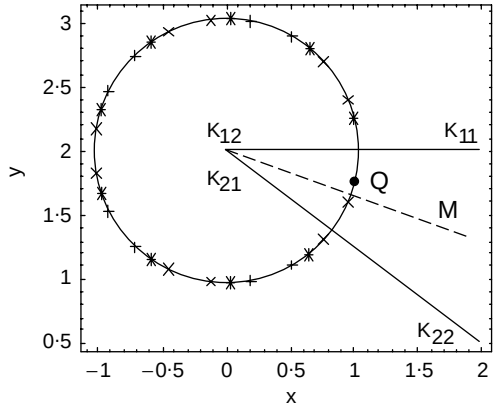

Figure 46. MS-method and SPP: $W1 = \{\{2, 2\},\{0, 2\}\}$, $W2 = \{\{0, 2\}, \{2, 0{\cdot}5\}\}$, $Q = \{1, 1{\cdot}75\}$, $o_{max} = 18$.

would mean poles of the field in (II). This must be excluded according to the condition of regularity of the scattered field.

A further example are parallel walls, i.e., the case of a flat duct; see Figure 45.

In the example of Figure 45 the chains of possible MS on both sides are arbitrarily interrupted. The chains would go to infinity with hard walls. The absorption of walls would produce some amplitude reduction with increasing order. This example will be used below to find interrupt criteria for chains of MS which, in principle, are infinitely long.

Below we also show some (computed) examples of MS in edges with no simple ratio of the wedge angle Θ to π. The walls W_1, W_2 are described by couples of end lines K_{ij}. The (dashed) median plane M always shows to the interior side of the room. The co-ordinates x, y may be arbitrarily normalized. The original source Q again is indicated by a black disc. The MS have no (literal) names. The used symbols for the MS suppose that they are shown for the sub-task $\sigma = w$, i.e., in the mirror reflection at M the source factor is multiplied with $R = -1$. When the resulting source factor is $\Pi R > 0$, the MS will be drawn with a $+$ sign; when $\Pi R < 0$ with a $\times$ (a minus sign would not permit to see coincidence of sources). Irrespective of inside and coincidence criteria the MS in Figure 46 are continued until $o_{max} = 18$.

The following examples (Figures 47–50) consider the inside and coincidence criteria. The resulting upper limits of the order on the two paths 1, 2 are indicated as $o1$, $o2, \ldots$. The

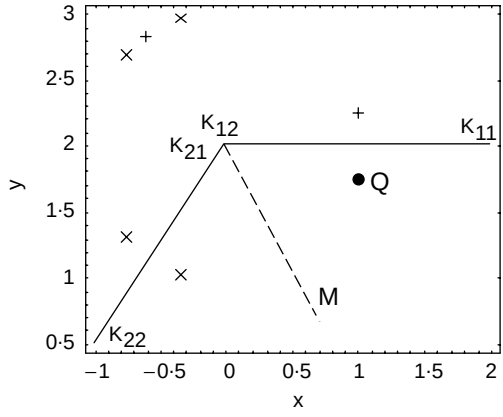

Figure 47. MS-method and SPP with interrupt: $W1 = \{\{2, 2\}, \{0, 2\}\}$, $W2 = \{\{0, 2\}, \{-1, 0{\cdot}5\}\}$, $Q = \{1, 1{\cdot}75\}$, $o1 = 3$, $o2 = 3$.

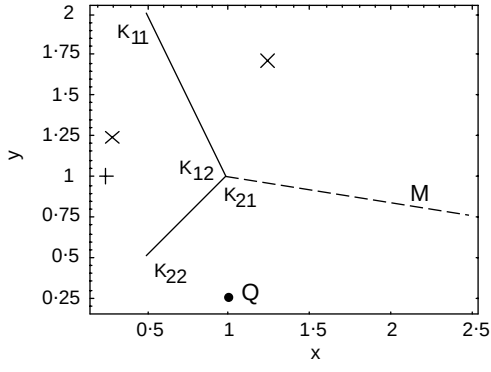

Figure 48. MS-method and SPP with interrupt: $W1 = \{\{0{\cdot}5, 2\}, \{1, 1\}\}$, $W2 = \{\{1, 1\}, \{0{\cdot}5, 0{\cdot}5\}\}$, $Q = \{1, 0{\cdot}25\}$, $o1 = 2$, $o2 = 1$.

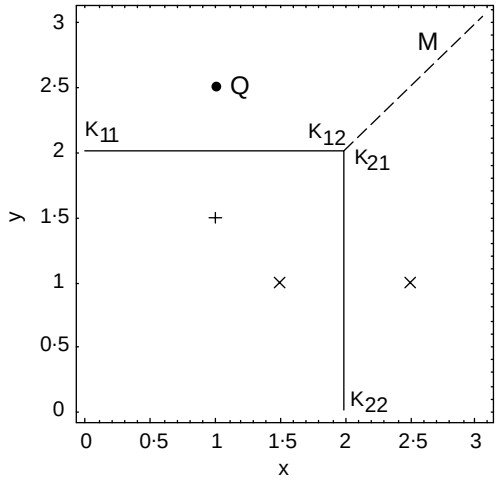

Figure 49. MS-method and SPP with interrupt: $W1 = \{\{0, 2\}, \{2, 2\}\}$, $W2 = \{\{2, 2\}, \{2, 0\}\}$, $Q = \{1, 2.5\}$, $o1 = 2$, $o2 = 1$. This convex, rectangular edge has for each zone (I), (II) only two sources.

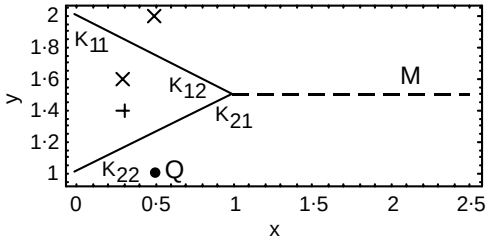

Figure 50. MS-method and SPP with interrupt: $W1 = \{\{0, 2\}, \{1, 1{\cdot}5\}\}$, $W2 = \{\{1, 1{\cdot}5\}, \{0, 1\}\}$, $Q = \{0{\cdot}5, 1\}$, $o1 = 2$, $o2 = 1$.

diagrams should be read as follows:

- Contributions to the field p_{I} in zone (I), containing the source Q, are made (besides Q) by those MS (in a direct sum, i.e., without sum factor 1/2) which are marked with $+$.
- The field in zone (II) is composed of contributions of the MS which are marked with $\times$.

More important than the examples of concave edges, shown up to now, are convex edges. The next example introduces the limit case of a semi-infinite thin screen.

In the limit case of a screen, the MS with $+$ coincides with the upper MS with $\times$, and the lower MS with $\times$ coincides with Q. But there it would produce a pole in zone (II); consequently, it is dropped. Consideration of the field angles of the MS with $+$, from which the lower MS with $\times$ was created by mirror reflection at M, leads to the same result, because the field angle does not include M. Also, the inside criterion permits only two MS with $+$ and $\times$ in the mirror point to Q. The field in (I) is produced by Q and its MS at F_1 (i.e., with source factor R for an absorbent flank), and the field in (II) is produced by one MS with a source factor $R = 1$ in the mirror point to Q (via field determination in (I) !). The limit case of a thin screen thus is described only with errors which, however, are in the order of magnitude of the errors of the traditional MS-method with absorbing flanks. This error can be checked against an independent evaluation of the sound field around screens (see below).

26. THE PSP FOR UNSYMMETRICAL ABSORPTION

The condition of symmetrical absorption for the application of the PSP to sound fields between couples of walls is a sensible restriction in applications. It will be tried, therefore, to resolve that restriction, if necessary by an approximation, which, however, should not introduce errors exceeding the errors of the traditional MS-method with absorbing walls.

First, we repeat the fundamental form of the PSP:

$$p_{\mathrm{I}}(x, z) = p_Q(x, z) + \tfrac{1}{2}(p_s^{(h)}(x, z) + p_s^{(w)}(x, z)),$$
$$p_{\mathrm{II}}(x, z) = \tfrac{1}{2}(p_s^{(h)}(x, -z) - p_s^{(w)}(x, -z)). \tag{43a}$$

If the scattered fields p_s are produced by MS, it reads

$$p_{\mathrm{I}}(x, z) = Q + \tfrac{1}{2}\left(\sum_i S_i^{(h)}(x, z) + \sum_i S_i^{(w)}(x, z)\right),$$
$$p_{\mathrm{II}}(x, z) = \tfrac{1}{2}\left(\sum_i S_i^{(h)}(x, -z) - \sum_i S_i^{(w)}(x, -z)\right). \tag{43b}$$

If the flanks have equal absorption, the MS contain source factors formed by products of reflection factors, which themselves are evaluated from the admittance of the flank F_1.

As was shown, the production of MS follows two paths: the first path begins with the mirror reflection at the real flank F_1 on the source side and produces in the first step the mirror source S_0 (in both sub-tasks $\sigma = h, w$); the other path begins with a mirror reflection at the median plane M.

If the flanks are symmetrical, the field in the sub-task $\sigma = h$ is symmetrical with respect to M (i.e., M is hard); in the sub-task $\sigma = w$ the field is antisymmetrical (i.e., M is soft). Symmetry and antisymmetry of the fields are solely determined by the source Q and the auxiliary sources of the PSP . If the walls are different, an antisymmetrical part of the field will arise due to the asymmetry of the walls.

26.1. A FIRST APPROXIMATION FOR DIFFERENTLY ABSORBING WALLS

It is always possible to compose an unsymmetrical field $p(x, z)$ in two *geometrically* equal halves (I) and (II) of a wedge with symmetrical and antisymmetrical field components:

$$p(x, z) = p^{(sy)}(x, z) + p^{(as)}(x, z),$$
$$p^{(sy)}(x, -z) = p^{(sy)}(x, z), \quad p^{(as)}(x, -z) = -p^{(as)}(x, z). \tag{44}$$

Whence follows

$$p^{(sy)}(x, z) = \tfrac{1}{2}(p(x, z) + p(x, -z)), \quad p^{(as)}(x, z) = \tfrac{1}{2}(p(x, z) - p(x, -z)). \tag{45}$$

M by definition is hard for the part $p^{(sy)}$ and soft for the part $p^{(as)}$. Therefore, these parts have a common characteristic with $p_s^{(h)}$, $p_s^{(w)}$ of the PSP with symmetrical flanks.

Further, the field $p(x, z)$ shall satisfy the boundary conditions at the flanks F_1, F_2:

$$p(F_1) = p^{(sy)}(F_1) + p^{(as)}(F_1) \stackrel{!}{=} v_\perp(F_1)/G_1,$$
$$p(F_2) = p^{(sy)}(F_1) - p^{(as)}(F_1) \stackrel{!}{=} v_\perp(F_2)/G_2. \tag{46}$$

In these boundary conditions, the parts $p^{(sy)}$, $p^{(as)}$ appear in the same combination as $p_s^{(h)}$, $p_s^{(w)}$ in the PSP. Thus, from formal considerations one arrives at an approximation for the PSP when applied to walls with different absorption.

Complete the PSP for acoustically different walls as follows.

- Apply in equation (43) for the evaluation of the field $p_{(I)}$ in zone (I) the sum

$$p_{(I)}(x, z) = Q + \tfrac{1}{2}\left(\sum_i p_{s,i}^{(h)}(x, z) + \sum_i p_{s,i}^{(w)}(x, z)\right),$$

using for the reflection factors the admittance of the flank F_1;

- apply in equation (43) for the evaluation of the field $p_{(II)}$ in zone (II) the difference

$$p_{(II)}(x, z) = \tfrac{1}{2}\left(\sum_i p_{s,i}^{(h)}(x, -z) - \sum_i p_{s,i}^{(w)}(x, -z)\right),$$

using for the reflection factors the admittance of the flank F_2.

This rule creates a field which satisfies the wave equation in the approximation of the MS-method for absorbent walls, satisfies the source condition, and satisfies the boundary conditions at F_1, F_2.

The question is whether the field is steady at M.

If R_1 is used in the sum and difference, the solution of the symmetrical problem with R_1 is obtained. If Q is displaced into its mirror-reflected position, and the substitution $F_1 \to F_2$ is supposed, then the solution of the symmetrical problem with R_2 is obtained. Both are steady at M, however with generally different values $p(M)$ due to the difference of R_1, R_2.

The rule above takes from the symmetrical problems with R_1, R_2, the parts in zones (I) and (II), respectively. The approximation produces in general a step of $p(x, z)$ at M.

It is an important question as to whether this jump is tolerable in the frame of precision of the MS-method with absorption. The field jump at M is of the order of magnitude of the difference of the reflection factors R_1, R_2. In the extreme case of one hard wall with $R_1 = 1$ and an absorbing opposed wall, one can consider the problem as the sub-task for zone (I) of a symmetrical PSP-problem. The traditional MS-method produces field jumps of about the same height for absorbing walls if one crosses the flanks of the field angles.

If the field point P is on the median plane M, one will take the average of both values according to the above rule of approximation.

26.2. A MORE PRECISE APPROXIMATION FOR DIFFERENTLY ABSORBING WALLS

We define

$$G^{(1)} = G_1 + G_2, \quad G^{(2)} = G_1 - G_2. \tag{47}$$

Choose the numbering so that $\mathrm{Re}\{G^{(2)}\} \geqslant 0$. It follows that

$$G_1 = \tfrac{1}{2}(G^{(1)} + G^{(2)}), \quad G_2 = \tfrac{1}{2}(G^{(1)} - G^{(2)}). \tag{48}$$

Solve the scattering task (43) with the PSP for both *symmetrical* cases with $G^{(\alpha)}$, $\alpha = 1, 2$. This gives

$$\begin{aligned} p_{\mathrm{I}}^{(\alpha)}(x, z) &= p_Q(x, z) + \tfrac{1}{2}(p_s^{(h,\alpha)}(x, z) + p_s^{(w,\alpha)}(x, z)), \\ p_{\mathrm{II}}^{(\alpha)}(x, z) &= \tfrac{1}{2}(p_s^{(h,\alpha)}(x, -z) - p_s^{(w,\alpha)}(x, -z)), \qquad \alpha = 1, 2. \end{aligned} \tag{49}$$

In the case $G_1 = G_2$ the object to $\alpha = 2$ is an edge with hard walls. Then the following procedure is not necessary because the normal PSP is applicable!

Below, we consider only particle velocities normal to the flanks or to the median plane M. Note the change of sign at the velocities in zone (II) (as a consequence of a subsequent mirror reflection):

$$\begin{aligned} v_{\mathrm{I}}^{(\alpha)}(x, z) &= v_Q(x, z) + \tfrac{1}{2}(v_s^{(h,\alpha)}(x, z) + v_s^{(w,\alpha)}(x, z)), \\ \mathrm{v}_{\mathrm{II}}^{(\alpha)}(x, z) &= -\tfrac{1}{2}(v_s^{(h,\alpha)}(x, -z) - v_s^{(w,\alpha)}(x, -z)). \end{aligned} \tag{50}$$

The boundary conditions of both symmetrical tasks $\alpha = 1, 2$ at the flank F_1 are

$$v_{\mathrm{I}}^{(\alpha)}(F_1) = G^{(\alpha)} p_{\mathrm{I}}^{(\alpha)}(F_1). \tag{51a}$$

The boundary conditions at the flank F_2 are formulated via

$$v_{\mathrm{II}}^{(\alpha)}(F_1) = G^{(\alpha)} p_{\mathrm{II}}^{(\alpha)}(F_1) \tag{51b}$$

and subsequent mirror reflection

$$-v_{\mathrm{II}}^{(\alpha)}(F_2) = G^{(\alpha)} p_{\mathrm{II}}^{(\alpha)}(F_2). \tag{51c}$$

These boundary conditions are satisfied by the PSP-method for both cases $\alpha = 1, 2$. If one inserts p_{I}, p_{II} in their forms of the PSP, one gets

$$\begin{aligned} v_Q(F_1) + \tfrac{1}{2}(v_s^{(h,\alpha)}(F_1) + v_s^{(w,\alpha)}(F_1)) &= G^{(\alpha)}[p_Q(F_1) + \tfrac{1}{2}(p_s^{(h,\alpha)}(F_1) + p_s^{(w,\alpha)}(F_1))], \\ -\tfrac{1}{2}(v_s^{(h,\alpha)}(F_1) - v_s^{(w,\alpha)}(F_1)) &= G^{(\alpha)}[\tfrac{1}{2}(p_s^{(h,\alpha)}(F_1) - p_s^{(w,\alpha)}(F_1))]. \end{aligned} \tag{52}$$

They can be applied to evaluate the particle velocities $v_s^{(\sigma,\alpha)}(F_i)$; $\sigma = h, w$; $\alpha = 1, 2$; $i = 1, 2$; from the scattering pressures $p_s^{(\sigma,\alpha)}(F_i)$ (we shall not use these forms for our further derivation).

The sound pressure field of the *unsymmetrical original task* is formulated as

$$p(x,z) = p_Q(x,z) + p_{sc}(x,z) \tag{53}$$

by the freefield p_Q of the source Q and a scattered field p_{sc}. The boundary conditions in the unsymmetrical wedge at both flanks F_1, F_2 are:

$$\begin{aligned} v_Q(F_1) + v_{sc}(F_1) &= G_1[p_Q(F_1) + p_{sc}(F_1)], \\ -(v_Q(F_2) + v_{sc}(F_2)) &= G_2[p_Q(F_2) + p_{sc}(F_2)]. \end{aligned} \tag{54}$$

Here the sign change in the second line considers the agreement that the particle velocities at both walls shall be directed into the walls, but in both lines they are components in the $+z$-direction.

The boundary conditions are linear operators. Therefore, a representation of $p(x,z)$ can be tried as a linear combination of the solutions of the symmetrical PSP:

in (I):

$$p_Q(x,z) + p_{sc}(x,z) = A p_{\mathrm{I}}^{(1)}(x,z) + B p_{\mathrm{I}}^{(2)}(x,z), \tag{55}$$

in (II):

$$p_Q(x,z) + p_{sc}(x,z) = a p_{\mathrm{II}}^{(1)}(x,z) + b p_{\mathrm{II}}^{(2)}(x,z). \tag{56}$$

With this formulation, the boundary conditions of the original task become

$$\begin{aligned} v_Q(F_1) + v_{sc}(F_1) &= A v_{\mathrm{I}}^{(1)}(F_1) + B v_{\mathrm{I}}^{(2)}(F_1) \\ &\overset{!}{=} G_1\,[p_Q(F_1) + p_{sc}(F_1)] = G_1[A p_I^{(1)}(F_1) + B p_{\mathrm{I}}^{(2)}(F_1)], \end{aligned} \tag{57a}$$

$$\begin{aligned} v_Q(F_2) + v_{sc}(F_2) &= a v_{\mathrm{II}}^{(1)}(F_2) + b v_{\mathrm{II}}^{(2)}(F_2) = -a v_{\mathrm{II}}^{(1)}(F_1) - b v_{\mathrm{II}}^{(2)}(F_1) \\ &\overset{!}{=} -G_1[p_Q(F_2) + p_{sc}(F_2)] = -G_2[a p_{\mathrm{II}}^{(1)}(F_1) + b p_{\mathrm{II}}^{(2)}(F_1)]. \end{aligned} \tag{57b}$$

Division with A or a gives for the ratios B/A and b/a with equations (51a) and (47)

$$B/A = -\frac{G_1 p_{\mathrm{I}}^{(1)}(F_1) - v_{\mathrm{I}}^{(1)}(F_1)}{G_1 p_{\mathrm{I}}^{(2)}(F_1) - v_{\mathrm{I}}^{(2)}(F_1)} = \frac{p_{\mathrm{I}}^{(1)}(F_1)}{p_{\mathrm{I}}^{(2)}(F_1)}, \tag{58}$$

and with equations (51b) and (47)

$$b/a = -\frac{G_2 p_{\mathrm{II}}^{(1)}(F_1) - v_{\mathrm{II}}^{(1)}(F_1)}{G_2 p_{\mathrm{II}}^{(2)}(F_1) - v_{\mathrm{II}}^{(2)}(F_1)} = \frac{G_1}{2G_2 - G_1}\,\frac{p_{\mathrm{II}}^{(1)}(F_1)}{p_{\mathrm{II}}^{(2)}(F_1)} = \frac{G^{(1)} + G^{(2)}}{G^{(1)} - 3G^{(2)}}\,\frac{p_{\mathrm{II}}^{(1)}(F_1)}{p_{\mathrm{II}}^{(2)}(F_1)}. \tag{59a}$$

In the case of symmetrical walls with $G^{(2)} = 0$ it would follow that

$$b/a \xrightarrow[G_2 \to G_1]{} -\frac{p_{\mathrm{II}}^{(1)}(F_1)}{p_{\mathrm{II}}^{(2)}(F_1)}. \tag{59b}$$

As an intermediate result one gets with equations (55) and (56) in (I):

$$p_Q(x,z) + p_{sc}(x,z) = A\left[p_{\mathrm{I}}^{(1)}(x,z) + \frac{p_{\mathrm{I}}^{(1)}(F_1)}{p_{\mathrm{I}}^{(2)}(F_1)} p_{\mathrm{I}}^{(2)}(x,z)\right], \tag{60}$$

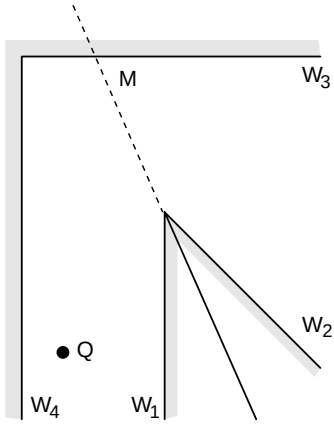

Figure 51. Combination of a corner source with the PSP.

in (II):

$$p_Q(x,z) + p_{sc}(x,z) = a\left[p_{\mathrm{II}}^{(1)}(x,z) + \frac{G_1}{2G_2 - G_1} \frac{p_{\mathrm{II}}^{(1)}(F_1)}{p_{\mathrm{II}}^{(2)}(F_1)} p_{\mathrm{II}}^{(2)}(x,z) \right], \tag{61}$$

If $z = 0$, i.e. for points on M, one has $p_{\mathrm{I}}^{(\alpha)}(M) \to p_{\mathrm{II}}^{(\alpha)}(M)$; at the same time the left-hand sides of equations (60) and (61) become equal. This leads to

$$\frac{a}{A} = \frac{p_{\mathrm{I}}^{(1)}(M) + (p_{\mathrm{I}}^{(1)}(F_1)/p_{\mathrm{I}}^{(2)}(F_1))p_{\mathrm{I}}^{(2)}(M)}{p_{\mathrm{II}}^{(1)}(M) + (G_1/(2G_2 - G_1))(p_{\mathrm{II}}^{(1)}(F_1)/p_{\mathrm{II}}^{(2)}(F_1))p_{\mathrm{II}}^{(2)}(M)}. \tag{62}$$

Up to now the right-hand sides of equations (55) and (56) are determined up to a common factor A. This factor finally follows from the source condition in (I) , i.e., from equation (60):

$$p_Q(Q) = A\left[1 + \frac{p_{\mathrm{I}}^{(1)}(F_1)}{p_{\mathrm{I}}^{(2)}(F_1)} \right] p_Q(Q), \quad A = \frac{p_{\mathrm{I}}^{(2)}(F_1)}{p_{\mathrm{I}}^{(1)}(F_1) + p_{\mathrm{I}}^{(2)}(F_1)}. \tag{63}$$

The result of this procedure solves the boundary conditions at the flanks, and it is steady at M, and it satisfies the source condition. The sound field in a wedge with differently absorbent walls is determined with the precision with which the two symmetrical scattering tasks are solved.

However, the procedure has some computational disadvantages.

One needs the solutions $p_{\mathrm{I}}^{(\alpha)}$, $p_{\mathrm{II}}^{(\alpha)}$ at the flanks and the median plane with precise source factors ΠR of the involved MS. They can hardly be substituted by approximate values, as it was possible for the interrupt criterion.

The field evaluation is split into the evaluations of four sub-tasks. The amount of programming may become prohibitively large.

Therefore one generally will apply the simpler rule of the previous section.

There is still one question open which shall be illustrated with Figure 51. The question is how the evaluation with the PSP for convex corners is combined with the corner source from wall couples. This question arises if one (or both) flank(s) of the wall couple end in a convex corner. As Figure 51 shows, the median plane M of that corner is a visible opposite wall to the corner source. So, either for the original source Q in the wedge of the wall couple (as shown in Figure 51), or for the corner source, the problem of scattering at the convex corner can be treated with the MS and PSP-method.

27. A GLOBAL APPLICATION OF THE PSP

Most auditoria have a constructional plane of symmetry M. So the room as a total satisfies the condition for the application of the PSP.

This means that one solves the task of field evaluation twice in the half of the room containing the source Q: once M is supposed to be hard and once M is supposed to be soft.

The computational advantage can be easily quantified in 2-D (similar relations hold in 3-D). The room is supposed to have N walls. In the sub-tasks of the PSP will appear the following numbers of walls (M included): $N/2 + 2$ walls, if M on both sides ends on walls; $(N - 1)/2 + 2$ walls if M ends on one side with a wall and on the other side in a corner; $N/2$ walls, if M ends on both sides in corners.

A reduction of the effective wall number begins (in the least favourable first case) with $N = 6$. For a relatively simple room geometry with $N = 20$, the effective wall number has reduced to 12. Since in the estimations of the needed MS for the traditional MS-method the wall number appears as base with the order as exponent, the computational advantage would be significant.

With this remark ends that part of the present paper which is concerned with the evaluation of the stationary sound field in rooms. It should be noticed that the described methods yield complex sound pressures in P. The computations will be somewhat simplified if one is satisfied with the magnitudes $|p_q|$ of the contributions of the effective sources (MS and corner sources). This is mostly done in room acoustical papers, although it is impossible to conclude from $|p_q|$ to $|p(P)|$ (the magnitude of a sum mostly is different from the sum of magnitudes ...).

We shall encounter that difference in the next section which deals with the determination of the room reverberation using the results of the field evaluation. Although reverberation is an instationary process, it should be possible to evaluate the most important room acoustical qualifier, the reverberation time, from the results of a computational field model. In doing that, one will be confronted with some lack of definition of reverberation in usual descriptions.

28. REVERBERATION TIME WITH RESULTS OF THE MS-METHOD

The method described above delivers the stationary, monochromatic field of a stationary, harmonic source in a room. It returns the complex sound pressure $p(P)$ in a point P, i.e., with magnitude and phase.

The most important room acoustical qualifier is the reverberation time; it is described in the literature (more or less) by "The reverberation time is the elapsed time for a decay of the sound pressure level of 60 dB after termination of a stationary sound excitation."

It is tacitly understood that "sound pressure" means the magnitude of the sound pressure, and in most experimental determinations of the reverberation time band noise is used with an average over the bandwidth. It is not mentioned (but it is important as we shall see below) that the rectification of the received signal (for the magnitude and band average) implies averaging over time intervals.

The reverberation process is instationary; our field evaluation is for stationary fields. Therefore, one needs a "switch-off model" for the evaluations. It should be reminded in that context, that the sound field in the room is created in the MS-method (as well as in the modified MS and PSP-method) by equivalent sources, which means that, after the equivalent sources have been installed in the right places and with the right amplitudes, the walls of the room can be taken away. The equivalent sources radiate into the free space.

One can imagine the distributed sources as a network of loudspeakers driven by the same signal generator. The network lines contain attenuators which model the source factors ΠR. If the signal generator is switched off, all loudspeakers are switched off instantly, but the sound waves radiated before switch-off still propagate. This model has the advantage that the boundary conditions at the walls are satisfied in every moment, because as long as a sound wave from a source hits a wall, the sound wave from its daughter source with that wall will also be present.

It may be mentioned that a different switch-off model can be designed which makes use of the above-mentioned reciprocity of the MS-method, i.e., which uses the "mirror-receiver model". In this model, microphones at the distributed receiver positions add their signals via attenuators (which again introduce the source factors ΠR). In this model only one loudspeaker, of the original source Q, must be switched off. But it is not so evident that the boundary conditions are satisfied every time. It is interesting to note that the implementation of this switch-off model produces a reverberation which corresponds to the method of the "integrated impulse response". Below we shall use only the above-mentioned model with the loudspeaker network.

The end of the contribution of a source q arrives in P after a time t after switch-off

$$t = \frac{dist(q,P)}{c_0} = \frac{k_0\, dist(q,P)}{\omega}, \quad \omega = 2\pi/T_p, \qquad \frac{t}{T_p} = \frac{k_0 dist(q,P)}{2\pi}. \tag{64}$$

Therein T_p is the time period of the sound wave. It is reasonable to measure t in units of periods T_p.

Imagine all evaluated MS (and their field contributions $p_s(P)$) sorted with increasing $k_0 dist(q,P)$ and indexed in this order with a number s ($s = 0$ may represent the original source Q). After some elapsed time t/T_p, those contributions will be summed in P, which are still travelling from their source to P. The decay curve $L(P)$ in P expressed as sound pressure level therefore is

$$L(t/T_p) = 10\lg \left| \sum_{k_0\, dist(q(s),P) \geqslant 2\pi t/T_p} p_s(P) \right|^2. \tag{65}$$

With increasing t/T_p the summation is performed over smaller and smaller remainders of the set of effective MS. This evaluation therefore will produce a steeper slope of $L(t/T_P)$ at the end of a time interval of observation when this end approaches fewer and fewer remaining MS. This increase in slope must not be confused with the slope produced by the decreasing amplitudes of MS with increasing distance (due to geometrical and/or acoustical reduction), but is a consequence of the finite size of the set of MS.

Equation (65) is a direct transcription of the reverberation process defined above verbally. Formation of magnitude and square is applied on the sum of contributions. Instead of proceeding on the t/T_p-axis in unit steps of s, one can proceed in steps $\Delta t/T_p$. Contributions within the interval $\Delta t/T_p$ are summed up (linearly!).

When applying equation (65) to 2-D rooms, curves of $L(t/T_p)$ are obtained which disagree with all expectations which one has for a reverberation curve. The reason for the discrepancy is the fact that in room acoustics, and therefore also in the definition of the reverberation time, magnitudes of the received signal, time-averaged over a time interval, are summed up (see e.g. reference [16, pp. 79, 96]). One also finds the reverberation defined as the "decay of the average energy density". The (effective) energy density implies the square of the sound pressure; averaging is performed over directions of the sound intensity and time intervals which are short compared with the reverberation time. Because tacitly the contributions of different sources are supposed to be incoherent also, the contributions

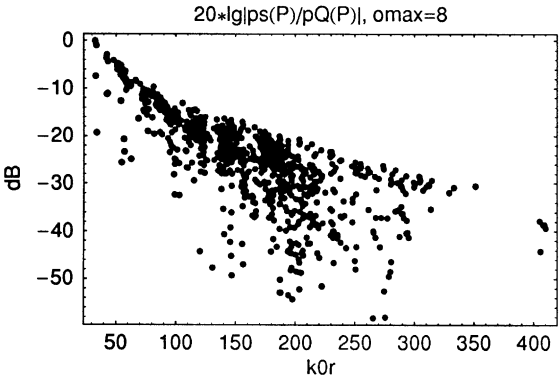

Figure 52. Sound pressure level of the contributions of MS in P, sorted after their travel distances.

of sources to the energy density can be added and they are proportional to the magnitude squared of their contributions $p_q(P)$ to the sound pressure $p(P)$:

$$E_q(P) = \frac{1}{2\,\rho_0 c_0^2} |p_q(P)|^2. \tag{66}$$

This definition leads to a reverberation curve

$$L(t/T_p) = 10\lg\left[\frac{1}{2\rho_0 c_0^2} \sum_{n\,>\,(t/T_p)/(\Delta t/T_p)} \frac{1}{\Delta s} \sum_{k_0\,dist(q(s),P)\,\subset\,2\pi\Delta t/T_p} |p(s)|^2\right]. \tag{67}$$

The outer sum indicates summation in steps of time intervals $\Delta t/T_p$ in which Δs sources are found, and this outer summation includes a decreasing number n of such steps. The interior sum forms a squared average (with the factor $1/\Delta s$) of the contributions in a time interval (this summation is skipped if $\Delta s = 0$).

29. A ROOM WITH CONCAVE EDGES AS EXAMPLE

We take the room of section 13 as a model room, with the same positions of the source Q and the receiver P as there. The evaluation of the mirror sources is performed for orders up to $o_{max} = 8$. The lower limit of $\Pi|R|$ was set to limit = 0·01; the upper limit for the distances was with $d_{max} = 100 dist(Q,P)$ set so high that it did not exclude a legal source. This produces 837 effective sources; the computing time for the determination of source positions and source factors was 320 s.

Figure 52 shows over $k_0 r$, with $r = dist(q,P)$, the sound pressure levels $p_q(P)$ of the contributions in P, relative to the contribution $p_Q(P)$ of the original source Q. The cloud of points has a typical triangular shape: the upper border has an about constant slope after a somewhat steeper slope for smaller $k_0 r$. The lower border lines are not so well defined, because there the points are disperse. The upwards going lower border line towards the right predominantly is determined by the termination with o_{max}. One can expect that the upper border line has some similarity with the reverberation curve.

The evaluation of equation (65) returns the reverberation curves of Figures 53(a–c) which differ from each other only in the value used for the time interval $\Delta t/T_p$.

Larger time intervals $\Delta t/T_p$ smoothen the curves, but they do not produce a similarity with a usual reverberation curve, when summation over complex sound pressure contributions is applied with magnitude squaring of the sum.

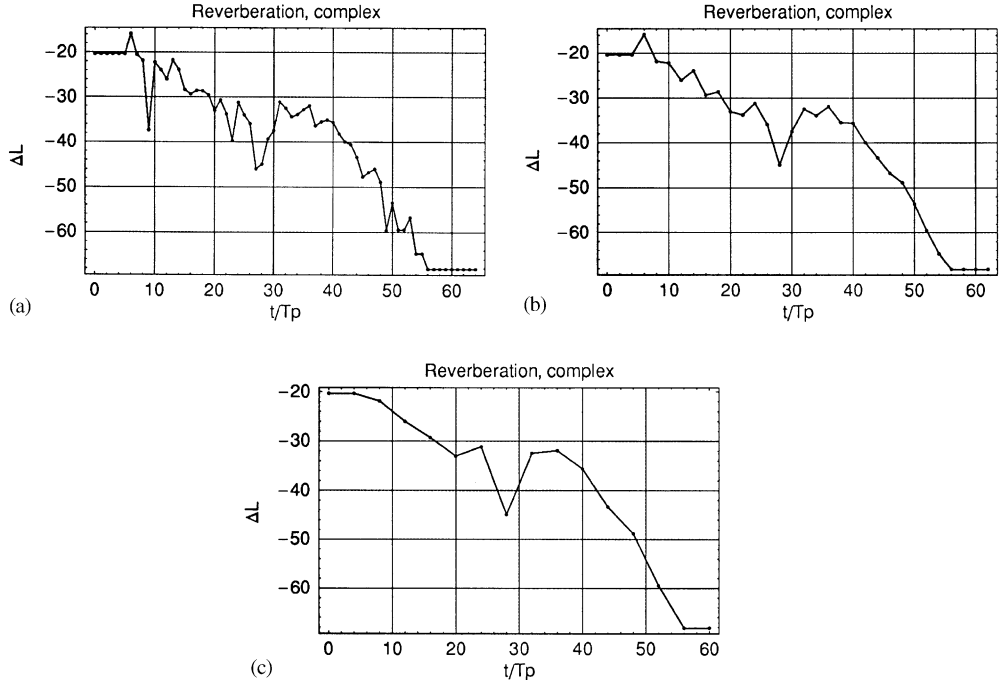

Figure 53. (a) Summation of complex contributions, with time interval $\Delta t/T_p = 1$. (b). Summation of complex contributions, with time interval $\Delta t/T_p = 2$. (c). Summation of complex contributions, with time interval $\Delta t/T_p = 4$.

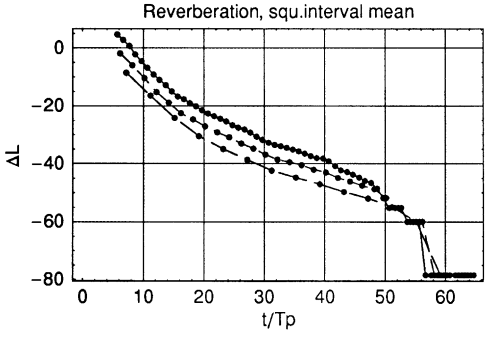

Figure 54. Reverberation curves with equation (67), for different values $\Delta t/T_p = 1, 2, 4$ (from high to low).

Figure 54 combines results of the evaluation of equation (67), again for different time intervals $\Delta t/T_p$ (within which now an averaging of squared magnitudes takes place); the values of the curves from high to low are $\Delta t/T_p = 1, 2, 4$. The points represent centres of the time intervals. The constant factor $1/(\rho_0 c_0^2)$ is omitted.

Except for the steep ends of the curves, which come from the termination of the MS-evaluation with o_{max}, as explained above, the curves now represent usual reverberation curves. They have a steeper "early reverberation" and not so steep "late reverberation". The choice of $\Delta t/T_p$ may influence to some degree the value of the reverberation time obtained from such curves, for example as the coefficient of a linear regression through the points within a given interval of observation for t/T_p. Figure 55 combines the points of the

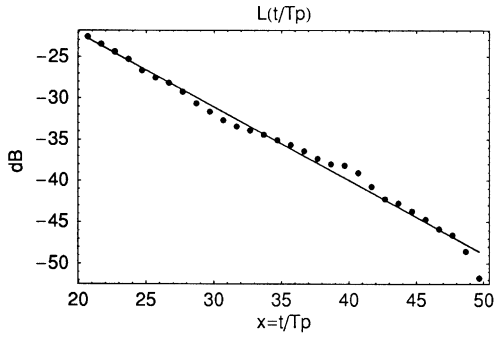

Figure 55. Combination of points from Figure 54, for $\Delta t/T_p = 1$ with a linear regression curve.

reverberation curve for $\Delta t/T_p = 1$ with the linear regression within the interval $20 \leqslant t/T_p \leqslant 50$. The reverberation time T_r in units of T_p is $T_r/T_p = 67{\cdot}46$.

30. SUMMARY

- One aim of the present paper was to free the MS-method from the horror visions of abundantly high numbers of needed mirror sources, by use of inherent interrupt criteria.
- Further, the nevertheless high number of needed mirror sources in the traditional MS-method is further reduced by the introduction of corner sources, which represent the sound field in corner areas between couples of walls.
- These corner sources can easily be mirror-reflected at opposite walls.
- The importance given to the corner areas brings the main part of evaluation from 3-D down to 2-D evaluations.
- The interrupt criteria restrict the number of mirror sources needed in a corner to low values, in most cases; and the corner sources as elementary units contain the most important field components for any field point P.
- Therefore, it can be expected that the source construction can be terminated after the first mirror reflection of the corner sources at opposite walls.
- The case of parallel walls is a special case of a wall couple. An easy-to-compute approximation is derived for this special case.
- The principal problem which the traditional MS-method has with convex corners is resolved with the help of a principle of superposition (PSP).
- The condition of symmetrical walls for the principle of superposition when applied to convex corners would be a severe restriction for applications in room acoustics. Approximations to the PSP are derived for unsymmetrical walls of a corner.

One must not compute everything anew if the frequency and/or the receiver position change. The source positions depend only on the relative positions of the original source and the walls. Preliminary checks of interrupt due to small source factors and/or to large distances can be made with some constant values of the reflection coefficients and a distance to the centre of the range in which the receiver point will change. One can find all needed information for the final evaluation of the reflection factors $R(\theta_s)$ with a new frequency and/or receiver position if one supplements the source lists in $tab(o)$ with the counting index s_m for the position of the list of the mother source in the table $tab(o-1)$.

If new assumptions are made for approximations, other than the inherent approximation of the traditional MS-method with absorbent walls, care was taken that the new errors of approximation remain in the frame of the errors of the original MS-method.

The MS-method, in its traditional and in the modified form, originally delivers complex sound pressures in a field point. Room acoustics often deals with sound pressure magnitudes. Then some simplifications can be applied to the MS-method. The difference between the squared magnitude of a sum of contributions and the sum of squared magnitudes of contributions is an important distinction in relation to the evaluation of the reverberation from numerical results of a room model and MS-method.

REFERENCES

1. A. KROKSTADT, S. STRØM and S. SØRSDAL 1968 *Journal of Sound and Vibration* **8**, 118. Calculating the acoustical room response by the use of a ray tracing technique.
2. J. J. EMBRECHTS 1982 *Acustica* **51**, 288. Sound field distribution using randomly traced sound ray techniques.
3. U. STEPHENSON 1985 *Acustica* **59**, 1. Eine Schallteilchen-Computersimulation zur Berechnung der für die Hörsamkeit in Konzertsälen maßgebenden Parameter.
4. M. VORLÄNDER 1989 *Thesis, Techn. Hochschule, Aachen, Faculty of Electrotechnics.* Untersuchungen zur Leistungsfähigkeit des raumaksustischen Schallteilchen-Modells.
5. U. STEPHENSON 1988 *Bericht BS* 201/88 aus Fraunhofer-Institut für Bauphysik, Stuttgart. Vergleich der Spiegelschallquellen-Methode mit der Schallteilchen-Simulations-Methode.
6. F. P. MECHEL 2000 *Acta Acustica* **86**, 203–215. A line source above a plane absorber.
7. F. P. MECHEL 1989 *Schallabsorber* (*Sound Absorbers*), Vol. I. Stuttgart: S. Hirzel Verlag, Chapter 13.
8. M. ABRAMOWITZ and I. A. STEGUN 1972 *Handbook of Mathematical Functions.* NY: Dover Publications; ninth edition.
9. F. P. MECHEL 1999 *Journal of Sound and Vibration* **219**, 105–132. Scattering at rigid building corners.
10. F. P. MECHEL 2000 *Acta Acustics* **86**, 759–768 "Modified mirror and corner sources with a principle of superposition.
11. F. P. MECHEL 2000 *Acta Acustica* **86**, 957–969. The corner source model.
12. F. P. MECHEL 1976 *Proceedings of the Noise Control Conference Warsaw*, p. 1. Why are silencers symmetrical?.
13. M. OCHMANN and U. DONNER 1994 *Acta Acustica* **2**, 247–255. Investigation of silencers with asymmetrical lining; I: theory.
14. F. P. MECHEL 1998 *Schallabsorber*, Vol. III. Stuttgart: S. Hirzel Verlag.
15. F. P. MECHEL 2000 *Acta Acustica* **86**, 970–984. A principle of superposition.
16. H. KUTTRUFF 1973 *Room Acoustics.* London: Applied Science Publishers.

APPENDIX A: GEOMETRICAL SUB-TASKS

A 3-D, right-handed Cartesian co-ordinate system x, y, z is supposed. Points, lines, planes will be considered in 3-D. Corresponding relations in 2-D are obtained either by setting one co-ordinate on a zero value, identically, or by easy direct derivations. Walls are defined by a list of subsequent edge points; the sequence of the edges in the list is so that they define a rotation which with the direction towards the interior of the room form a right-handed system. Mostly not the polygon of a wall is considered below, but the plane which contains the wall.

1. *Distance d between two points* $P_1(x_1, y_1, z_1)$, $P_2(x_2, y_2, z_2)$:

$$dPP = \sqrt{(x_2 - x_1)^2 + (y_2 - y_1)^2 + (z_2 - z_1)^2}. \tag{A.1}$$

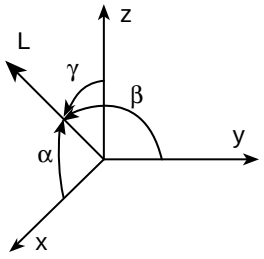

Figure A1. The direction angles α, β, γ of an oriented line L are the angles between the axes and the line.

2. *Direction cosines of the line from* $P_1(x_1, y_1, z_1)$ to $P_2(x_2, y_2, z_2)$:

$$\cos\alpha = \frac{x_2 - x_1}{dPP}, \quad \cos\beta = \frac{y_2 - y_1}{dPP}, \quad \cos\gamma = \frac{z_2 - z_1}{dPP}. \tag{A.2}$$

3. *Cosine of the angle* φ *between two lines*: The directions of the lines given by their direction angles α_i β_i γ_i,

$$\cos\varphi = \cos\alpha_1 \cos\alpha_2 + \cos\beta_1 \cos\beta_2 + \cos\gamma_1 \cos\gamma_2. \tag{A.3}$$

4. *Normal form* $Ax + By + Cz + D = 0$ *of a plane*: The plane is given by three points P_1, P_2, P_3 on it. A possible form of the plane equation (coming of a zero value of the vector triple product of the vectors (P, P_1), (P_2, P_1), (P_3, P)) is

$$\begin{vmatrix} x - x_1 & y - y_1 & z - z_1 \\ x_2 - x_1 & y_2 - y_1 & z_2 - z_1 \\ x_3 - x_1 & y_3 - y_1 & z_3 - z_1 \end{vmatrix} = 0. \tag{A.4}$$

whence follow the parameters A, B, C, D:

$$\begin{aligned} A &= y_1(z_2 - z_3) + y_2(z_3 - z_1) + y_3(z_1 - z_2), \\ B &= -x_1(z_2 - z_3) - x_2(z_3 - z_1) - x_3(z_1 - z_2), \\ C &= x_1(y_2 - y_3) + x_2(y_3 - y_1) + x_3(y_1 - y_2), \\ D &= x_1(y_3 z_2 - y_2 z_3) + y_1(x_2 z_3 - x_3 z_2) + z_1(x_3 y_2 - x_2 y_3). \end{aligned} \tag{A.5}$$

5. *Reduced normal form* $ax + by + cz + d = 0$ *of a plane*:

$$a = \frac{A}{\sqrt{A^2 + B^2 + C^2}}, \; b = \frac{B}{\sqrt{A^2 + B^2 + C^2}}, \; c = \frac{C}{\sqrt{A^2 + B^2 + C^2}}, \; d = \frac{D}{\sqrt{A^2 + B^2 + C^2}}. \tag{A.6}$$

This reduced normal form should not be confused with Hesse's normal form:

$$a'x + b'y + c'z - p = 0,$$

$$a' = \frac{A}{\pm\sqrt{A^2 + B^2 + C^2}}, \quad b' = \frac{B}{\pm\sqrt{A^2 + B^2 + C^2}}, \quad c' = \frac{C}{\pm\sqrt{A^2 + B^2 + C^2}},$$

$$p = \frac{D}{\pm\sqrt{A^2 + B^2 + C^2}} \geqslant 0, \tag{A.7}$$

where the sign of the root is taken so that p is positive. This additionoal convention in Hesse's normal form makes it unsuited for inside checks.

The parameters a, b, c of the reduced normal form are the direction cosines $\cos\alpha$, $\cos\beta, \cos\gamma$ of the normal vector on the plane (pointing to the interior side).

6. *Foot point $P = (x, y, z)$ of a point $P_1 = (x_1, y_1, z_1)$ on a plane*: The "foot point" P is the projection of P_1 on the plane. The plane is given by the parameters of its reduced normal form:

$$\begin{aligned} x &= (b^2 + c^2)x_1 - a(d + by_1 + cz_1), \\ y &= (a^2 + c^2)y_1 - b\,(d + a\,x_1 + cz_1), \\ z &= (a^2 + b^2)z_1 - c(d + ax_1 + by_1). \end{aligned} \tag{A.8}$$

7. *Mirror point $P = (x, y, z)$ of a point $P_1 = (x_1, y_1, z_1)$ at a plane*:

$$\text{Let } P_F \text{ be the foot point of } P_1 \text{ on the plane. Then } P = 2P_F - P_1. \tag{A.9}$$

8. *Direction cosines of intersection line of two planes*: Let the planes W_i be given by the parameters a_i, b_i, c_i, d_i of their reduced normal forms:

$$\begin{aligned} \cos\alpha &= \frac{\Delta_1}{\Delta}, \quad \cos\beta = \frac{\Delta_2}{\Delta}, \quad \cos\gamma = \frac{\Delta_3}{\Delta}, \\ \Delta_1 &= \begin{vmatrix} b_1 & c_1 \\ b_2 & c_2 \end{vmatrix}, \quad \Delta_2 = \begin{vmatrix} c_1 & a_1 \\ c_2 & a_2 \end{vmatrix}, \quad \Delta_3 = \begin{vmatrix} a_1 & b_1 \\ a_2 & b_2 \end{vmatrix}, \\ \Delta &= \sqrt{\Delta_1^2 + \Delta_2^2 + \Delta_2^2}. \end{aligned} \tag{A.10}$$

The rotation $W_1 \to W_2$ and the direction of the intersection line form a right-handed system.

9. *Point of intersection $X = (x, y, z)$ of a line through two points $P_i = (x_i, y_i, z_i)$ with a plane*: Let the plane W be given by the parameters a, b, c, d of its reduced normal form:

$$\begin{aligned} x &= -d(x_1 - x_2) + b(x_2y_1 - x_1y_2) + c(x_2z_1 - x_1z_2)/xx, \\ y &= -d(y_1 - y_2) + a(x_1y_2 - x_2y_1) + c(y_2z_1 - y_1z_2)/xx, \\ z &= -d(z_1 - z_2) + a(x_1z_2 - x_2z_1) + b(y_1z_2 - y_2z_1)/xx, \\ xx &= a(x_1 - x_2) + b(y_1 - y_2) + c(z_1 - z_2). \end{aligned} \tag{A.11}$$

10. *Foot point $P = (x, y, z)$ of a point $P_1 = (x_1, y_1, z_1)$ on the intersection line of two planes W_1, W_2*:

Let the planes W_i be given by the parameters a_i, b_i, c_i, d_i of their reduced normal forms:

$$\begin{aligned} x &= (\Delta_3(b_1d_2 - b_2d_1) + \Delta_2(c_2d_1 - c_1d_2) + \Delta_1(\Delta_1x_1 + \Delta_2y_1 + \Delta_3z_1))/\Delta^2, \\ y &= (\Delta_3(a_2d_1 - a_1d_2) + \Delta_1(c_1d_2 - c_2d_1) + \Delta_2(\Delta_1x_1 + \Delta_2y_1 + \Delta_3z_1))/\Delta^2, \\ z &= (\Delta_2(a_1d_2 - a_2d_1) + \Delta_1(b_2d_1 - b_1d_2) + \Delta_3(\Delta_1x_1 + \Delta_2y_1 + \Delta_3z_1))/\Delta^2, \end{aligned} \tag{A.12}$$

with Δ and Δ_i from equations (A.10).

11. *Bisectrice plane between two intersecting planes W_1, W_2*: Let the planes W_i be given by the parameters a_i, b_i, c_i, d_i of their reduced normal forms. The parameters of the

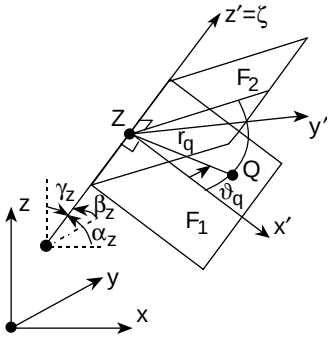

Figure A2. x', y', z' is a right-handed system, like x, y, z. The rotation $F_1 \to F_2$ forms with z' a right-handed system.

bisectrice plane (containing the intersection line) are

$$a = (a_1 + \lambda a_2), \quad b = (b_1 + \lambda b_2), \quad c = (c_1 + \lambda c_2), \quad d = (d_1 + \lambda d_2), \tag{A.13}$$

with $\lambda = \pm 1$.

12. *Two planes parallel or anti-parallel*: Parallel: the three parameters a, b, c of the reduced normal form are pairwise equal; anti-parallel: two of the parameters are pairwise equal, the other differs in sign.
13. *Distance between two anti-parallel planes*: Let the planes W_i be given by the prameters a_i, b_i, c_i, d_i of their reduced normal forms. Distance δ:

$$\delta = |d_1 - d_2|. \tag{A.14}$$

14. *Inside check of a point $P = (x, y, z)$ relative to a plane given by three points $P_i = (x_i, y_i, z_i)$*: The check is performed with and returns

$$\operatorname{sign}\begin{vmatrix} x - x_1 & y - y_1 & z - z_1 \\ x - x_2 & y - y_2 & z - z_2 \\ x - x_3 & y - y_3 & z - z_3 \end{vmatrix} = \left\{ \begin{array}{ll} +1 & \text{if } P \text{ is inside } W \\ 0 & \text{if } P \text{ is on } W \\ -1 & \text{if } P \text{ is outside } W \end{array} \right\}, \tag{A.15}$$

where $| \ldots |$ indicates a determinant, and $\operatorname{sign}(x)$ checks the sign of x.

15. *Inside check of a point $P = (x, y, z)$ relative to a plane given by its reduced normal form parameters*: The check is performed with and returns

$$\operatorname{sign}(ax + by + cz + d) = \left\{ \begin{array}{ll} +1 & \text{if } P \text{ is inside } W \\ 0 & \text{if } P \text{ is on } W \\ -1 & \text{if } P \text{ is outside } W \end{array} \right\}. \tag{A.16}$$

16. *Co-ordinate transformation*: The system x, y, z is rotated and shifted as shown in the graph of Figure A2. The new axis $z' = \zeta$ in the applications is the intersection line of two planes F_1, F_2; the new origin Z is the foot point of the original source Q on the intersection line.

The transformation $x, y, z \to x', y', z'$ is done by

$$\begin{pmatrix} x' \\ y' \\ z' \end{pmatrix} = \begin{pmatrix} \cos\alpha_x & \cos\beta_x & \cos\gamma_x \\ \cos\alpha_y & \cos\beta_y & \cos\gamma_y \\ \cos\alpha_z & \cos\beta_z & \cos\gamma_z \end{pmatrix} = \begin{Bmatrix} x - x_Z \\ y - y_Z \\ z - z_Z \end{Bmatrix}. \tag{A.17}$$

The inverse transformation $x', y', z' \to x, y, z$ is done (with the transposed matrix) by

$$\begin{pmatrix} x \\ y \\ z \end{pmatrix} = \begin{pmatrix} \cos\alpha_x & \cos\alpha_y & \cos\alpha_z \\ \cos\beta_x & \cos\beta_y & \cos\beta_z \\ \cos\gamma_x & \cos\gamma_y & \cos\gamma_z \end{pmatrix} \begin{pmatrix} x' \\ y' \\ z' \end{pmatrix} + \begin{pmatrix} x_Z \\ y_Z \\ z_Z \end{pmatrix}. \tag{A.18}$$

APPENDIX B: INPUT DATA OF THE MODEL ROOMS

B.1. CONCAVE ROOM

The vertical and the horizontal cuts through the room in Figure B1 show the counting numbers of the walls and their form and arrangement, as well as the positions of the original source Q and receiver point P. The co-ordinates indicated in the horizontal cut are arbitrary; normally, they will be scaled in the MS-computations. The table below gives the values of the edge co-ordinates.

walls = {{{−100·0, 0·0, 25·0}, {100·0, 0·0, 25·0}, {200·0, 100·0, 0·0}, {−200·0, 100·0, 0·0}},
{{−200·0, 100·0, 0·0}, {200·0, 100·0, 0·0}, {250·0, 150·0, 0·0}, {−250·0, 150·0, 0·0}},
{{−250·0, 150·0, 0·0}, {250·0, 150·0, 0·0}, {150·0, 600·0, 75·0}, {−150·0, 600·0, 75·0}},
{{−150·0, 600·0, 75·0}, {150·0, 600·0, 75·0}, {150·0, 600·0, 162·5}, {125·0, 600·0, 175·0},
{−125·0, 600·0, 175·0}, {−150·0, 600·0, 162·5}, {−150·0, 600·0, 75·0}},
{{125·0, 150·0, 225·0}, {−125·0, 150·0, 225·0}, {−125·0, 375·0, 200·0},
{125·0, 375·0, 200·0}},
{{125·0, 100·0, 225·0}, {−125·0, 100·0, 225·0}, {−125·0, 150·0, 225·0},
{125·0, 150·0, 225·0}},
{{100·0, 0·0, 175·0}, {−100·0, 0·0, 175·0}, {−125·0, 100·0, 225·0}, {125·0, 100·0, 225·0}},
{{100·0, 0·0, 25·0}, {−100·0, 0·0, 25·0}, {−100·0, 0·0, 175·0}, {100·0, 0·0, 175·0}},
{{100·0, 0·0, 25·0}, {100·0, 0·0, 175·0}, {250·0, 150·0, 175·0}, {250·0, 150·0, 0·0},
{200·0, 100·0, 0·0}},
{{250·0, 150·0, 0·0}, {250·0, 150·0, 175·0}, {150·0, 600·0, 162·5}, {150·0, 600·0, 75·0}},
{{−150·0, 600·0, 75·0}, {−150·0, 600·0, 162·5}, {−250·0, 150·0, 175·0},
{−250·0, 150·0, 0·0}},
{{−100·0, 0·0, 25·0}, {−200·0, 100·0, 0·0}, {−250·0, 150·0, 0·0}, {−250·0, 150·0, 175·0},
{−100·0, 0·0, 175·0}},
{{−100·0, 0·0, 175·0}, {−250·0, 150·0, 175·0}, {−125·0, 100·0, 225·0}},
{{−125·0, 100·0, 225·0}, {−250·0, 150·0, 175·0}, {−125·0, 150·0, 225·0}},
{{−125·0, 150·0, 225·0}, {−250·0, 150·0, 175·0}, {−150·0, 600·0, 162·5},
{−125·0, 600·0, 175·0}},
{{250·0, 150·0, 175·0}, {125·0, 150·0, 225·0}, {125·0, 600·0, 175·0}, {150·0, 600·0, 162·5}},
{{250·0, 150·0, 175·0}, {125·0, 100·0, 225·0}, {125·0, 150·0, 225·0}},
{{250·0, 150·0, 175·0}, {100·0, 0·0, 175·0}, {125·0, 100·0, 225·0}},
{{125·0, 375·0, 200·0}, {−125·0, 375·0, 200·0}, {−125·0, 600·0, 175·0},
{125·0, 600·0, 175·0}}}.

The co-ordinates of the original source Q and receiver point P are:

$Q = \{-75·0, 50·0, 30·0\}$,
$P = \{50·0, 350·0, 50·0\}$,

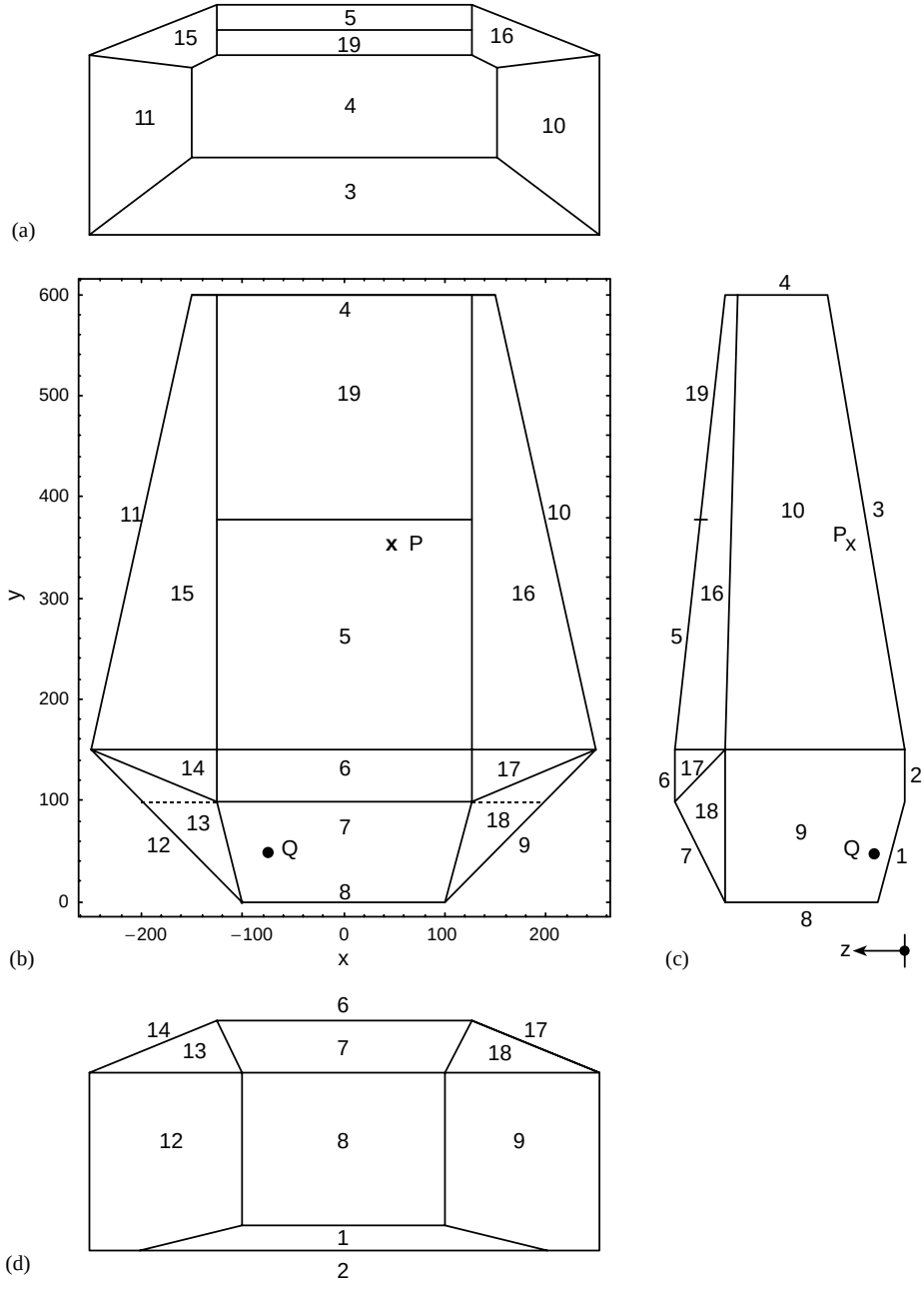

Figure B1. (a–d): A concave room.

The normalized wall admittances $Z_0 G$ are

$$Z_0 G = \{0{\cdot}0141 + 0{\cdot}000379\text{j},\ 0{\cdot}0141 + 0{\cdot}000379\text{j},\ 0{\cdot}0758 - 0{\cdot}0118\text{j},\ 0{\cdot}214 + 0{\cdot}158\text{j},\ 0{\cdot}0311 - 0{\cdot}00394\text{j},\ 0{\cdot}150 - 0{\cdot}123\text{j},\ 0{\cdot}0311 - 0{\cdot}00394\text{j},\ 0{\cdot}0769 - 0{\cdot}0748\text{j},\ 0{\cdot}0311 - 0{\cdot}00394\text{j},\ 0{\cdot}0758 - 0{\cdot}0118\text{j},\ 0{\cdot}0758 - 0{\cdot}0118\text{j},\ 0{\cdot}0311 - 0{\cdot}00394\text{j},\ 0{\cdot}0311 - 0{\cdot}00394\text{j},\ 0{\cdot}0311 - 0{\cdot}00394\text{j},\ 0{\cdot}0311 - 0{\cdot}00394\text{j},\ 0{\cdot}0311 - 0{\cdot}00394\text{j},\ 0{\cdot}0311 - 0{\cdot}00394\text{j},\ 0{\cdot}110 - 0{\cdot}125\text{j}\}.$$

They produce absorption coefficients α_{dif} for diffuse sound incidence:

α_{dif} = {0·10, 0·10, 0·40, 0·70, 0·20, 0·60, 0·20, 0·40, 0·20, 0·40, 0·40, 0·20, 0·20, 0·20, 0·20, 0·20, 0·20, 0·20, 0·49}.

The parameters a, b, c, d of the reduced normal form of the wall equations are

normal form =

{{0·0, 0·242536, 0·970143, −24·2536}, {0·0, 0·0, 1·0, 0·0}, {0·0, −0·164399, 0·986394, 24·6598},
{0·0, −1·0, 0·0, 600·0}, {0·0, −0·110432, −0·993884, 240·189}, {0·0, 0·0, −1·0, 225·0},
{0·0, 0·447214, −0·894427, 156·525}, {0·0, 1·0, 0·0, 0·0}, {−0·707107, 0·707107, 0·0, 70·7107},
{−0·976187, −0·21693, 0·0, 276·586}, {0·976187, −0·21693, 0·0, 276·586},
{0·707107, 0·707107, 0·0, 70·7107}, {0·485071, 0·485071, −0·727607, 175·838},
{0·371391, 0·0, −0·928477, 255·331}, {0·369231, −0·107692, −0·923077, 270·0},
{−0·36943, −0·102619, −0·923575, 269·376}, {−0·371391, 0·0, −0·928477, 255·331},
{−0·485071, 0·485071, −0·727607, 175·838}, {0·0, −0·110432, −0·993884, 240·189}}.

B.2. ROOM WITH CONVEX CORNERS

The walls are re-numbered (compared with the concave room). An orchestra pit is arranged below the stage. See Figure B2 with the cuts through the room for wall numbering, source and receiver positions.

walls = {{{215·0, 135·0, 0·0}, {250·0, 175·0, 0·0}, {−250·0, 175·0, 0·0}, {−215·0, 135·0, 0·0}},
{{250·0, 175·0, 0·0}, {150·0, 600·0, 75·0}, {−150·0, 600·0, 75·0}, {−250·0, 175·0, 0·0}},
{{150·0, 600·0, 75·0}, {150·0, 600·0, 162·5}, {125·0, 600·0, 175·0}, {−125·0, 600·0, 175·0},
{−150·0, 600·0, 162·5}, {−150·0, 600·0, 75·0}},
{{125·0, 600·0, 175·0}, {125·0, 375·0, 200·0}, {−125·0, 375·0, 200·0},{−125·0, 600·0, 175·0}},
{{125·0, 375·0, 200·0}, {125·0, 175·0, 225·0}, {−125·0, 175·0, 225·0}, {−125·0, 375·0, 200·0}},
{{125·0, 175·0, 225·0}, {125·0, 100·0, 225·0}, {−125·0, 100·0, 225·0}, {−125·0, 175·0, 225}},
{{125·0, 100·0, 225·0}, {100·0, 0·0, 175·0}, {−100·0, 0·0, 175·0}, {−125·0, 100·0, 225·0}},
{{100·0, 0·0, 175·0}, {100·0, 0·0, 25·0}, {−100·0, 0·0, 25·0}, {−100·0, 0·0, 175·0}},
{{100·0, 0·0, 25·0}, {185·0, 100·0, 25·0}, {−185·0, 100·0, 25·0}, {−100·0, 0·0, 25·0}},
{{185·0, 100·0, 25·0}, {185·0, 100·0, 15·0}, {−185·0, 100·0, 15·0}, {−185·0, 100·0, 25·0}},
{{185·0, 100·0, 15·0}, {125·0, 30·0, 15·0}, {−125·0, 30·0, 15·0}, {−185·0, 100·0, 15·0}},
{{125·0, 30·0, 15·0}, {125·0, 30·0, −40·0}, {−125·0, 30·0, −40·0}, {−125·0, 30·0, 15·0}},
{{125·0, 30·0, −40·0}, {210·0, 130·0, −40·0}, {−210·0, 130·0, −40·0}, {−125·0, 30·0, −40·0}},
{{210·0, 130·0, −40·0}, {210·0, 130·0, 15·0}, {−210·0, 130·0, 15·0}, {−210·0, 130·0, −40·0}},
{{210·0, 130·0, 15·0}, {215·0, 135·0, 0·0}, {−215·0, 135·0, 0·0}, {−210·0, 130·0, 15·0}},
{{210·0, 130·0, 25·0}, {100·0, 0·0, 25·0}, {100·0, 0·0, 175·0}, {210·0, 130·0, 175·0}},
{{250·0, 175·0, 0·0}, {215·0, 135·0, 0·0}, {210·0, 130·0, 15·0}, {210·0, 130·0, 175·0}, {250·0, 175·0, 175·0}},
{{250·0, 175·0, 0·0}, {250·0, 175·0, 175·0}, {150·0, 600·0, 160·0}, {150·0, 600·0, 75}},
{{250·0, 175·0, 175·0}, {100·0, 0·0, 175·0}, {125·0, 100·0, 225·0}},
{{250·0, 175·0, 175·0}, {125·0, 100·0, 225·0}, {125·0, 175·0, 225·0}},
{{250·0, 175·0, 175·0}, {125·0, 175·0, 225·0}, {125·0, 600·0, 175·0}, {150·0, 600·0, 160·0}},
{{210·0, 130·0, 25·0}, {210·0, 130·0, −40}, {125·0, 30·0, −40·0}, {125·0, 30·0, 15·0},
{185·0, 100·0, 15·0},

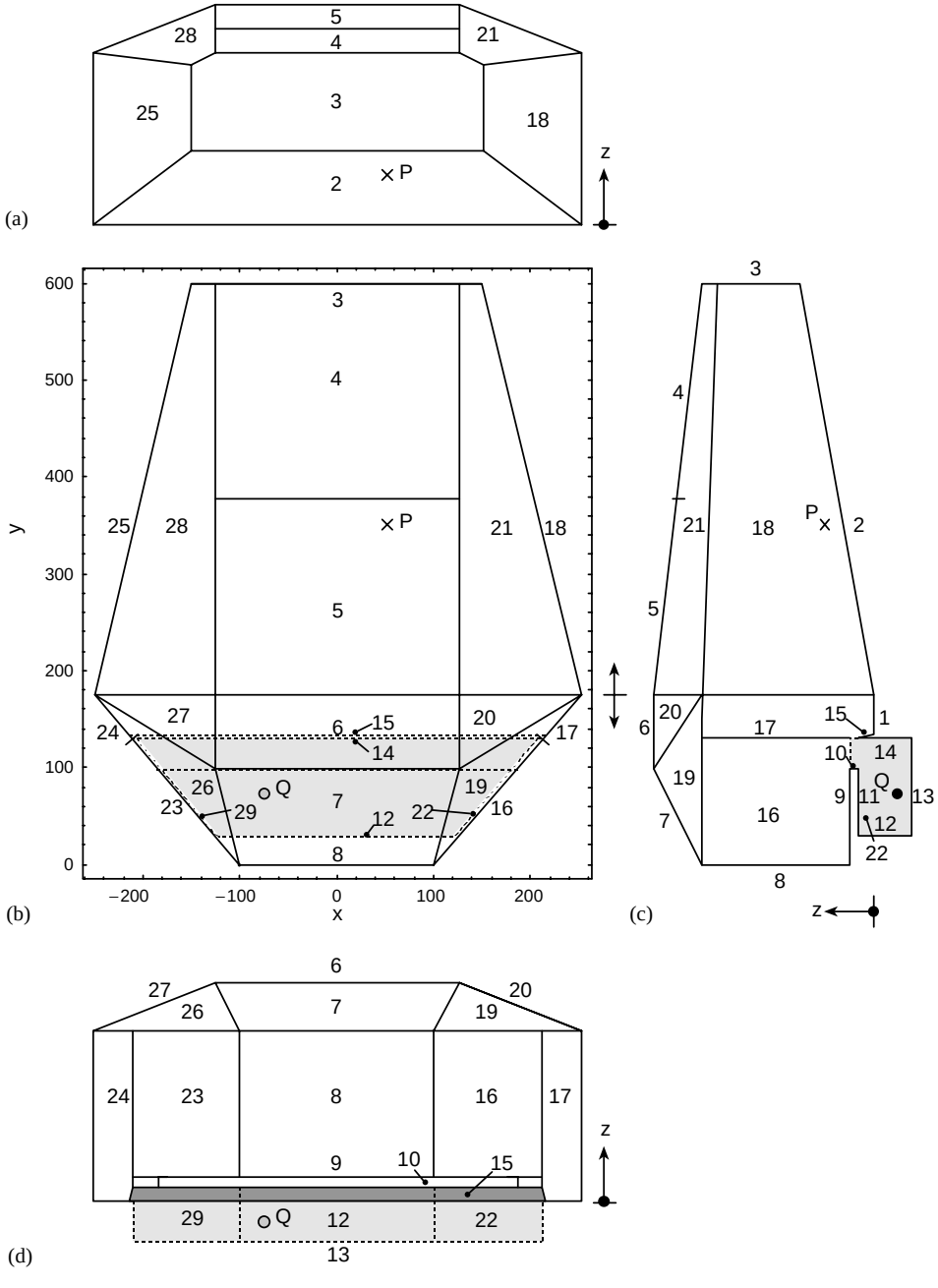

Figure B2. (a–d): A room with convex corner.

{185·0, 100·0, 25·0}},
{{−210·0, 130·0, 175·0}, {−100·0, 0·0, 175·0}, {−100·0, 0·0, 25·0}, {−210·0, 130·0, 25·0}},
{{−250·0, 175·0, 175·0}, {−210·0, 130·0, 175·0}, {−210·0, 130·0, 15·0}, {−215·0, 135·0, 0·0}, {−250·0, 175·0, 0·0}},
{{−150·0, 600·0, 75}, {−150·0, 600·0, 160·0}, {−250·0, 175·0, 175·0}, {−250·0, 175·0, 0·0}},
{{−125·0, 100·0, 225·0}, {−100·0, 0·0, 175·0}, {−250·0, 175·0, 175·0}},

{{−125·0, 175·0, 225·0}, {−125·0, 100·0, 225·0}, {−250·0, 175·0, 175·0}},
{{−150·0, 600·0, 160·0}, {−125·0, 600·0, 175·0}, {−125·0, 175·0, 225·0}, {−250·0, 175·0, 175·0}},
{{−125·0, 30·0, 15·0}, {−125·0, 30·0, −40·0}, {−210·0, 130·0, −40·0}, {−210·0, 130·0, 25·0},
{−185·0, 100·0, 25·0}, {−185·0, 100·0, 15·0}}}

Q = {−75·0, 75·0, −38·5},

P = {50·0, 350·0, 50·0},

Aperture = {{185·0, 100·0, 25·0}, {210·0, 130·0, 25·0}, {−210·0, 130·0, 25·0}, {−185·0, 100·0, 25·0}},

$Z_0 G$ = {0·0141 + 0·000379j, 0·0758 − 0·0118j, 0·0758 − 0·0118j, 0·11 − 0·125j,
0·0311 − 0·00394j, 0·15 − 0·123j, 0·0311 − 0·00394j, 0·0769 − 0·0748j,
0·0141 + 0·000379j, 0·0141 + 0·000379j, 0·0758 − 0·0118j, 0·15 − 0·123j,
0·0141 + 0·000379j, 0·0758 − 0·0118j, 0·0141 + 0·000379j,
0·0311 − 0·00394j, 0·0758 − 0·0118j, 0·0758 − 0·0118j,
0·0311 − 0·00394j, 0·0311 − 0·00394j, 0·0311 − 0·00394j,
0·0758 − 0·0118j, 0·0311 − 0·00394j, 0·0758 − 0·0118j, 0·0758 − 0·0118j,
0·0311 − 0·00394j, 0·0311 − 0·00394j, 0·0311 − 0·00394j, 0·0758 − 0·0118j}.

The wall admittances produce sound absorption coefficients for diffuse sound incidence:

α_{dif} = {0·1, 0·4, 0·4, 0·5, 0·2, 0·6, 0·2, 0·4, 0·1, 0·1, 0·4, 0·6, 0·1, 0·4, 0·1, 0·2, 0·4, 0·4, 0·2, 0·2, 0·2, 0·4, 0·2, 0·4, 0·4, 0·2, 0·2, 0·2, 0·4}.

The parameters {a, b, c, d} of the reduced normal form of the walls are

normal form = {{0·0, 0·0, 1·0, 0·0}, {0·0, −0·173785, 0·984784, 30·4124}, {0·0, −1·0, 0·0, 600·0},
{0·0, −0·110432, −0·993884, 240·189}, {0·0, −0·124035, −0·992278, 244·969},
{0·0, 0·0, −1·0, 225·0}, {0·0, 0·447214, −0·894427, 156·525}, {0·0, 1·0, 0·0, 0·0},
{0·0, 0·0, 1·0, −25·0}, {0·0, 1·0, 0·0, −100·0}, {0·0, 0·0, −1·0, 15·0}, {0·0, 1·0, 0·0, −30·0},
{0·0, 0·0, 1·0, 40·0}, {0·0, −1·0, 0·0, 130·0}, {0·0, 0·948683, 0·316228, −128·072},
{−0·763386, 0·645942, 0·0, 76·3386}, {−0·752207, 0·658181, −0·031342, 72·8701},
{−0·973417, −0·229039, 0·0, 283·436}, {−0·558217, 0·478471, −0·677834, 174·443},
{−0·371391, 0·0, −0·928477, 255·331}, {−0·369195, −0·108587, −0·922987, 272·824},
{−0·761939, 0·647648, 0·0, 75·813}, {0·763386, 0·645942, 0·0, 76·3386},
{0·747409, 0·664364, 0·0, 70·5887}, {0·973417, −0·229039, 0·0, 283·436},
{0·558217, 0·478471, −0·677834, 174·443}, {0·371391, 0·0, −0·928477, 255·331},
{0·511898, −0·100372, −0·853163, 273·514}, {0·761939, 0·647648, 0·0, 75·813}}.